Imperial College London

THÈSE

Présentée par

Cédric FIEZ-VANDAL

Pour obtenir le grade de

Docteur de l'Université Louis Pasteur – Strasbourg I

Mention : Sciences de la Vie et de la Santé
Spécialité : Aspects Moléculaires et Cellulaires de la Biologie

---

Vers l'Étude Structurale des Récepteurs Couplés aux Protéines G

(Towards Structural Studies on G Protein-Coupled Receptors)

Soutenue publiquement le 18 avril 2008
au Collège Doctoral Européen des Universités de Strasbourg

Devant les membres du jury :

Dr. Franc PATTUS	Directeur de thèse
Prof. So IWATA	Co-directeur de thèse
Prof. Marcel HIBERT	Rapporteur interne
Prof. Eva PEBAY-PEYROULA	Rapporteur externe
Prof. Andreas ENGEL	Rapporteur externe
Dr. Niek DEKKER	Examinateur

À Jan

"Mr. Fiez-Vandal was a member of the European Doctoral College of the University of Strasbourg during the preparation of his Ph.D., from 2005 to 2008, René Cassin year class 2005-2006. During his three-year membership, he benefited from specific financial supports offered by the College and, along with his mainstream research, was able to follow a special course offered by the College, concerning topics of general European interests presented by a few renowned international experts. This Ph.D. research project has been led with the collaboration of two universities: Imperial College London and the Louis Pasteur University in Strasbourg."

Dr. Jur. Michael Vorbeck
(former Head of Higher Education and Research at the Council of Europe)

Contents

Abstract

G protein-coupled receptors (GPCRs) mediate the majority of cellular responses to hormones and neurotransmitters. Consequently, they constitute the largest family of pharmaceutical targets. Efforts in applying structure-based drug design and *in silico* screening to facilitate drug discovery for this important class of molecules is limited by the lack of high-resolution structural information. Indeed, Bovine rhodopsin and the human β_2-adrenoreceptor are the only GPCRs for which a high-resolution structure is available[1-3]. Here, we report progress made in expressing and purifying mammalian GPCRs from the MePNet collection in the methylotrophic *Pichia pastoris* yeast expression system. Beginning initially with flask cultures and subsequently with medium cell density fermentor cultures, GPCRs, expressed with N-terminal FLAG epitope and decahistidine, and C-terminal biotinylation fusion tags, were subjected to various purification methods. The use of home-made streptavidine-coated beads in batch gave the most success in purifying these GPCRs. After having checked their oligomerization state by size exclusion chromatograhy, dynamic light scattering and electronic microscopy, three-dimensional crystallization trials were conducted by using the sitting-drop technique. Other approaches included generating fusion proteins to enhance expression and stability, and to increase the amount of hydrophilic surface area. In particular, functional fusions with G proteins yielded promising results. In order to increase the likelihood of crystal formation, we also fused the well-know and highly stable β-barrel protein OmpA, to the N-terminal end of some GPCRs. Preliminary expression results with such latter fusions encourage us to go further in this direction.

Résumé

La famille des Récepteurs Couplés aux Protéines G (RCPG) est caractérisée par la présence de sept domaines transmembranaires (« seven transmembrane receptors » ou 7TM en anglais). Ces récepteurs contrôlent l'activité physiologique de la majorité des cellules et sont la cible privilégiée de la plupart des drogues et de plus de 50 % des médicaments connus.

L'étude de cette famille de récepteurs présente donc un intérêt scientifique majeur. L'enjeu économique est énorme puisque l'exploitation des RCPG ouvre la porte à la découverte et au développement de composés actifs sur la plupart des pathologies humaines. La taille du marché visé représente à terme plusieurs centaines de milliards d'euros. La concurrence est très significative et la plupart des grosses sociétés pharmaceutiques ont mis en place des programmes de criblage à haut débit ciblant exclusivement ces récepteurs. Mais elles manquent encore de données structurales leurs permettant d'améliorer ces projets de « drug discovery ». En effet, seules deux structures tridimensionnelles de RCPG ont été résolues jusqu'à présent, celle de la rhodopsine bovine[1], et très récemment, celle du récepteur β_2-adrenergique humain[2-4]. Si ces deux structures apportent des informations précieuses, elles restent néanmoins insuffisantes. De nombreux consortiums se sont donc mis en place ces dernières années pour lever les écueils propres à l'expression, la production et la cristallisation de ces récepteurs membranaires.

Ce travail de thèse s'inscrit ainsi dans le programme MePNet (Membrane Protein Network, http://www.mepnet.org/)[5] réunissant plus d'une demi-douzaine de grands groupes pharmaceutiques (Abbott, AstraZeneca, Daiichi-Sankyo, GlaxoSmithKline, Kyowa, Novartis, Pfizer, Sanofi Aventis). Son objectif est de mettre en place des stratégies de production pour les RCPG en utilisant le système d'expression *Pichia pastoris*.

La première partie de ce travail a été consacrée au récepteur à la dopamine de type D_2 (D_2DR humain), une cible thérapeutique majeure dans le traitement des addictions, de la maladie de Parkinson et de la schizophrénie. Des expériences de fermentation utilisant la levure *Pichia pastoris* et visant à produire en grande quantité ce récepteur ont été menées

avec succès. La quantité de récepteur produit a été évaluée qualitativement (tests de fixation de ligands à l'équilibre) et par Western-blots. L'effet de différents paramètres sur l'expression du récepteur en fermenteur (diminution de la température d'induction, présence ou non de chaperons chimiques et pharmacologiques) a également été abordé. Les résultats obtenus en fermenteur dans des conditions optimisées d'expression se sont révélés être du même niveau que ceux obtenus en fiole. Ces résultats très encourageants nous ont permis de transposer avec succès l'expression du D_2DR humain dans de grandes unités de fermentation.

Une collaboration avec le Prof. Philip G. Strange (University of Reading, School of Pharmacy, Royaume-Uni) a été amorcée pour caractériser plus finement d'un point de vue pharmacologique (mesures de B_{max}) ce récepteur produit sous forme recombinante.

De nombreux essais de purification, combinant plusieurs types de résines (SP Sepharose Fast Flow, IMAC resins, avidin agarose resin, anti-FLAG M2 affinity gel, entre autres), en batch ou en colonne, n'ont malheureusement permis de ne récupérer qu'une très faible fraction du récepteur exprimé.

C'est pourquoi, dans la seconde partie de cette étude, nous avons développé et ensuite appliqué à de nombreux autres récepteurs une technique de purification en une étape. Cette technique est basée sur l'affinité de l'extrémité C-terminale biotinylée des récepteurs pour des billes couplées à la streptavidine. Le récepteur à la dopamine de type D_2, le récepteur α_{2B}-adrénergique (α_{2B}AR humain), le récepteur aux cannabinoïdes de type 2 (CB_2R humain), le récepteur aux opioïdes de type κ (κOR humain), le récepteur à la neurokinine de type 3 (NK_3R humain), le récepteur du neuropeptide Y1 (NPY1R humain) et le récepteur A_{2A} de l'adénosine (A_{2A}R humain) ont ainsi été purifiés et soumis à des essais de cristallogenèse. Pour certains d'entre eux, des expériences de gel filtration, de microscopie électronique ou de diffusion dynamique de la lumière ont permis d'apprécier leur degré d'oligomérisation.

Nous avons également cherché à stabiliser certains de ces récepteurs en les fusionnant ou en les co-exprimant avec la sous-unité Gα de leur protéine G. Le récepteur à la dopamine de type D_2, le récepteur à la neurokinine de type 2 (NK_2R murin) et le récepteur A_{2A} de l'adénosine ont ainsi été respectivement fusionnés, à leur extrémité C-terminale, avec la sous-unité $G\alpha_{oA}$, la sous-unité $G\alpha_q$, et la version courte ou longue de la sous-unité $G\alpha_s$. Dans le cadre de notre collaboration avec le Prof. Philip G. Strange, nous avons utilisé un analogue non hydrolysable du GTP ($[^{35}S]GTP\gamma S$) pour évaluer l'effet de différents agonistes ou antagonistes sur les fusions D_2DR:$G\alpha_{oA}$ et $A_{2A}R$:$G\alpha_s$. Ces diverses constructions, si elles se

sont révélées très intéressantes d'un point de vue pharmacologique, n'ont par contre pas amélioré les rendements de purification.

Toujours avec le souci de stabiliser ces récepteurs pour faciliter leur purification et leur cristallisation, nous avons enfin fusionné, en position N-terminale cette fois-ci, une protéine de la membrane externe bactérienne, OmpA, avec le D_2DR humain et le récepteur aux cannabinoïdes de type 2. Ces dernières constructions ont été exprimées avec succès dans *Pichia pastoris* et des expériences de purification sont en cours.

Foreword

The Magnificent Seven

To any movie buff, TM7 refers to the 1960 John Sturges' movie, The Magnificent Seven, in which a 30-year-old Steve McQueen burst onto the scene fighting alongside Yul Brynner, Charles Bronson, Robert Vaughn, and James Coburn to defend the homes of an oppressed Mexican peasant village. But flip it to 7TM and it's a different allusion altogether. Nowadays every biomedical scientist knows that 7TM refers to a receptor class, the G protein-coupled receptors (GPCRs), which have taken center stage in drug discovery. But considering the amount of information about the pharmacology of these receptors acquired over the past several decades, it is surprising that we don't know more about how they really work. How does an agonist ligand activate a receptor? How is ligand specificity achieved? Of course, the simple answer is that we need more information about receptor structure and dynamics.

Almost exactly 23 years have passed since the first human GPCR was cloned and characterized by Jeremy Nathans while he was a graduate student at Stanford Medical School[6]. Another two years passed before a team from Merck Research Laboratories, Duke University Medical School, and Howard Hughes Medical Institute, headed by Richard Dixon and Robert Lefkowitz, cloned the β_2-adrenergic receptor (β_2AR) and showed that it was homologous to rhodopsin[7]. A frenzy of receptor-gene cloning followed, leading to a new era of molecular pharmacology based on some knowledge of receptor structure – mainly from site-directed mutagenesis studies – in both academic and industrial settings.

Research groups recorded major advances in understanding the molecular pathophysiology of various human ailments. Perhaps the keynote early advance was the striking elucidation, again by Nathans, of the genetic basis of color blindness and a modern

molecular proof of Thomas Young's nearly 200-year-old hypothesis of trichromatic color vision[8,9]. Mutagenesis and biophysical studies of visual pigments also provided a reasonable understanding of the physical chemistry underlying visual spectral tuning. How do different visual pigments, which absorb light over a wide range of wavelengths from ultraviolet to far red, tune the same basic chromophore cofactor, 11-*cis*-retinal?

But the visual-pigment, or opsin, gene family of typically just a few genes (four in humans) makes up only a small part of the GPCR superfamily. The seminal work of Linda Buck and Richard Axel at Columbia University College of Physicians and Surgeons and Howard Hughes Medical Institute in 1991 – recognized by the 2005 Nobel Prize in physiology or medicine – suggested that a large number of seven-helical receptors make up the olfactory receptor system in mammals[10], for example. GPCRs existed for ligands that were not even endogenous to the organism harboring the receptors.

Taxonomies of hundreds of cloned receptor genes suggested evolutionary relationships among receptors for widely disparate natural ligands: from proteins, to lipids, to nucleotides, to calcium. Orphan receptors – those genes that have the molecular hallmarks of GPCRs, and are expressed, but have no known endogenous ligand – became targets for extensive "deorphaning" programs, mainly in the maturing biotech industry. The hope was that many of those receptors might be drug targets for the next generation of blockbuster therapeutic agents with billion-dollar-per-year sales. After all, small-molecule GPCR modulators have been estimated to make up more than one-half of all commercial pharmaceuticals, including some former best sellers such as the β-adrenergic receptor blockers, and more recently the selective serotonin reuptake inhibitors.

The long-term goal of obtaining an atomic resolution structure of a GPCR had only been achieved in 2000. Rhodopsin, the prototypical GPCR, became the first receptor to be crystallized[1]. However, bovine rhodopsin is unusual in that it is highly abundant from natural sources and is structurally stabilized by the covalently bound ligand 11-*cis*-retinal, which maintains the receptor in a dark-adapted, non-signalling conformation. In contrast, all other GPCRs are activated by diffusible ligands and are expressed at relatively low levels in native tissues. Although the structure determination of rhodopsin was important, many questions remained concerning the conformational changes between different activation states for each receptor, as well as the structural differences among receptors that accommodate the very large diversity of ligands.

Five months ago, after considerable efforts, researchers from Stanford University and the Scripps Research Institute, led by Brian Kobilka and Ray Stevens, have finally determined

the first high-resolution view of a human GPCR bound to a diffusible ligand. More than 40 years after beta blockers were first used clinically, scientists can now got a close-up look at the drugs' molecular target: the β_2-adrenergic receptor. Published online October 21 as an Advance Online Publication in *Nature* and in the October 25 issue of *Science* Express[2-4], this work represents a technical tour de force that required the kind of innovation that was applied to the channel field by Rod MacKinnon and colleagues at the Rockefeller University and Howard Hughes Medical Institute.

However, despite this first success, many more receptor structures will be required to improve any computational method for deorphaning or rational drug design. So the real bulk of future efforts should be focused on trying to obtain high-resolution structures of additional GPCRs, and not only of the rhodopsin-type family A receptors, but of other classes of GPCRs as well.

Illkirch, March 2008

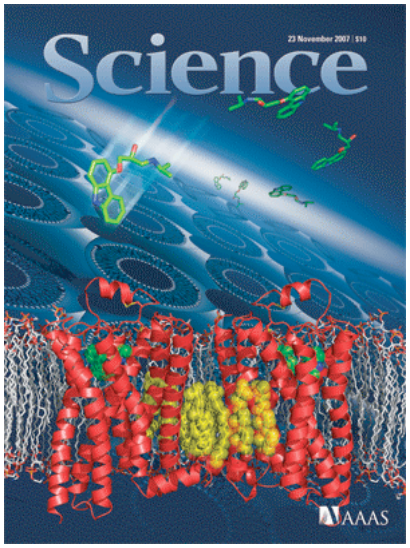

Cover of the 23 November 2007 issue of Science. Structure of the human β_2-adrenergic receptor (red) embedded in a lipid membrane and bound to a diffusible ligand (green), with cholesterol (yellow) between the two receptor molecules. A cartoon of the lipidic cubic phase used for crystallization of the receptor is shown in the background. Image: Yekaterina Kadyshevskaya and the Stevens Laboratory, Scripps Research Institute, CA, USA.

Chapter 1

General Introduction to GPCRs

Cells contain a panoply of transmembrane receptor molecules that can recognize external signals and initiate intracellular signalling events. G protein-coupled receptors (GPCRs), the largest and most diverse group of these receptors, occur in nearly every eukaryotic cell[11-14]. They have a major role in regulating the overall homeostasis of complex organisms, such as mammals, but are also found in primitive species such as *Dictyostelium* (slime mold)[15] and yeast[16]. The GPCR superfamily is diverse[17,18], and sequencing of the human genome has revealed more than a thousand GPCRs-encoding genes[19,20]. The diversity of the GPCRs is matched equally by the variety of ligands that activate them, including odorants[21], taste ligands[22], light[23], metals[24], biogenic amines[25], fatty acids[26], amino acids[27], peptides[28], proteins[29], nucleotides[30], lipids[31-33], Krebs-cycle intermediates[34] and steroids[35]. GPCRs are one of the most important drug targets for the pharmaceutical industry, and up to 40% of all marketed therapeutics act on them[36,37], with no less than a quarter of the top 200 drugs based on GPCRs[38]. Out of the 800 GPCR genes identified in the human genome, up to 340 are believed to be potential drug targets[39]. However, the drugs prescribed today exert their action on only ~30 of them[40], mainly biogenic amine receptors, so there is enormous potential within the pharmaceutical industry to exploit the remaining family members, including more than one hundred orphan receptors[41] for which no existing ligands have so far been identified. A few examples of drugs and their respective targets and related diseases include prazosin (α_1-adrenoreceptor; hypertension)[42], pirenzepine (muscarinic M_1 receptor; gastric ulcers)[43], famotidine (histamine H_2 receptor; duodenal and gastric ulcers)[44], and haloperidol (dopamine D_2 receptor; schizophrenia)[45].

1.1 Structure

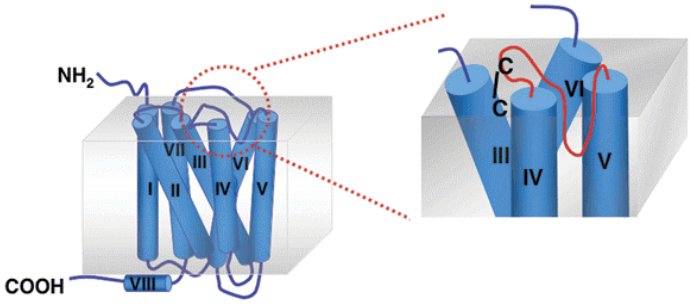

Figure 1.1. The general organization of a GPCR is shown, with the extracellular N-terminus, the seven transmembrane helices (TMs 1-7) arranged counterclockwise and the intracellular C-terminus. Inset: proposed spatial organization of the second extracellular loop (in red). The loop is restrained by a disulfide bridge between conserved cysteines, and folded down between helix 4 and 5. (Massotte and Kieffer, 2001)

All GPCRs share a central hydrophobic core domain structure composed of seven transmembrane helices (TMs), which are connected by three intracellular and three extracellular loops[46] (Fig. 1.1). Two cysteine residues are also conserved in most GPCRs, forming a disulphide bridge between the first and second extracellular loops. This is thought to stabilize the structure by limiting the number of possible orientations adopted by the transmembrane helices[47]. In addition to the Cys-Cys disulphide bridge, also conserved are the D(E)RY motif sequence in TM3 and NPXXY in TM7, both of which are thought to play important functional roles[47]. Topologically, GPCRs possess extracellular N-terminal domains and intracellular C-terminal domains, which can vary both in length and function.

The GPCR superfamily can be subdivided into 6 classes: class A rhodopsin-like, class B secretin-like, class C metabotropic glutamate/pheromone, class D fungal pheromone, class E cAMP receptors, and the frizzled/smoothened family[39]. Some of these classes are not found in mammals, while some are represented by only members found in a single species. Indeed, the classification of GPCRs is still a matter of contention, largely due to the low sequence homology shared between GPCRs both within and across species[39]. Furthermore, in addition to those receptors with known functions, there are approximately 200 receptors with no known function[48]. These are termed “orphan receptors”, for which cognate ligands need to be investigated and identified[49].

1.2 Function

GPCRs are thought to mediate signalling by stimulating membrane-associated heterotrimeric GTP-binding proteins (G proteins) on the cytoplasmic side of the plasma

membrane. Upon activation, the G protein undergoes a GDP release/GTP-binding dependant dissociation step to form the Gα subunit and Gβγ subunit complex, which activate downstream effectors, such as adenylate cyclase (also known as adenylyl cyclase) and phospholipase C (PLC), to produce second messengers (Fig. 1.2). Adenylate cyclase converts adenosine triphosphate into cyclic adenosine monophosphate (cAMP). Phospholipase C catalyzes the hydrolysis of phosphoinositol biphosphate into soluble inositol triphosphate (IP_3) and membrane-bound diacylglycerol (DAG). Other effectors include protein kinases and ion channel, e.g. activation of inward rectifying K^+ channel by metabotropic glutamate receptors[50] and chloride channels by M_2 acetylcholine receptors[51]. The production of downstream messenger molecules, e.g. cAMP, IP_3 and DAG, facilitates downstream signalling cascades, effecting numerous physiological changes. Due to the rapid nature of the signal amplification resulting from these processes, small changes in receptor activation can lead to dramatic changes in downstream signalling.

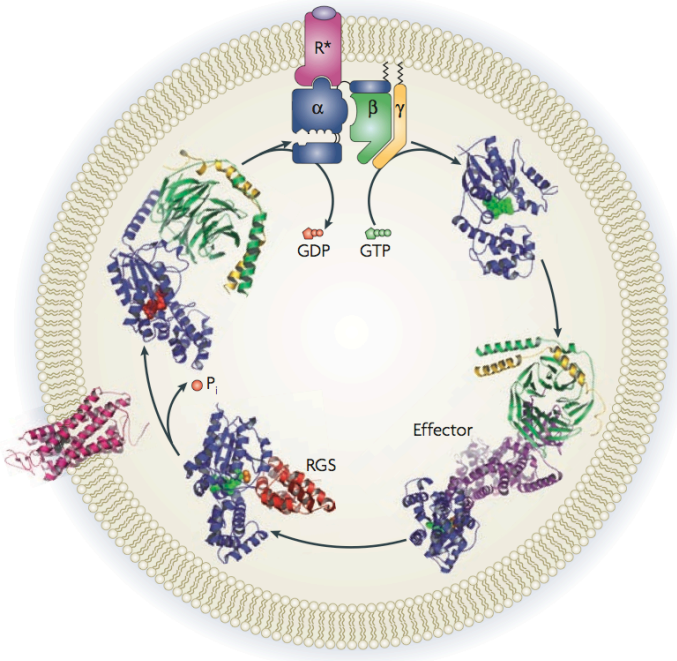

Figure 1.2. The G protein cycle. The receptor–G-protein complex remains the only major G protein conformation for which atomic-scale structural information is unavailable. In the resting state, G proteins are heterotrimers of GDP-bound α- (blue), β- (green) and γ- (yellow) subunits ($G_{t/i}\alpha\beta_1\gamma_1$; Protein Data Bank (PDB) ID code 1GOT). On binding of an extracellular stimulus (light purple for instance), receptors (pink) (such as bovine rhodopsin; PDB ID code 1F88) undergo a conformational change that permits G protein binding and catalyzes GDP release from Gα. Once GDP is released, a stable, high-affinity complex is formed between the activated receptor (R^*) and G protein. Binding of GTP (green) to Gα destabilizes this complex, allowing both subunits, Gα(GTP) ($G_t\alpha$(GTPγS); PDB ID code 1TND) and Gβγ, to interact with downstream effector proteins (purple) ($G_{i/q}\alpha(GDP{\cdot}AlF_4^-){\cdot}GRK2{\cdot}G\beta_1\gamma_2$; PDB ID code 2BCJ). The signal is terminated on hydrolysis of GTP to GDP by Gα, which may be catalyzed by regulator of G protein signalling (RGS) proteins (dark red) ($G_{t/i}\alpha(GDP{\cdot}AlF_4^-){\cdot}$RGS9; PDB ID code 1FQK). (Oldham and Hamm, 2007)

The complexity in downstream signalling can be largely attributed to the large number of G protein isoforms that exist. In the mammalian system, there are thought to be 20 Gα, 5 Gβ and 12 Gγ isoforms[52,53] which can assemble in various combinations to form a multitude of different trimeric Gαβγ complexes. This variety provides the potential for precise modulation and integration of signals from extracellular stimuli. Activation of each GPCR leads to a very specific cellular response, despite the apparently overlap in effectors and second messengers. Indeed, this can be attributed to a complex interplay of spatial and modulating factors, such as (i) cell- or tissue-specific expression and processing of GPCRs, G proteins and downstream effectors; (ii) the relative proportions of each of these components; (iii) compartmentalization of various signalling sub-systems to control "cross-talk"; (iv) modulation of the signals by accessory proteins which interact with GPCRs.

Recently, it has become apparent that GPCRs interact with a range of other proteins, which can have a significant influence on their expression and function, regulating the strength, efficiency or specificity of signal transfer. For instance, the molecular chaperone, NinaA, has been shown to form a stable complex with rhodopsin in *Drosophila melanogaster*[54]. NinaA mutants displayed an inability to transport rhodopsin to the plasma membrane of photoreceptor cells, greatly reducing its expression level. It was also demonstrated quantitatively that NinaA was required for proper expression of rhodopsin.

In addition, modulation of angiotensin II type-1 receptor (ATR) function by the ATR-associated protein (ATRAP) was demonstrated by expressing ATRAP in COS-7 cells. Overexpression of ATRAP was found to attenuate the downstream activation of phospholipase C by ATR[55]. Furthermore, investigation of ATRAP function in adult vascular smooth muscle cells, showed that it significantly increased ligand-induced desensitization and internalization of the receptor[56]. Similarly, a study by Strittmatter *et al.* showed that the neuronal protein, GAP-43, increased the M_2 muscarinic receptor-mediated GTP hydrolysis of $G\alpha_o$ and receptor-induced chloride channel opening, when injected into *Xenopus* oocytes[57]. From these select examples, it is already apparent that the consequence of GPCR-mediated signalling is not fully determined by ligand activation alone. Rather, it is modulated by cellular components that directly and indirectly affect the signalling mechanism and efficacy, as well as GPCR biology.

Indeed, although investigation into the consequences of many of these GPCR-accessory protein interactions is still on going, from what is known, it is evident that GPCR-mediated signalling is a complex process. The availability of high-resolution structural

data will provide deeper insight into their biochemistry and the mechanisms underlying their function *in vivo*.

1.3 GPCR localization & oligomerization

The classical view of the GPCR signalling process is based on random collisions between the proteins that freely diffuse in the plasma membrane, where the specificity of interaction is entirely dependent on the 3D structure of the respective molecules and their matching recognition surfaces. However, recent evidence suggests that the whole system is less mobile than previously predicted, and that cells may concentrate GPCRs and their cognate G proteins, by way of membrane microdomains or compartments, such as lipid rafts and caveolae[58-69]. This compartmentalization may be a major regulator of receptor-effector coupling[70].

The oligomerization of GPCRs was first proposed in the 1970s and 1980s based on cooperative ligand binding[71,72] and radiation inactivation studies[73]. However, it received few supporters due partly to the fact that results could be accounted for by considering GPCRs as functionally distinct units, with no apparent mechanistic need for oligomerization for their activation or activation of downstream G proteins. Although a number of studies have convincingly demonstrated that receptor monomers can be fully functional in activating G proteins and transducing a signal[74], mounting evidence in the past decade suggests that GPCRs can undergo both homo- and hetero-oligomerization in living cells, and that oligomerization may be important for receptor synthesis and expression, and receptor function[75-78]. In the work by Maggio *et al.*, chimeras of α_{2C}-adrenergic and M_3 muscarinic receptors, which had the C-terminal TM6 & 7 segments exchanged between the receptors, were used to transfect COS-7 cells[79]. The chimeric receptors were found to be non-functional when transfected individually. However, co-transfection restored both ligand binding and G protein signalling functions, demonstrating that GPCRs have the capacity to interact with each other at a molecular level.

The prominent current hypothesis is that GPCRs assemble as dimers shortly after synthesis in the endoplasmic reticulum (ER), and traffic as such throughout their life in the cell. The metabotropic γ-aminobutyric acid B ($GABA_B$) receptor has been instrumental in establishing this idea. $GABA_B$ receptors are responsible for presynaptic inhibition of neurotransmitter release in the mammalian brain, and function as heterodimers that consist of $GABA_{B1}$ and $GABA_{B2}$ subunits. When expressed alone, $GABA_{B1}$ receptor is retained intracellularly as an immature protein because it has a carboxy-terminal ER retention motif[80],

whereas $GABA_{B2}$ receptor reaches the cell surface but is not functional. Following their co-expression, heterodimerization masks the subtype-1 ER retention signal, allowing the proper targeting of a functional heterodimeric $GABA_B$ receptor to the plasma membrane. Although a general role for heterodimerization and/or homodimerization in GPCR quality control and ER export has not yet been established, studies using cellular fractionation and fluorescence or bioluminescence resonance energy transfer (FRET and BRET, respectively) have revealed that several GPCRs dimerize in the ER[81-84]. Consistent with the idea that GPCR dimerization occurs early in the secretory pathway is the observation that truncated mutants of vasopressin V_2R[85], dopamine D_3[86], GnRH gonadotropin-releasing hormone[87] and CCR_5 chemokine[88,89] receptors, as well as rhodopsin mutants[90] behave as dominant-negatives of their respective wild-type receptors by preventing their expression on the cell surface. As the physical interaction between wild-type and mutant receptors was confirmed by co-immunoprecipitation in some of these studies[85,86,88], the dominant-negative action was taken as evidence that early heterodimerization between wild-type and mutant receptors leads to their ER retention. For naturally occurring mutations this could have pathophysiological consequences. For example, it has been suggested that the loss of cell-surface expression of CCR_5 observed following its co-expression with the ER-retained $CCR_5\Delta32$ mutant contributes to the delayed onset of AIDS in HIV-infected patients that harbour a $CCR_5/CCR_5\Delta32$ genotype[88]. A series of rhodopsin mutants was also proposed to cause retinal degeneration in *Drosophila* by interfering with the maturation of the wild-type photoreceptor[90].

The first convincing evidence that GPCR dimerization or oligomerization could have a role in pharmacological diversity came from studies on the δ- and κ-opioid receptors[91]. Co-expression of both receptors in HEK298 and COS cells led to the formation of a stable heterodimer with a very low affinity for either the δ- and κ-selective ligand alone. However, high affinity was restored following the combination of the two ligands, suggesting the occurrence of positive cooperativity. Although the direct link between heterodimerization itself and the changes in pharmacological properties has not been formally established, positive or negative ligand binding cooperativity that occurs after receptor co-expression has been interpreted as resulting from receptor heterodimerization for many other GPCRs. These include the metabotropic $GABA_{B1}/GABA_{B2}$[92], opioid δ/μ[93], muscarinic M_2/M_3[94], somatostatin $SSTR_5$/dopamine D_2[95] and adenosine A_{2A}/dopamine D_1[96] receptors. More recently, several

groups have also shown how homo- and heterodimerization can modify the pharmacology of receptors and the specificity of antagonists in native cells[97-101].

But probably the most striking illustration of GPCR oligomerization to date comes from atomic force microscopic studies* of rhodopsin in dark-adapted native retinal disks, which depict large arrays of GPCR homodimers[102,103] (Fig. 1.3).

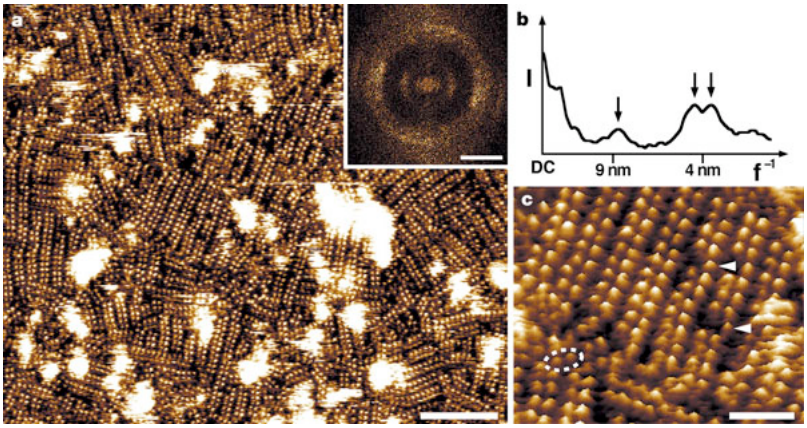

Figure 1.3. Organization and topography of the cytoplasmic surface of rhodopsin. **a**, Topograph obtained using atomic-force microscopy, showing the paracrystalline arrangement of rhodopsin dimers in the native disc membrane. Inset, arcs in the calculated powder-diffraction pattern reflect the regular arrangement of rhodopsin in the membrane. **b**, Angularly averaged powder-diffraction pattern, showing peaks at $(8.4\ nm)^{-1}$, $(4.2\ nm)^{-1}$ and $(3.8\ nm)^{-1}$. **c**, Magnification of a region of the topograph in a, showing rows of rhodopsin dimers, as well as individual dimers (inside dashed ellipse), presumably broken away from one of the rows, and occasional rhodopsin monomers (arrowheads). The rhodopsin molecules protrude from the lipid bilayer by 1.4 ± 0.2 nm (n = 111). The topograph in c is shown in relief, tilted by 5°. Scale bars: a, 50 nm; inset, $(5\ nm)^{-1}$; c, 15 nm. (Fotiadis *et al.*, 2003)

1.4 GPCR constitutive activity and inverse agonism

Constitutive activity is a feature of many GPCRs. The ability of GPCRs to adopt a spontaneously active conformation in the absence of agonist as well as the discovery of ligands that act as inverse agonists is very much a recent development. An inverse agonist is an agent that binds to the same receptor-binding site as an agonist, effecting conformational changes to reduce the constitutive activity level of the receptor.

Leading up to the mid-1990s, it was thought that there were possibly five GPCRs which exhibited constitutive activity and whose inverse agonists had been identified. These

* This microscopy technique uses a tiny stylus on a cantilever that is dragged across the crystal surface, and the deflections recorded are used to map the surface topology. Simon Scheuring from Andreas Engel's group in Basel, Switzerland, made the analogy to a blind man scanning the environment with a stick to explore the road ahead. Deflections of his stick are recorded and assembled into an image in his brain. The technique does not provide resolution as high as that obtained using either electron or X-ray crystallography, but unlike these other methods, it allows the user to monitor conformational changes of the proteins *in situ*.

included the β_2-adrenergic receptor[104], serotonin $5HT_{2C}$ receptor[105], δ-opioid receptor[106], bradykinin B_2 receptor[107] and the frog atria muscarinic acetylcholine receptor[108]. The list has since grown to include several dozen members[75]. Ligands which were originally thought to act as antagonists, have come to be reclassified as partial or full inverse agonists[109]. Because inverse agonism requires experimental characterization, much of this progress is attributed to the development of recombinant expression systems, which allow the overexpression of GPCRs and mammalian G proteins, to the levels required for accurate quantitation of ligand-induced changes in activity level[110-112].

Many wild-type GPCRs display only low levels of constitutive activity in the absence of agonist. However, they can be modified to display much higher basal activity. Indeed, many disease states are associated with mutations that lead to increases in constitutive activity. Mutations in the TM2 (G90D) and TM7 domains (A292E, K296E) of rhodopsin have been noted to result in enhanced basal activity, which manifests itself as congenital night blindness in patients[113,114]. Similarly, the expression of the constitutively active Kaposi's sarcoma-associated herpesvirus-GPCR (KSHV-GPCR), a homolog of the human chemokine receptor, $CXCR_2$, leads to cellular changes and the vascular overgrowth characteristic of Kaposi's sarcoma[115]. Indeed, a D128V mutation in $CXCR_2$, which leads to enhanced constitutive activity, also causes similar cellular changes[116].

As such, inverse agonists are potentially important therapeutical agents for the treatment of diseases that are caused by mutations that enhance constitutive activity. For instance, the discovery that an inverse agonist for the human cannabinoid CB_2 receptor blocks the recruitment of leukocytes, could potentially be used in the development of therapeutic drugs against allergies and other inflammatory disorders[117]. Similarly, inverse agonists for the KSHV-GPCR[118] may be useful for treating Kaposi's sarcoma.

1.5 First structures of 7TM receptors

Early studies on seven transmembrane proteins focused on the highly expressed members, bacteriorhodopsin, related halobacteria proteins – halorhodopsin and sensory rhodopsins I & II – and rhodopsin.

Bacteriorhodopsin is a light-driven proton pump from halobacteria[119]. It exists as a functional trimer *in vivo*. It is responsible for the pumping of protons outwards across the plasma membrane, creating a cytosolic environment 10,000-fold more alkali than the exterior. The flow of protons back into the cell generates a proton motive force, which is coupled to ATP synthesis. Initial structural studies on bacteriorhodopsin were first carried out using

electron microscopic analysis of two-dimensional crystals[120]. This led to the determination of an atomic model for bacteriorhodopsin by Henderson *et al.* (1990)[121]. Since 1990, a combination of electron microscopic and X-ray crystallographic studies have led to many more structures being published, ranging in resolution from 6 to 1.55 Å[122-124].

In addition to bacteriorhodopsin, halobacteria possess a light-driven chloride-ion pump, halorhodopsin[125], for which the structure has been solved[126], and two sensory rhodopsins, which are involved in phototaxis. Of the two, the structure of sensory rhodopsin II has been solved[127-129]. The members of the bacteriorhodopsin family of proteins share structural similarities with rhodopsin. Each protein contains seven TM α-helical domains, with a chromophore covalently bound at approximately the centre of helix 7. Topologically, the proteins also have their N- (outside) and C-termini (inside) arranged in a similar fashion with respect to the cytosolic environment. The structures of bacterial seven TM proteins provided the first glimpse of the possible TM domain arrangements for this class of protein. However, subsequent comparisons with structures of a GPCR, rhodopsin[1], revealed differences in the arrangement of the helices, and size and organisation of the extramembrane regions.

The first mammalian GPCR structure to have been solved to high-resolution is that of bovine rhodopsin[1,130] (Fig. 1.4a). Bovine rhodopsin is a photoreceptor protein responsible for dim-light vision. Rhodopsin is composed of a 348 amino acid apoprotein, opsin, and a light-sensitive ligand, the 11-*cis*-retinal chromophore (Fig. 1.4b). The 11-*cis*-retinal constitutes an inverse agonist covalently bound to opsin via a Schiff-base linkage to a Lys 296 side chain on helix 7[131] (Fig. 1.4c and d). Consequently, the receptor is held tightly in a non-activated conformation by its retinoid ligand.

Upon absorption of a photon (498 nm), the chromophore undergoes photoisomerization to all-*trans*-retinal, inducing a correspondent change in the opsin from its inactive to its active conformation. The active form, known as Meta II, – which can be considered analogous to the agonist-bound state of many ligand-binding GPCRs – then recruits and binds intracellular G proteins, transducins, continuing the visual signal cascade that culminates in an electrical impulse to the visual cortex of the brain. The absorption of a single photon brings about the activation of hundreds of transducin molecules[132], illustrating the magnitude of the signal amplification achieved by GPCRs. Inactivation of the receptor is brought about by a hydrolysis reaction, which releases the retinoid[133,134].

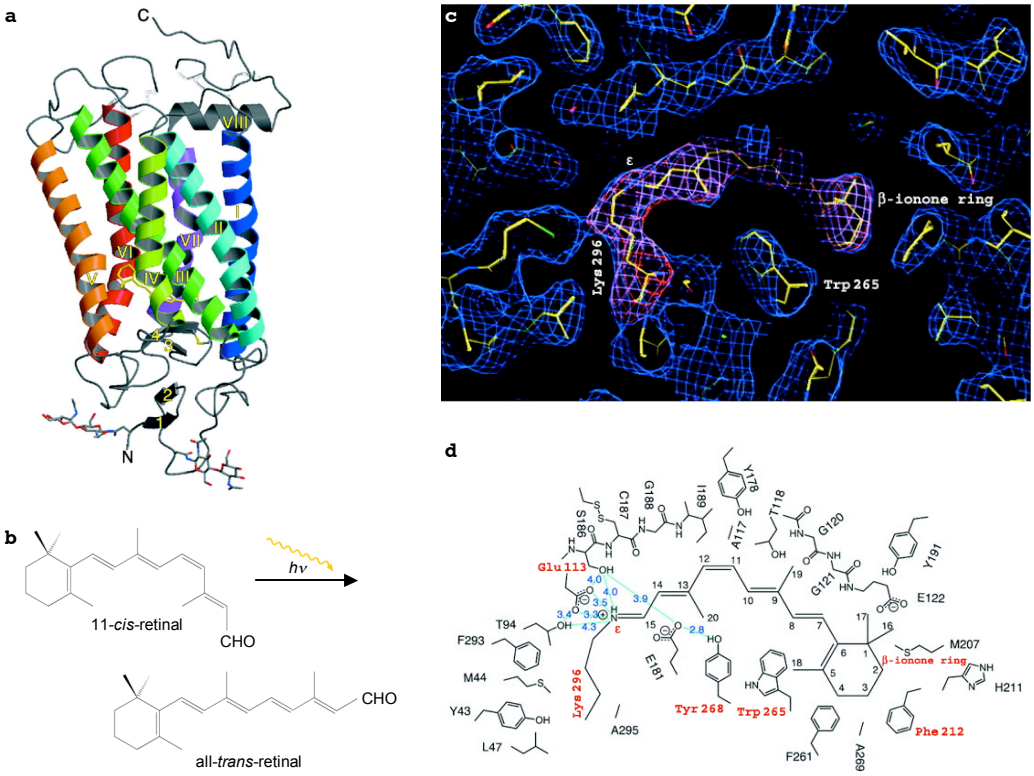

Figure 1.4. a, Side view of the bovine rhodopsin (PDB ID code 1F88) with the intracellular region at the top. The extracellular portion of rhodopsin has many flexible regions. The second extracellular loop between helix 4 and 5 contributes to the stabilization of the retinoid by forming a cap over the retinal binding pocket (Yan *et al.*, 2002). Intracellular loops 2 and 3 are believed to be points of interaction with the G protein, transducin (Terakita *et al.*, 2002). **b**, Schematic representation of the isomerization reaction which takes place when 11-*cis*-retinal (above left) absorbs a photon of light at 498 nm to form all-*trans*-retinal (bottom right) **c**, Electron density for the 11-*cis*-retinal chromophore (red) with the current model refined against the 2.8 Å data set. **d**, Schematic presenting the residues within 4.5 Å distance from retinal molecule. The β-ionone ring of retinal extends deep into the binding pocket of rhodopsin and contacts residues on helix 5 and 6, where it is sandwiched between Phe 212 and Tyr 268, and interacts with the highly conserved Trp 265. It has been proposed that changes in the rotamer of Trp 265 occur upon activation of rhodopsin and related family members, and constitutes the "toggle switch" for receptor activation (Schwartz *et al.*, 2006). Accordingly, the interactions between *cis*-retinal and Trp 265 are likely to contribute to the absence of basal activity in rhodopsin. Blue labels indicate the distances between Schiff base nitrogen atom and charged or polar atoms within 4.5 Å. (a, c and d; adapted from Palczewski *et al.*, 2000)

There are many factors that contributed to the success of structural studies of bovine rhodopsin. Firstly, it is expressed in large amounts from natural sources (rod outer segment membrane). Secondly, rhodopsin is covalently bound to its inverse agonist, the 11-*cis*-retinal, thereby increasing its stability. Thirdly, the protein is comparatively stable in detergent solution, demonstrating significant stability at up to 40 °C in a wide variety of common detergents, e.g. LDAO, octyl-β-D-glucoside, dodecyl-β-D-maltopyranoside, tetraethylene glycol monooctyl ether[135]. Lastly, the presence of the spectroscopically active bound chromophore facilitates efficient identification and quantitation during purification.

1.6 First structure of a recombinant GPCR: the human β_2-adrenoreceptor

The human β_2-adrenoreceptor (β_2AR) is a GPCR activated by adrenaline that plays important parts in cardiovascular and pulmonary physiology. In contrast to rhodopsin, β_2AR – like many other GPCRs for hormones and neurotransmitters – exhibits significant basal, agonist-independent G protein activation. This basal activity has been associated with inherent structural instability and flexibility[136,137].

The β_2AR was efficiently expressed in Sf9 insect cells and was purified to homogeneity using antibody and ligand affinity chromatography[138]. Extensive sparse matrix screening (over 2,000 conditions at 4 °C and 20 °C) failed to produce diffraction-quality crystals of wild-type β_2AR. This was probably due to conformational variability of the flexible third intracellular loop and C-terminus, as well as the relatively small polar surface available for crystal contacts.

In an effort to provide conformational stability while increasing the polar surface available for crystal contacts, the groups of Brian Kobilka (Stanford, CA, USA) and Gebhard Schertler (MRC, Cambridge, UK) generated a monoclonal antibody that binds to the third intracellular loop of native, but not denatured receptor protein[139]. The β_2AR was then crystallized in complex with Fab fragments generated from this monoclonal antibody (see further Fig. 1.9b) and the structure determined at an anisotropic resolution of 3.4 Å/3.7 Å[4] – carazolol-bound β_2AR-Fab complex were grown in dimyristoylphosphatidylcholine (DMPC) bicelles and the size and uniformity of the crystals were improved by removing 48 amino acids from the unstructured C-terminus (β_2AR365). The cytoplasmic ends of the transmembrane segments and the connecting loops are well resolved, whereas the extracellular regions and the ligand-binding site of the receptor are not seen (Fig. 1.5a).

To obtain high-resolution structural information on the β_2AR and to provide a more detailed picture of extracellular loops as well as the ligand-binding site, Brian Kobilka and Ray Stevens (The Scripps Research Institute, CA, USA) used an alternative approach. They replaced the third intracellular loop (IC3) of β_2AR365 with a small, stable protein known as T4 phage lysozyme (T4L). The T4L protein promotes crystal-lattice formation in the same way as the antibody fragment previously (Fig. 1.5a). The optimized β_2AR-T4L fusion protein*, bound to carazolol, was crystallized in a cholesterol-doped lipidic cubic phase

* Rosenbaum *et al.*[3] report a systematic functional analysis of β_2AR bound to T4L to establish its physiological relevance. The engineered receptor displays wild-type binding to antagonists and inverse agonists but increased affinity for agonists, a profile similar to that of constitutively active mutants. However, only minor differences

(see further Fig. 1.11) and the resulting 2.4 Å resolution crystal structure reveals the interface between the receptor and the ligand[2,3].

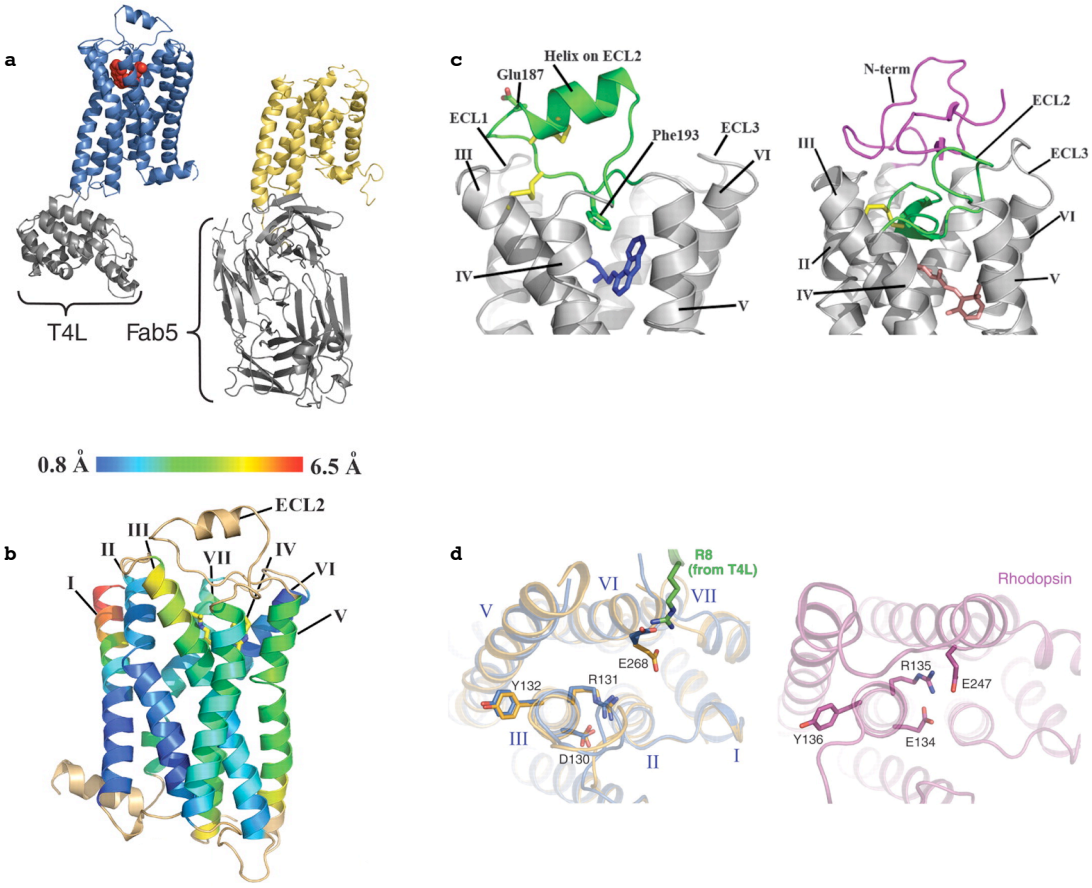

Figure 1.5. a, Side-by-side comparison of the crystal structures of the β_2AR-T4L fusion protein and the complex between β_2AR365 and a Fab fragment. The receptor component of the fusion protein is shown in blue (with modeled carazolol as red spheres), whereas the receptor bound to Fab5 is yellow. **b**, Comparison of β_2AR-T4L helical orientations with those of rhodopsin (PDB ID code 1U19). β_2AR-T4L is rendered as a ribbon trace colored with a blue-to-red spectrum corresponding to observed distances between Cα positions in the two structures [root mean square deviation (RMSD) 2.7 Å between all residues in the transmembrane region]. Helix II shows very little movement, whereas the entire lengths of helices III, IV, and V shift substantially. Helix VIII and loops were not included in the comparison and are colored tan. **c**, Comparison of the extracellular sides of β_2AR-T4L and rhodopsin. (Left panel) The N-terminus is missing from the experimental density in the β_2AR-T4L structure and is not shown. ECL2 is shown in green and contains a short helix and two disulfide bonds (yellow). The intraloop disulfide bond constrains the tip of ECL2, which interacts with ECL1. The second disulfide bond links ECL2 with helix III. There is one interaction between ECL2 and carazolol (blue) through Phe 193. The entire loop is held out of the ligand-binding site by a combination of the rigid helical segment and the two disulfide bonds. (Right panel) In contrast, ECL2 (green) in rhodopsin assumes a lower position in the structure that occludes direct access to the retinal-binding site and forms a small β sheet in combination with the N-terminal region (magenta) directly above the bound retinal (pink). **d**, Analogous interactions to the ionic lock between the E(D)RY motif and Glu 247 seen in rhodopsin (right panel, purple) are broken in both structures of the β_2AR (left panel, blue and yellow as in a). (Cherezov *et al.*, 2007; Rosenbaum *et al.*, 2007)

---

were observed when the receptor chimera structure was compared to the 3.4 Å structure of the wild-type β_2AR crystallized in complex with Fab fragments.

Although the overall structure of β_2AR is similar to rhodopsin, with seven transmembrane helices and an eighth helix that runs parallel to the cytoplasmic face of the membrane (Fig. 1.5b), there are several new findings. With regard to ligand binding, carazolol is located deep within the transmembrane helices, at a site that is consistent with the retinal binding pocket (Fig. 1.5c), and some key interactions are consistent with findings in the rhodopsin structure. For example, the inactive state of rhodopsin maintained by 11-*cis*-retinal is thought to be stabilized in part by direct conformational restriction of a conserved tryptophan (Trp 265) side chain[140] (see Fig. 1.4c and d). The analogous tryptophan in the β_2AR is similarly restrained (although indirectly) by carazolol. This finding provides a structural basis for interpreting prior mutation studies, which showed that signal propagation mechanisms are largely conserved in members of the GPCR family. However, the data also indicate variation that may permit specialized responses to specific ligands. A helical structure in the second extracellular loop (ECL2) of β_2AR-T4L makes direct contact with carazolol. This feature is not conserved in rhodopsin (Fig. 1.5c). Cherezov *et al.*[2] and Rosenbaum *et al.*[3] suggest that the novel structure in ECL2 and disorder in the N-terminal region of β_2AR may provide a path for diffusible ligands to the binding pocket and contribute to ligand selectivity. Thus, although conformational changes associated with GPCR activation might be conserved in the family, specific kinetic and thermodynamic details of ligand recognition might be specified through modular variation of extracellular loop regions. The β_2AR structure also differs from rhodopsin in having weaker interactions between the cytoplasmic ends of TM3 and TM6, involving the conserved E(D)RY sequences (Fig. 1.5d). These differences may be responsible for the relatively high basal activity and structural instability of the β_2AR, and contribute to the challenges in obtaining diffraction-quality crystals of non-rhodopsin GPCRs.

1.7 Activation mechanism

The various molecular binding modes seem to be coupled to specific "triggers" within GPCRs[141]. For family A receptors, one such trigger is the "ionic lock" – an electrostatic interaction between a triad of charged amino acids that tether TM3 and TM6 together (Fig. 1.6a and b). The ionic lock stabilizes the inactive state of the receptor[141]. The specific amino acids that form the lock – the conserved E(D)RY motif at the end of TM3 and an acidic amino acid at the cytoplasmic border of TM6 – are similar in most GPCRs; mutations that change this sequence can disrupt the lock and increase the constitutive activity[142]. Agonist binding is expected to disrupt, mostly indirectly, this interaction, promoting thereby

the active conformation of the receptor. A second trigger, called the "toggle", is also known, and is thought to involve a cluster of amino acids that are in contact with the agonist-binding site (Fig. 1.6a). The toggle also seems to constrain the receptor in an inactive state; it is thought to be released when strong agonists bind to the receptor. However, this "two-state" model does not apply for all receptors in family A[143,144]. Besides, numerous data indicate that GPCRs are highly plastic molecules that can adopt a large variety of structural conformations, with many intermediates between the inactive and fully active states[141,145].

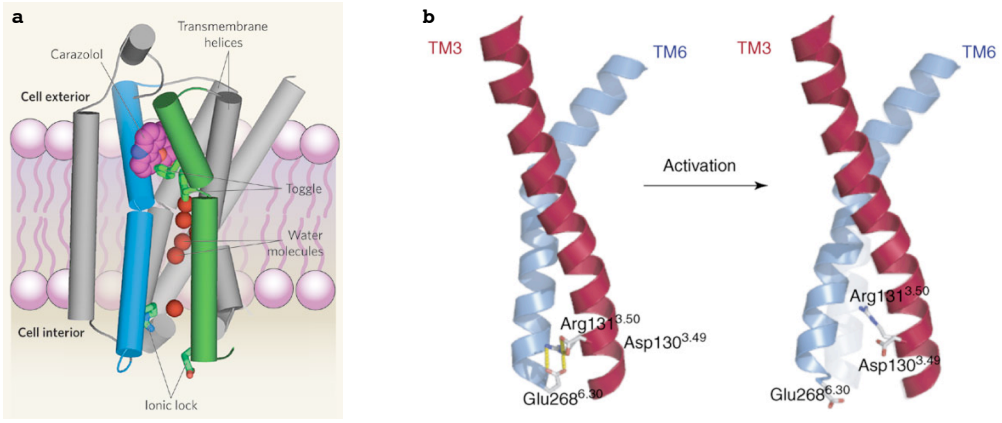

Figure 1.6. a, The cartoon shows the partial crystal structure of the β_2AR-T4L chimera, as reported by Cherezov *et al.* (2007). Seven helices (TM1-7) cross the cell membrane, although TM5 is not shown as it would obscure the other helices. Ligand molecules bind at a site between TM3 (blue) and TM6 (green); carazolol was used to stabilize the site in order to obtain this structure. The amino acids just below carazolol form a "toggle" that stabilizes the inactive state of the receptor. The amino acids indicated at the bottom can form an "ionic lock" that performs the same function, but this crystal structure and that of Rasmussen *et al.* (2007) show that the lock is broken in β_2AR. Water molecules occupy a loosely packed channel; this may provide room for movement of the TM helices upon activation of the receptor, and allow binding of a G protein near the base of TM5 and TM6. **b**, Disruption of the ionic lock in β_2AR. Model of TM3 (red) and TM6 (blue) from β_2AR, highlighting the amino acids that comprise the ionic lock at the cytoplasmic end of these TM segments. (Kobilka and Deupi, 2007).

Some receptors can adopt "active" conformations in the absence of ligands, leading to constitutive activity. Each ligand is expected to stabilize (or induce) one or a restricted set of these possible conformations, which determines its pharmacological properties as partial or full (inverse) agonist. The range of conformational states of a receptor also explains how specific ligands can display differential "efficacies" toward various signalling pathways.

A surprise finding from the two recent β_2AR crystal structures[2-4] is that the ionic lock is broken (as expected in an active state) despite the presence of an inverse agonist (which promotes the inactive state). Had only one crystal form of β_2AR been available, it could have been argued that this was an artefact of the experimental conditions – either a consequence of

the artificial lipid environments, or because of perturbation of the third intracellular loop. But because the lipid supports and IC3 region are different in each structure, it is unlikely that the same misleading result could have occurred in both cases. Moreover, the TM regions in both structures align well with each other, further corroborating the results. Thus, the weak constitutive activity of β_2AR might be attributed to the breaking of the ionic lock; this can be compared with rhodopsin, which retains the lock and shows no such activity – in this view, the ionic-locked state of rhodopsin is an extreme case; a specialized, more fully inactivated state that provides for the remarkable level of silencing of receptor activity required to suppress noise in the dark-adapted state of photoreceptor neurons. In contrast, the toggle is intact in the two β_2AR structures, just as it is in inactivated rhodopsin, despite considerable differences in the binding modes adopted by the ligand molecules for these two GPCRs. Perhaps stronger inverse agonists than carazolol would stabilize the ionic lock and fully inactivate β_2AR, whereas agonists would release both lock and toggle. But these speculations have yet to be confirmed, reinforcing the need for additional structural data about receptors, their ligand binding domains and complexes in various states of the activation process.

1.8 GPCR drug discovery

Drugs targeting GPCRs represent the core of modern medicine. They account for the majority of best-selling drugs and about 40% of all prescription pharmaceuticals on the market[146] (Fig. 1.7). Notable examples include Eli Lilly's Zyprexa®, Schering-Plough's Clarinex®, GlaxoSmithKline's Zantac®, and Novartis's Zelnorm®. And there is broad consensus that GPCRs will remain at the hub of drug development activities for the foreseeable future.

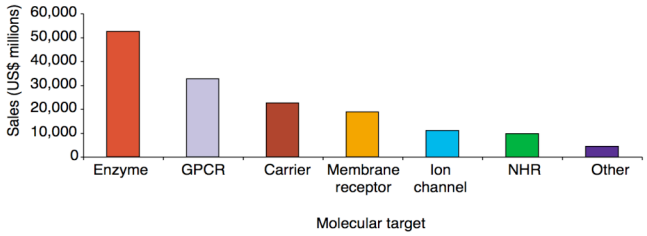

Figure 1.7. Global sales of the 100 best-selling drugs in 2002, arranged according to the target class to which they belong. Abbreviation: NHR, nuclear hormone receptors. (Betz, 2005) Four out of the top ten individual drugs sold in 2006 target GPCRs: the long-acting β_2 selective adrenoreceptor agonist salmeterol (Advair®, US$6.3 billion), the platelet ADP receptor antagonist clopidogrel (Plavix®, US$5.8 billion), the dopamine receptor antagonist olanzapine (Zyprexa®, US$4.7 billion) and the selective monoaminergic antagonist risperidone (Risperdal®, US$4.6 billion). (Source: IMS Health 2006)

Due to their relevance to many disease states, GPCRs are prominent components of pipelines in small and large drug companies alike, and many drug discovery programs focus exclusively on these receptors[38]. In addition to combinatorial chemical and ultra-high-throughput screening approaches, many of these programs are now often supplemented by *in silico* methods to maximize the probability of finding attractive novel lead compounds[147]. The development of an accurate three-dimensional receptor pharmacophore aids in this process. A receptor pharmacophore describes the physicochemical features required for the optimal molecular interactions necessary to elicit a desired receptor response. Structure-activity relationship analysis of ligands can highlight potential functional groups, which aid in providing these key molecular interactions. Similarly, studying the receptor-binding site allows the identification of key residues and physicochemical properties that are likely to determine ligand recognition. Often, ligand- and receptor-based pharmacophore development complement each other and work synergistically in identifying favourable physicochemical interactions.

In receptor-based development, the accuracy and usefulness of the pharmacophore is subjected to the intrinsic inaccuracies of the receptor model generated. In the absence of protein structures, homology modeling has been one technique used to generate models. Combining ligand-based pharmacophore and receptor homology modeling may increase the likelihood of finding novel agonists and antagonists. The work of Evers and Klabunde[148], with the α_{1A}-adrenoceptor, serves as a prime example of this approach. The model of the α_{1A}-adrenoceptor that was built was used in a virtual screen of a filtered in-house compound library (target-unspecific filters, such as molecular weight and number of rotatable bonds, and target-specific filters, such as a pharmacophore model) of 22,950 compounds. Using this approach, 37 compounds with binding affinities below 10 μM were discovered, three of which were found to bind in the single digit nanomolar range.

Additional biochemical studies serve to highlight key functional residues and validate the accuracy of the model. Mutagenesis screening, for instance, helps uncover the key ligand-receptor contacts responsible for drug recognition by the receptor. This approach was first demonstrated by Strader *et al.*[149] by observing ligand affinity constants of epinephrine derivatives binding to β_2-adrenergic receptor mutants. By modifying the 3- and 4-hydroxyls of epinephrine, and mutating the Ser 204 and Ser 207 residues, it was proposed that the 3-OH interacted with Ser 204 and 4-OH with Ser 207 by hydrogen bonding. Govaerts and colleagues[150,151], and more recently Rob Leurs[152], have described a similar approach that combines mutation studies with receptor modeling to elucidate the mechanism of

chemokine-induced activation of CCR_5 and to characterize important steps in the activation of the human histamine H_1 receptor.

However, homology modeling of GPCR structures based on the bovine rhodopsin structure is marked by significant difficulties[153]. Firstly, due to low sequence homology across the GPCR superfamily[39], generating an accurate sequence alignment becomes difficult. Secondly, the bovine rhodopsin structure presented is that of an inactive conformation, whereas the mechanisms of ligand binding are associated with the active state of GPCRs. Thirdly, whereas rhodopsin might serve as a reasonable structural template for class A GPCRs, there remains a distinct need for an equivalent representative for members from the other classes.

The precision required for designing a drug specific to only one particular GPCR makes the solving of other GPCR structures to high-resolution even more pertinent. Indeed, although ligands have been successfully developed which possess sub-micromolar affinities using homology modeling[154], it remains uncertain if they also possess significant binding affinities to other GPCRs, which can bring about unwanted side effects *in vivo*[*]. In the absence of structural data, the accurate high-throughput screening of designer ligands against other GPCRs for unwanted interactions remains impossible. It is hoped that the recent release of the β_2AR structures (PDB ID codes 2R4R, 2R4S and 2RH1) in November 2007[2-4] would facilitate more accurate modeling based on homology.

I would also like briefly to mention two interesting *de novo* GPCR structure-based methods that do not rely on rhodopsin homology.

Goddard and colleagues have developed at Caltech new computational strategies and techniques based solely on the primary amino acid sequence for predicting the tertiary structure of GPCRs (MembStruk) and for predicting a putative binding site for small-molecule ligands in the TM, which might or might not overlap with the retinal binding site in rhodopsin (HierDock). Using this approach, the Goddard group was able to predict accurately a rhodopsin structure covalently bound to retinal, close to that observed for the experimental structure[155]. Given these encouraging results, they applied their

[*] However, drugs that exhibit GPCR promiscuity can, in some circumstances, be desirable and there are examples of drugs that target more than one GPCR, which is therapeutically advantageous. A good example of this is the antipsychotic drug olanzapine (Zyprexa®), which was developed by Eli Lilly to compete in the CNS market with the rival drug clozapine (Clozaril®), marketed by Novartis. Although both drugs were initially developed to target dopamine D_2 receptors, olanzapine binds with high affinity to more than 12 GPCRs (Roche *et al.*, 2002). At first glance, this broad range of activities might seem to limit the therapeutic usefulness of olanzapine but that has not been the case and it is, in fact, one of the most successfully marketed drugs of the past few years. In this case, the ability of the drug to block 5HT and dopamine receptors is probably an advantage because it is thought that both receptors have a role in schizophrenia.

structure-prediction algorithms to several other receptors[156-159] including the β_2AR[156] and the dopamine D_2 receptor[157] .

Epix Pharmaceuticals Israel (formerly Predix Pharmaceuticals) uses the concept of "structural decoys" to predict *de novo* GPCRs structures[160]. Its PREDICT algorithm combines protein sequence information with membrane environment property factors to determine the most stable three-dimensional structure of a receptor's transmembrane domain. The PREDICT method generates many alternative structures, which are simultaneously optimized. This technique avoids a structure becoming trapped in a local minimum without sufficiently exploring its conformational space. The company recently published five examples of successful early-stage discovery projects that led to "very promising lead compounds" validated via *in vitro* and *in vivo* assays[161]. Each was initiated by screening libraries virtually against PREDICT-generated structures, including of two different serotonin receptors.

1.9 Challenges of working with membrane proteins

A relatively small number of membrane protein structures has been solved (154) compared to more than 45,000 soluble proteins[162-164]. This reflects the difficulty in obtaining crystals of membrane proteins that diffract to a sufficient high-resolution for modeling. The structural study of GPCRs poses many challenges, from the stage of their expression and purification, to their crystallization.

1.9.1 Recombinant expression systems

It is a sobering thought that most of the membrane proteins whose structures have been solved are stable proteins from abundant natural sources, some of which even naturally form 2D arrays, e.g. bacteriorhodopsin in the purple membrane of *Halobacterium salinarum*. The solving of the bovine rhodopsin structure by X-ray crystallography, for instance, was possible due in large part to its abundance in the retina – up to 50 mg per 100 vertebrate retinas. However, in general, GPCRs are present in only a small number of copies per cell, presumably to allow tight control of the signal transduction amplification. This makes their isolation from natural sources unfeasible, both due to the amount of tissue material required in order to produce a sufficient amount of receptor, as well as the high level of backgrounds from contaminating membrane proteins in proportion to the target receptor. In the case of the neuropeptide Y receptor type-2, for example, 1,000 pig brains were needed to obtain 190 μg of purified receptor for functional studies[165]. As such, it has been necessary to express GPCRs in recombinant systems to generate the amounts required for pharmalogical, biochemical and

structural studies.

The expression systems employed to date can be broadly arranged in three categories; bacterial, lower eukaryotic and higher eukaryotic systems (reviewed in[166]). Several comprehensive reviews covering the main advantages and disadvantages of using the various expression systems for producing membrane proteins are available[167-169]. In addition, a recent review also covers the expression of mammalian GPCRs[170]. Here, the focus will be on the *Pichia pastoris* expression system.

1.9.2 *Pichia pastoris*

The yeast expression systems commonly used include *Saccharomyces cerevisiae*, *Schizosaccharomyces pombe* and *Pichia pastoris*. The story of *P. pastoris* begins forty years ago, when Koichi Ogata first described the ability of certain yeasts to utilize methanol as a sole source of carbon and energy[171]. These methylotrophs attracted immediate attention as potential sources of single-cell protein (SCP), to be used as high-protein animal feed. In the early seventies, Philips Petroleum Company developed media and protocols for cultivating *P. pastoris* on methanol at high densities. Soon after, the idea concerning animal feeds was abandoned for economic reasons, but the company contracted with the Salk Institute of Biotechnology in California and continued developing the *P. pastoris* system for heterologous protein expression. The expression system has been commercially available from the Invitrogen Company since 1993. To date, the *P. pastoris* system has been documented to have been used to successfully express a number of mammalian GPCRs. These include human β_2-adrenergic[172], endothelin ET_B[173] and μ-opioid receptors[174], mouse serotonin $5HT_{5A}$ receptor[172,175] and bovine rhodopsin[176]. Like all yeast, *P. pastoris* possesses a short generation time (approximately 2 hours), grows on relatively simple, inexpensive media, and requires only simple genetic manipulation. It is well characterized genetically, allowing the use of a number of promoters for the expression of recombinant protein as well as the production of knockout cell lines. For instance, the strain used in this work, SMD1163 (*his*4, *pep*4, *pbr*), is a protease deficient strain, which facilitates the relatively simple isolation of multicopy clones based on both histidine auxotrophism and geneticin resistance. *P. pastoris* is also readily adapted for growth in fermentors, allowing large-scale production.

Unlike *Escherichia coli*, a commonly used bacterial expression system, yeast possess the capacity to perform post-translational modifications[177] – signal sequence processing, protein folding, disulphide bridge formation, lipid addition and O- and N-linked glycosylation – which can sometimes be important for recombinant protein function[178]. However,

differences do exist. For instance, the N-linked glycans added by yeast are different from those added by mammalian cells, which might disrupt proper functioning of proteins sensitive to the structure of the glycans added[179].

Yeast and mammalian cells differ in the sterol composition of their membranes. Whereas mammalian cells produce cholesterol, yeasts produce ergosterol. Sterols, in general, play an important role in modulating the physicochemical properties of lipid bilayer by ordering the hydrocarbon tails of lipid molecules[180]. In the case of cholesterol, it is also understood to modulate the function of a number of membrane proteins, including GPCRs, either by specific molecular interactions between cholesterol and the membrane protein[181], or by altering the physical properties of the membrane[180,182]. The two sterols – cholesterol and ergosterol – have different effects on the lipid environment. For instance, ergosterol molecules demonstrate a greater ability to order saturated lipid chains, compared to cholesterol. The difference in lipid composition between the heterologous and native membrane environments may attenuate the stability and function of some GPCRs when expressed recombinantly[183].

P. pastoris differs from many of the other yeast expression systems in that it can metabolize methanol. The enzymes associated with this methanol metabolism, under the control of strongly regulated and highly inducible promoters, can constitute up to 80% of the cell's protein content. The exploitation of these methanol-inducible promoters, such as AOX1, allows the expression of large quantities of recombinant protein. The low constitutive level of expression under non-inducing conditions also improves the yield of proteins that may be toxic to the host cell, by preventing their expression until optimal cell density has been reached. *P. pastoris* has also proven amenable to medium and high cell fermentation (up to 500 g wet cell weight per liter) with its ability to grow up to extremely high cell densities, thereby facilitating the production of a large amount of cell material.

1.9.3 Crystallizing membrane proteins

Whereas the production of large quantities of a protein of interest is requisite for good structure results, it is no guarantee of success. In spite of the recent methodological advances, there is no easy route to a membrane protein structure. While NMR methods are useful for looking at isolated helices or loop regions[184-189], X-ray diffraction and electron microscopy are currently the only routes to obtaining high-resolution membrane protein structures.

When properly folded, GPCRs and other integral membrane proteins display hydrophilic surfaces exposed to the surrounding solution, and hydrophobic surfaces in contact

with the lipid bilayer. Their extraction from the membrane requires the use of amphipathic detergents, which possess polar head groups and hydrophobic tails. The detergent molecules serve to disrupt the lipid membrane and cover the hydrophobic surfaces of the protein in a detergent micelle. The presence of lipids within these detergent micelles acts to stabilize the interactions. Indeed, the addition of cholesterol or cholesteryl hemisuccinate (CHS) has been shown to drastically improve the stability of some mammalian GPCRs in detergent micelles[190,191], while binding experiments also show increased activity.

Crystal formation depends largely on the regular association of protein molecules in three dimensions. Membrane proteins generally can form two types of crystal packing[192,193]. Type I represents stacks of two-dimensional (2D) crystals ordered in the third dimension via interactions of hydrophilic parts of membrane proteins (Fig. 1.8a). Type II crystals are composed of membrane proteins whose hydrophobic part is shielded by a detergent micelle, and all crystal contacts are formed through hydrophilic, solvent-exposed parts of protein molecules (Fig. 1.8b).

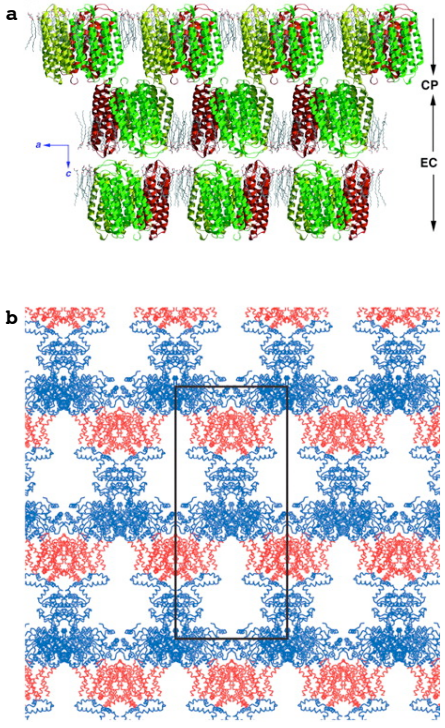

Figure 1.8. Packing arrangements of 3D membrane protein crystals that are used in X-ray crystallography. **a**, Type I: crystal packing of the trimeric halorhodopsin in a cubic monoolein-water-KCl phase. Crystal contacts in the *ab* plane are exclusively derived from protein-lipid-protein interactions, whereas direct protein-protein interactions occur only in the *c* direction, mainly by symmetric contacts involving loops and the C-termini of symmetry-related molecules. Lipids between halorhodopsin trimers were modeled as monoolein. Abbreviations: CP, cytoplasmic side; EC, extracellular side (Kolbe *et al.*, 2000) **b**, Type II: crystal lattice structure of the mammalian Kv1.2 channel in complex with an oxido-reductase β subunit showing integral membrane components (pore and voltage sensors) in red and extramembranous components (T1 domain and β subunit) in blue. A single unit cell is outlined in black. (Long *et al.*, 2005)

Apart from the addition of detergents, type II membrane protein crystals are growing using the same precipitants and techniques applied to the crystallisation of soluble proteins. However, the addition of detergents has two impeding effects. The first is that detergent-solubilized membrane proteins generally have relatively small areas available for

protein-protein contacts, due to the association of the detergent micelle to the hydrophobic regions. One technique developed to address this issue is the production of artificial binders in the form of Fab or single-chain Fv fragments, to bind and to extend the hydrophilic regions of membrane proteins. This technique was initially developed by Michel and colleagues to solve the structure of *Parococcus denitrificans* cytochrome *c* oxidase[194,195]. Antibody fragment-mediated crystallization has since proven its value with yeast cytochrome bc_1 complex[196], the potassium channels KscA[197] (Fig. 1.9a) and KvAP[198], the chloride channel ClC[199] and, more recently, the human β_2-adrenoreceptor[4] (Fig. 1.9b). However, this method is limited by the difficulties and expense associated with producing monoclonal antibodies to an appropriate exposed epitope on the target protein*. The second impeding influence from the use of detergents is the requirement that the detergent micelle must fit perfectly in the solvent gaps between the protein molecules of the crystal lattice. Since the size of this space is unknown before solving the structure, the detergent is found by trail and error.

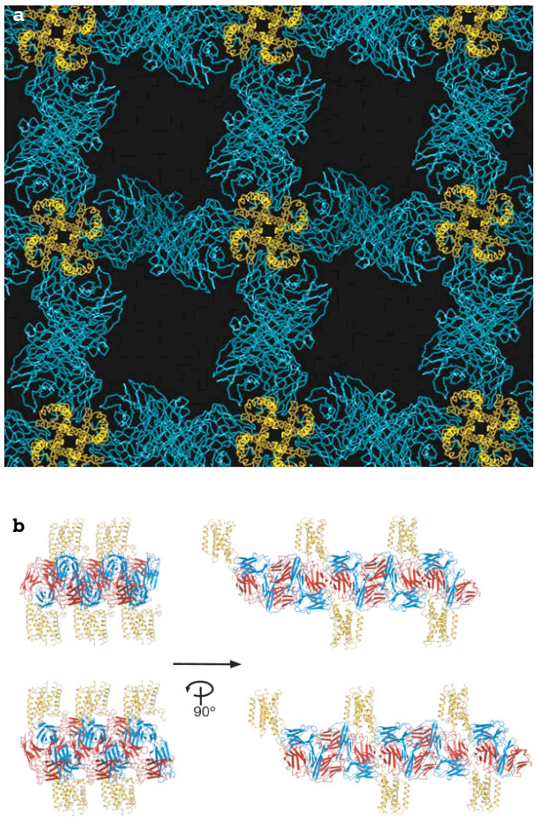

Figure 1.9. Fab attachment and crystal packing. **a**, KcsA (yellow) was crystallized as a complex with an antibody Fab fragment (blue). One Fab fragment is bound to the extracellular-facing turret on each K^+ channel subunit. View down the four-fold crystallographic axis of the *I*4 cell, which corresponds to the molecular four-fold axis of the K^+ channel. (Zhou *et al.*, 2001) **b**, β_2AR (gold) was crystallized in a lipid environment when bound to an inverse agonist (carazolol) and in complex with a Fab (heavy chain, blue; light chain, red) that binds to the third intracellular loop. (Rasmussen *et al.*, 2007)

* One possible solution to overcome these obstacles is to use monoclonal antibodies with known peptide-binding epitopes[200,201]. This can allow systematic engineered introduction of the required motif at optimal locations within the target membrane protein, chosen based on available knowledge concerning the membrane protein under investigation, so as to minimize the potential for deformation of the structure.

In general, crystallization trials for type II membrane protein crystals involve the screening of many crystallization conditions to find a promising starting point for optimization. This has been facilitated by the use of 96-well sitting-drop screens, which utilize nanolitre volumes of protein sample, thereby decreasing sample wastage. Once a promising starting condition has been established, optimization is performed by screening of various parameters, including the identity and concentration of salt, detergents, and precipitants used, as well as the inclusion of additives available, in the form of commercial additive screens, or by the addition of small amounts of lipids or detergent of a different identity to modify the detergent micelle composition and size. Often, shrinking the detergent micelle by using detergents with shorter hydrophobic tails can both increase the tendency for a protein to crystallize. The crystallization of cytochrome bo_3 ubiquinol oxidase[202] was only possible when octyl-glucoside was used instead of DDM. Additionally, the inclusion of small amphiphiles such as heptane triol or butane diol, can aid in the shrinking of the micelle. However, in general, due to the large solvent content, loose crystal packing, and the presence of the detergent micelle, membrane protein crystals tend not to diffract as well as soluble proteins.

A new approach to efficiently generating well-ordered type I 3D crystals, the lipidic-cubic phase method, has been extremely successful in providing crystals of bacteriorhodopsin (bR) in the ground and intermediate states[123,203-205]. The lipidic-cubic phase is a special 3D arrangement of lipids that form a continuous curved bilayer with a cubic structure, between which aqueous solutions can move (Fig. 1.10a). Membrane proteins can be incorporated into this bilayer and diffuse freely within it. The basic premise behind this method is that membrane proteins should crystallize more readily in a lipid bilayer than in a nonbilayer environment, provided that they can retain their native properties. One of the drawbacks of this approach is that, despite being a more natural environment for membrane proteins, conditions for crystal formation must be determined empirically for each protein (as is the case for other detergent/lipid-based methods). Ehud Landau (Galveston, TX, USA) was very successful in obtaining highly ordered crystals of bacteriorhodopsin using this approach[123]. Less ordered crystals were also obtained for several other membrane proteins with different structural characteristics – two photosynthetic reaction centers from *Rhodopseudomonas viridis* (RCvir) and *Rhodobacter sphaeroides* (RCsph), the light harvesting complex 2 (LH2) from *Rhodopseudomonas acidophila*, halorhodopsin (hR) from *Halobacterium salinarum*[126,206,207] – and in last November, Ray Stevens and colleagues published in *Science*[2,3] the lipidic cubic phase crystal structure of the human β_2AR adrenaline

receptor. By setting up an automated, nanovolume cholesterol-doped monoolein cubic phase, they were able to produce crystals of an engineered β_2AR-T4L fusion protein that diffracted to a resolution of 2.2 Å (Fig. 1.10b and 1.11). The successful diffraction screening and data collection that led to this structure determination required overcoming a number of technological barriers that encompassed the growth and harvest of microcrystals, crystal imaging, and collection of diffraction data. Indeed, because of their transparency, β_2AR-T4L crystals were often visually obstructed by the frozen lipidic mesophase material and therefore could not be confidently imaged by traditional beamline cameras; moreover, owing to the extremely small size and radiation sensitivity of these crystals, data collection required the use of microbeam technology in which X-ray beams are focused and then further collimated to diameters between 5 and 10 μm[208,209]. It remains now to be seen whether non-engineered GPCRs can be crystallized in these lipid bicontinuous cubic phases.

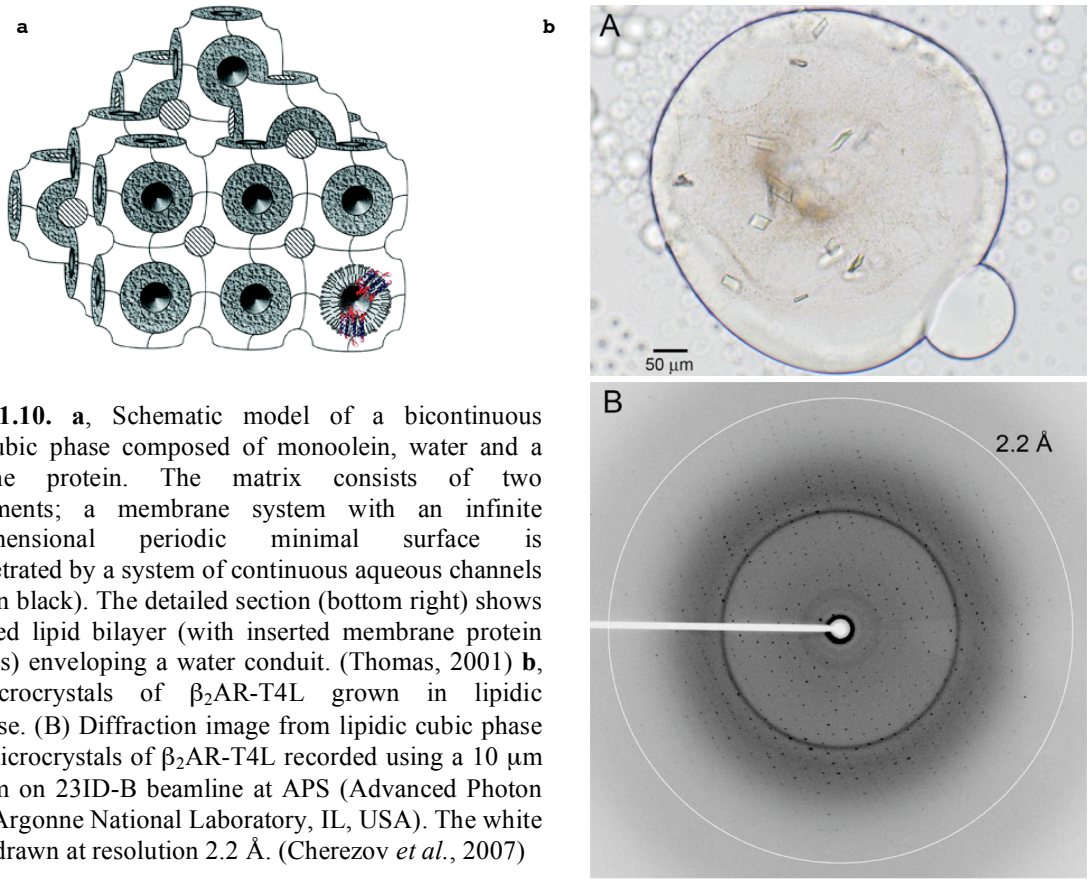

Figure 1.10. a, Schematic model of a bicontinuous lipidic-cubic phase composed of monoolein, water and a membrane protein. The matrix consists of two compartments; a membrane system with an infinite three-dimensional periodic minimal surface is interpenetrated by a system of continuous aqueous channels (shown in black). The detailed section (bottom right) shows the curved lipid bilayer (with inserted membrane protein molecules) enveloping a water conduit. (Thomas, 2001) **b**, (A) Microcrystals of β_2AR-T4L grown in lipidic mesophase. (B) Diffraction image from lipidic cubic phase grown microcrystals of β_2AR-T4L recorded using a 10 μm minibeam on 23ID-B beamline at APS (Advanced Photon Source, Argonne National Laboratory, IL, USA). The white circle is drawn at resolution 2.2 Å. (Cherezov *et al.*, 2007)

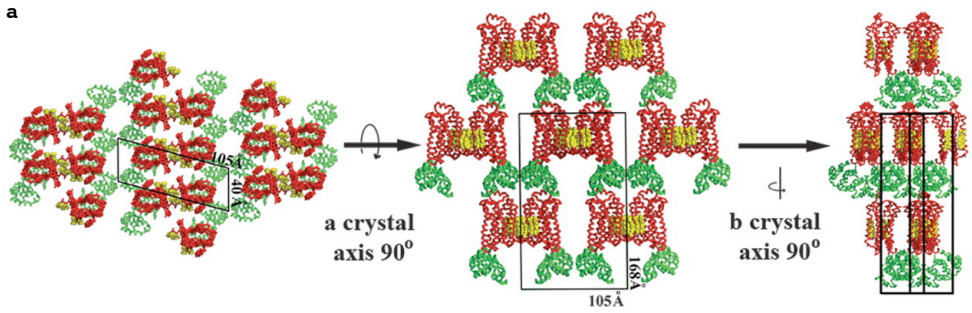

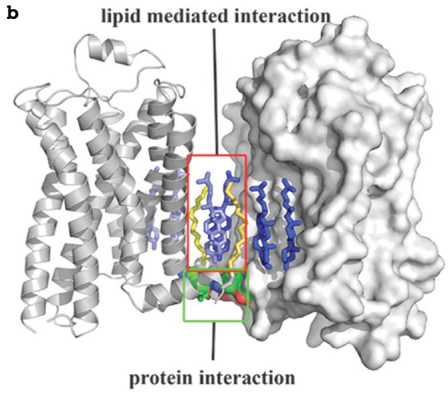

Figure 1.11. Crystal-packing interactions in the lipidic mesophase-crystallized β_2AR-T4L. **a**, There are four main contact areas, two of which are mediated by T4L in the plane of the membrane with itself through a two-fold symmetry axis and translation. The third interaction is normal to the membrane plane between T4L and lumen-exposed loops of β_2AR. The fourth interaction is generated by the two-fold symmetry axis, packing one receptor to another in the plane of the membrane. **b**, The receptor crystal-packing interface is composed mainly of lipids, with two cholesterol molecules and two palmitic acid molecules forming the majority of the interactions. A network of ionic charge interactions exists on the cytoplasmic end of the interface, forming the only interreceptor protein contacts. (Cherezov *et al.*, 2007)

Electron crystallography of two-dimensional (2D) crystals is a powerful alternative to X-ray crystallography. Werner Kühlbrandt (Frankfurt, Germany) stressed the advantages of using 2D crystals; only relatively small quantities of starting material are required for such studies (an important consideration for membrane proteins), and these kinds of crystals form relatively easily compared to those needed for 3D methods. Unfortunately, obtaining the large flat crystals that are required for cryo-electron microscopy (cryo-EM) is very difficult and labour-intensive. Also the highest resolution ever achieved by this method is much lower (1.9 versus 1 Å), probably because of the less rigid structure of the 2D lattice compared to the 3D lattice. However, the method does work, as exemplified by the recent solution of the structure of the lens-specific aquaporin-0 (AQP0)[210]. In this case, 3D information was obtained from 2D crystals by recording a series of cryo-EM images with the crystals progressively tilted away from the horizontal. This method resolved the structure of the protein to 1.9 Å (Fig. 1.12). The real advantage with 2D crystals is that one can probably do more with them en-route to a high-resolution structure (i.e. collect data for a projection map and study the surface topology using atomic force microscopy), which makes it slightly safer when commencing a project solely aimed towards producing a structure. Ideally though, 2D and 3D methods should be used in combination.

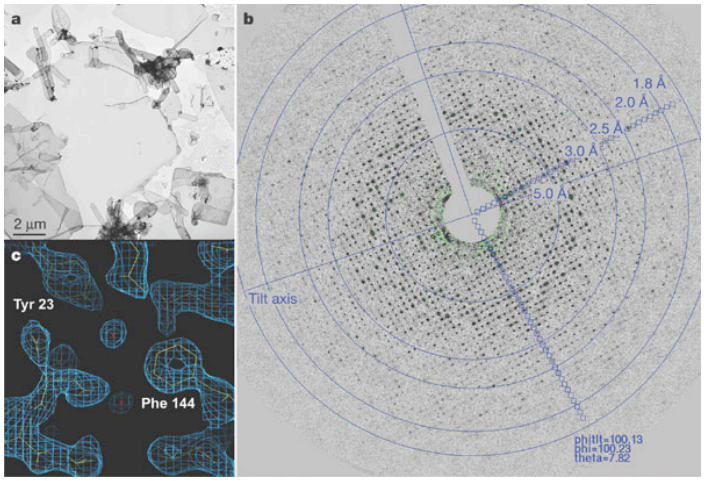

Figure 1.12. Electron crystallography of AOP0 junctions. **a**, Double-layered AQP0 2D crystals (several micrometres in size). **b**, A typical electron diffraction pattern recorded from an untilted AQP0 2D crystal prepared by the carbon sandwich technique (Gyobu *et al.*, 2004), showing diffraction spots to a resolution beyond 2 Å. **c**, Region of the final $2F_o$ - F_c map of AQP0 refined to 1.9 Å resolution. Two aromatic residues, Tyr 23 and Phe 144, that line the water pore in AQP0 are represented by doughnut-shaped densities. (Gonen *et al.*, 2005)

1.10 MePNet initiative

In light of the pressing need to obtain the structures of more GPCRs, many international consortia have been formed to address the issues hindering progress in this field[211]. The Membrane Protein Network (MePNet) is one such European collaboration. By applying a high-throughput approach to a large number of GPCR targets, it is hoped that a few will progress to producing well-diffracting crystals sufficient for structural studies. Within MePNet, more than 100 mammalian GPCRs have been subjected to overexpression in bacterial, yeast and mammalian cells, followed by purification and crystallization studies[5]. The 20-30 best expressing clones have since been isolated and are now undergoing further optimisation. Amongst many others, examples of targets under investigation include the human dopamine, α-adrenergic and cannabinoid receptors.

1.10.1 Human dopamine receptors

Dopamine (Fig. 1.13) is a key neurotransmitter that is important for many physiological functions including motor control, mood, and the reward pathway. Many of these functions are integrated by the medium spiny neurons of the striatum, which lie below the cortex in the brain and respond to dopamine. Dopamine exerts its effects on neurons through five known subtypes of dopamine receptors (DRs) (D_1, D_2, D_3, D_4, and D_5). The DRs may be subdivided based on their pharmacological behavior into the D_1-like and the D_2-like

subfamilies*. When dopamine binds to $G_s\alpha$-coupled D_1-like receptors (D_1 and D_5), the enzyme adenylate cyclase is activated and the secondary messenger cAMP is produced. In contrast, when dopamine binds to the $G_{i/o}\alpha$-coupled D_2-like receptors (D_2, D_3, and D_4), adenylate cyclase activity is blocked and cAMP production is reduced[221]. Neurons in the midbrain project their axons to the striatum and release dopamine, which modulates cAMP production by activating D_1 and D_2 receptors expressed by striatal neurons. These receptors work antagonistically to modulate synthesis of cAMP. Moreover, D_2 receptors have been shown to activate a large diversity of second messenger pathways, including stimulation of phospholipase C[222], potentiation of arachidonic acid release[223], regulation of K^+ and Ca^{2+} channels activity[224,225], as well as modulation of the activity of the Na^+/H^+ exchanger [226].

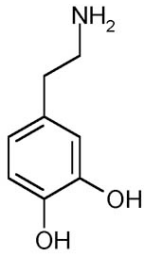

Figure 1.13. Dopamine

Communication in the dopamine system is particularly important because a variety of neurological and neuropsychiatric disorders, including schizophrenia, attention deficit, hyperactivity disorder, Tourette syndrome, obsessive-compulsive disorder, Parkinson's disease, Huntington's disease, and drug addiction, result from impaired dopamine receptor signalling. Many of the drugs used to treat these disorders target dopamine receptors. For example, D_2 antagonists such as haloperidol and risperidone are effective at reducing psychosis while piribedil, a D_2/D_3 agonist, is used as monotherapy in the treatment of Parkinson's disease.

The first three-dimensional models of the dopamine receptors have been created based on the structure of bacteriorhodopsin[227-229] and on a low resolution structure of

* The D_1-like receptors have short third intracellular loops and long carboxyl terminal tails whereas the D_2-like receptors have long third intracellular loops and short carboxyl terminal tails. This provides a structural basis for the division of the receptors into two subfamilies but is also likely to have a functional significance possibly related to the specificity of receptor/G protein interaction. Indeed, the third intracellular loop of these receptors is thought to be important for the interaction of receptor and G protein and for the D_2-like receptors, variants of these subtypes exist based on this loop. For example, there are short and long variants of the D_2 and D_3 receptors with the long forms having an insertion (29 amino acids for the D_2) in this loop[212,213]. Polymorphic variants of the D_2 receptor have been described with single amino acid changes in this loop[214]. For the D_4 receptor there are polymorphic variants in the human population with different length insertions in this loop[215]. In some cases these D_2-like receptor variants may have differential abilities to couple to or activate G proteins[214,216,217] and may also exhibit slightly different pharmacological properties[218,219]. The variants of the D_4 receptor have not been found to exhibit any differences in the binding of ligands or in coupling to G proteins[220].

rhodopsin[230]. More recently, researchers from the University of Michigan and the University of Kansas used computational homology modeling techniques to determine a three-dimensional structure of the human dopamine D_3 receptor, a potential target for drug addiction, Parkinson's disease, and schizophrenia. They found potential ligands via computational pharmacophore and structure-based screening, several of which displayed substantial inhibition in a D_3 binding assay.

These models, combined with extensive characterization of the receptors by site-directed mutagenesis[230], have provided a limited amount of information about each dopamine receptor's ligand preferences and G protein specificities. A detailed understanding of the differences between the receptor subclasses, however, requires structural information at atomic resolution.

1.10.2 Human α_2-adrenoreceptors

Adrenoceptors (ARs) are located throughout the body on neuronal and non-neuronal tissues where they mediate a wide range of responses to the endogenous catecholamines noradrenaline and adrenaline (Fig. 1.14). Many adrenergic ligands are currently in widespread clinical use, and provide an effective therapy for hypertension and asthma. The adrenoreceptor family was first divided into two subtypes, the α- and β-adrenoreceptors as determined by pharmacological studies in isolated tissue[231]. A quarter of a century later, the α-adrenoreceptors were further subdivided based on their anatomical location, with α-adrenoreceptors located on peripheral sympathetic nerve terminals designated α_2-adrenoreceptors and those located post-synaptically designated α_1-adrenoreceptors[232].

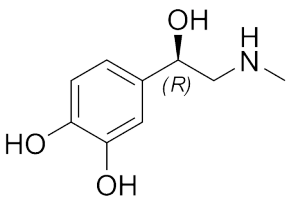

Figure 1.14. The isolation of adrenaline (right panel) – the first hormone to be obtained in its pure form and called "the blood-pressure-raising principle of the suprarenal glands" – was first reported in 1901. The work was done in a small independent laboratory run by Jokichi Takamine (left panel), a Japanese chemist who spent most of his adult life in the United States. His success in isolating adrenalin was a surprise to the scientific community, especially because his competitors included much better-known figures as John Jacob Abel of Johns Hopkins University and Otto von Fürth of Straßburg, Germany (now France).

Three human α_2-adrenoreceptor subtypes, designated by their chromosomal location α_2-C10, α_2-C2 and α_2-C4, have been cloned to date[233-235]. They are the pharmacologically defined subtypes α_{2A}, α_{2B}, and α_{2C}, respectively[236].

All three subtypes of α_2ARs appear to couple to the same signalling systems in the native target cells, which include inhibition of adenylate cyclase through coupling to pertussis toxin*-sensitive (PTX) $G_{i/o}$ proteins†, activation of receptor-operated K^+ channels, and inhibition of voltage-gated Ca^{2+} channels[238]. Reports of additional coupling mechanisms have been described in heterologous cell systems expressing cDNAs encoding α_2AR subtypes, which include coupling to mitogen-activated protein kinases (MAPKs)[239-242], phospholipase A_2[243], phospholipase C[244-246] and phospholipase D[247].

The α_2-adrenoreceptor subtypes play a pivotal role in a myriad of diverse cell functions and physiological actions, and hence have long been potential targets for drug development[248-251]. In the central nervous system (CNS) these receptors play an important role in regulating neurotransmitter release, and their importance in regulating the release of both noradrenaline and serotonine has resulted in the investigation and development of α_2-antagonists such as idazoxan for use in the treatment of depression. These receptors also mediate central cardiovascular responses and α_2-agonists such as clonidine induce hypotension and bradycardia[252]. Tizanidine, a structural analog of clonidine, is an effective muscle relaxant, useful in treatment of spasticity resulting from stroke, cerebral trauma or multiple sclerosis[253-255]. Guanfacine and gunanbez have been used in the therapy of withdrawal syndromes and as analgesics, in addition to lowering of blood pressure[248]. *p*-Aminoclonidine (apraclonidine) and brimonidine are used as eye drops to treat glaucoma; these drugs decrease the intraocular pressure by reducing aqueous humour production[256].Moreover, exploitation of the sedative properties of α_2-agonists, mediated by the somatodendritic autoreceptors on the *locus cereleus* has resulted in the development of veterinary sedatives and anesthetics such as dexmedetomidine, demotidine and xylazine. The α_2-agonists also have analgesic properties being mediated by the α_2-adrenoreceptors in the spinal cord. However, the currently available α_2-drugs cannot differentiate between the three subtypes, leading to major side effects. For instance, stimulation of α_2ARs by agonists decreases blood pressure and heart rate, thus limiting their use. New data, including ligand binding and structural insights, should enable design of subtype specific drugs and alleviate

* A compound that inhibits the guanine nucleotide binding proteins G_i and G_o via ADP-ribosylation.
† But stimulation of adenylate cyclase through coupling to $G\alpha_s$ proteins has also been reported[237].

the above-mentioned problems.

1.10.3 Human adenosine $A_{2(A)}$ receptors

Adenosine receptors are major targets of caffeine (Fig. 1.15b), the most commonly consumed drug in the world. There is growing evidence that they could also be promising therapeutic targets in a wide range of conditions, including cerebral and cardiac ischaemic diseases, sleep disorders, immune and inflammatory disorders and cancer.

Extracellular adenosine (Fig. 1.15a) acts as a local modulator with a generally cytoprotective function in the body[30]. Its effects on tissue protection and repair fall into four categories: increasing the ratio of oxygen supply to demand; protecting against ischaemic damage by cell conditioning; triggering anti-inflammatory responses; and the promotion of angiogenesis[257].

There are four known subtypes of adenosine receptors (ARs) – referred to as A_1, A_{2A}, A_{2B} and A_3 – each of which has a unique pharmacological profile, tissue distribution and effector coupling. Among the human ARs, the most similar are the A_1 and A_3 ARs (49% sequence similarity) and the A_{2A} and A_{2B} ARs (59% similarity).

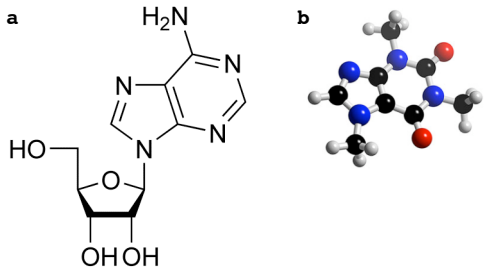

Figure 1.15. a, Adenosine. **b**, By virtue of its purine structure, caffeine is a competitive antagonist at adenosine receptors and produces a range of central and physiological effects that are opposite those of adenosine. Recently, caffeine has been shown to enhance dopaminergic activity, presumably by competitive antagonism at adenosine receptors that are co-localized and interact functionally with dopamine receptors. Thus, caffeine, as a competitive antagonist at adenosine receptors, may produce its behavioral effects by removing the negative modulatory effects of adenosine from dopamine receptors, thus stimulating dopaminergic activity.

Activation of the A_{2A}AR increases adenylate cyclase activity. G_s seems to be the major G protein associated with A_{2A}ARs in the peripheral systems but not in the striatum, where A_{2A}AR density is the highest. It has been shown that striatal A_{2A}ARs mediate their effects predominantly through activation of G_{olf}[258], which is similar to G_s and also couples to adenylate cyclase. In rat-tail arteries, facilitation of noradrenaline release by activation of the A_{2A}AR triggers the PLC and adenylate cyclase pathways[259]. Activation of the A_{2A}AR also induces formation of inositol phosphates to raise intracellular calcium and activate protein

kinase C in COS-7 cells via pertussis toxin-insensitive $G\alpha_{15}$ and $G\alpha_{16}$ proteins[260], which have limited tissue distribution and interact with most GPCRs.

The $A_{2A}AR$ is involved in vasodilation in the aorta and coronary artery[30]. It was suggested that the tachycardic effect of $A_{2A}AR$ activation is mediated by centrally located receptors, whereas its hypotensive effect is mediated by the peripheral $A_{2A}AR$[261]. In the late 1960s and 1970s, metabolically stable AR agonists were tested clinically as antihypertensives, and this was an intended use of the $A_{2A}AR$ agonist CGS21680. However, its clinical path was curtailed following canine haemodynamic studies due to *in vivo* non-selectivity related to spare receptors. In platelets, an $A_{2A}AR$ agonist was shown to inhibit aggregation by increasing intra-cellular cAMP levels, suggesting that adenosine agonists might have utility as antithrombotic agents[262]. Recently, there has been an effort to further improve subtype-selectivity of $A_{2A}AR$ agonists for novel therapeutic applications, including imaging. Adenosine, under the name Adenoscan® (Astellas Pharma), is used in myocardial stress imaging to evaluate coronary artery disease by achieving vasodilation in patients unable to exercise adequately. Regadenoson (CVT-3146), a potent and selective $A_{2A}AR$ agonist, is being evaluated in Phase III studies for the same purpose during myocardial perfusion imaging[263]. The selective $A_{2A}AR$ agonist binodenoson (WRC-0470) has entered Phase III clinical trials and seems to be well tolerated as a short-lived coronary vasodilator and acts as an adjunct to radiotracers in imaging[264]. ATL-146e, the most selective of these $A_{2A}AR$ agonists, has also entered Phase III clinical trials for coronary imaging.

1.10.4 Human cannabinoid receptors

Cannabinoid receptors (CBs) are the primary targets of the psychoactive components of marijuana (*Cannabis sativa)*, such as *trans*-Δ^9-tetrahydrocannabinol (Δ^9-THC) (Fig. 1.16), as well as endogenous cannabinoid-like compounds, such as *N*-arachidonoylethanolamine (anandamide)[265] and 2-arachidonylglycerol[266]. To date, two subtypes of the human cannabinoid receptor, CB_1 and CB_2, have been identified, and their cDNA has been cloned in the early 1990s[267,268]. Despite the high homology in their amino acid sequence [44% sequence identity overall and 68% in the transmembrane regions], they possess different pharmacological profiles. CB_1 mediates the psychoactive effects of marijuana in the CNS, but is also present in peripheral tissues[269]. In contrast, CB_2 is localized primarily in cellular tissues within the immune system, including the marginal zone of the spleen, and therefore contributes to the development and modulation of the immune system cytokine network[270].

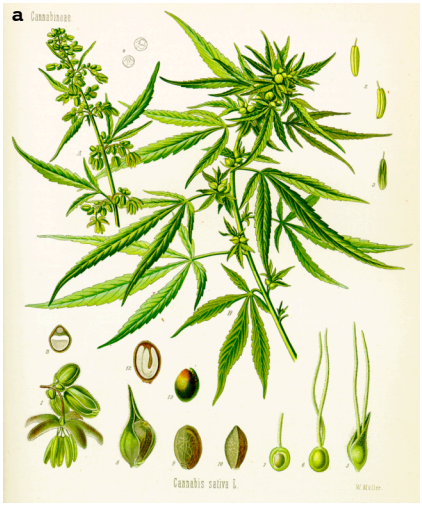

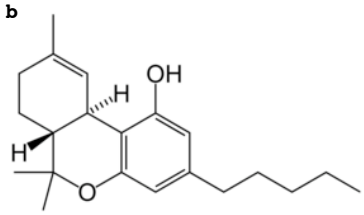

Figure 1.16. **a**, *Cannabis sativa*, scientific drawing published in Franz Eugen Koehler, *Koehlers Medizinal-Pflanzen in naturgetreuen Abbildungen und kurz erläuterndem Texte*, Gera, Germany, 1883-1914. **b**, *trans*-Δ^9-tetrahydrocannabinol (Δ^9-THC)

Biochemical characterization of the signal transduction of CB_1 and CB_2 expressed in cultured cells has suggested that the activation of both receptors results in the inhibition of cAMP accumulation[271,272]. This coincides with the notion that functional coupling to the inhibitory G protein (G_i) is one of the major signalling pathways for cannabinoid receptors[273]. CB_1 has also been shown to mediate the inhibition of presynaptic N- and P/Q-type Ca^{2+} channels in neuroblastoma cells[274], and the activation of inwardly rectifying K^+ channels in AtT-20 cells[275]. These effects were not observed in AtT-20 cells transfected with CB_2[271]. This suggests that CB_1 and CB_2 functionally couple to other effector systems that are independent of G_i and are not shared between the two subtypes.

Endogenous cannabinoids (endocannabinoids) most probably have both neuromodulatory and immunomodulatory roles that include inhibition of ongoing transmitter release through retrograde signalling[276], as well as regulation of cytokine release and immune cell migration[277,278]. It is also now generally accepted that there are certain disorders in which endocannabinoid release increases in particular tissues**;** this upregulation of the endocannabinoid system leads in some cases to suppression of unwanted signs and symptoms and is therefore "autoprotective". In other cases, this same upregulation can lead to the production of undesirable effects[279]. For example, there is evidence that endocannabinoid release ameliorates spasticity in multiple sclerosis and inflammatory pain on one hand, but contributes to obesity in some individuals or impairs fertility in certain woman on the other hand. As a result, there is enormous interest, not only in directly acting upon cannabinoid receptor agonists and antagonists, but also in compounds that can affect the activity of the endocannabinoid system indirectly by allosterically modulating endocannabinoid-induced activation of cannabinoid receptors.

1.10.5 Human opioid receptors

It is now clear from work carried out in many laboratories over the last twenty years that there are three well defined or "classical" types of opioid receptors, designated μ, δ and κ. Genes coding for these receptors have been cloned[280-282]. Opioid receptors mediate the effects of endogenous opioid peptides in the central, peripheral and enteric nervous systems. The μ-opioid receptor is also the molecular target of opioid drugs – made from the opium poppy *Papaver somniferum L.*[*] – such as morphine, heroin, fentanyl and methadone (Figure 1.17)[283]. Knockout mice lacking a functional μ-opioid receptor do not display analgesia, tolerance or physical dependence to opioid drugs[284].

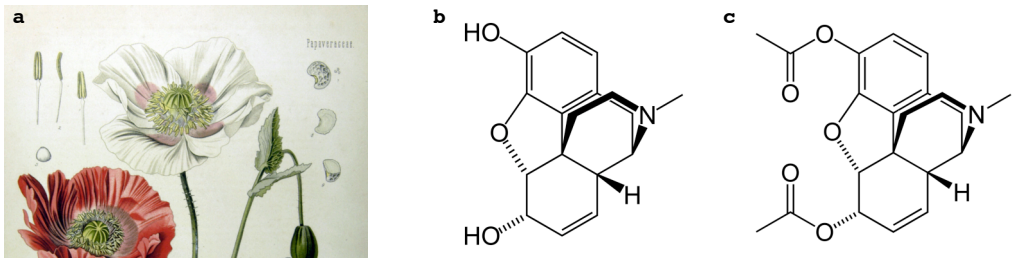

Figure 1.17. **a**, *Papaver somniferum L.*, scientific drawing published in Franz Eugen Koehler, *Koehlers Medizinal-Pflanzen in naturgetreuen Abbildungen und kurz erläuterndem Texte*, Gera, Germany, 1883-1914. **b**, Morphine. **c**, Heroin.

The opioid receptor family is somewhat unusual in that all of the cloned opioid receptor types belong to the G_i/G_o-coupled superfamily of receptors. Opioid receptors do not couple directly with G_s and G_q and none of the cloned receptors forms a ligand-gated ion channel. It was originally thought that μ- and δ-receptors coupled through G_i/G_o proteins to activate an inwardly rectifying K^+ conductance and to inhibit voltage-operated Ca^{2+} conductances whereas κ-receptors only inhibit voltage-operated Ca^{2+} conductances. However, it is now known that the κ-receptor is, in some cell types, also coupled to activation of an inwardly rectifying K^+ conductance[285]. It seems highly likely, therefore, that all of the opioid receptors will share common effector mechanisms.

[*] Preparations of the opium poppy *Papaver somniferum L.* have been used for many hundreds of years to relieve pain. In 1803, Sertürner isolated a crystalline sample of the main constituent alkaloid, morphine, which was later shown to be almost entirely responsible for the analgesic activity of crude opium. The rigid structural and stereochemical requirements essential for the analgesic actions of morphine and related opioids led to the theory that they produce their effects by interacting with a specific receptor.

Among the receptors for the many neuropeptides that exist in the nervous system, the opioid receptors are unique in that there existed before the discovery of the natural agonists, an abundance of non-peptide ligands with which the pharmacology of the receptors was already defined. In current terms relating to the drug-discovery process, I would consider the 4,5-epoxy-methylmorphinan opioid alkaloids morphine, codeine and thebaine as "natural-product hits" on which were based chemical programmes to design analogues with improved pharmacology. The effect of morphine to reduce sensitivity to pain or to inhibit intestinal motility and secretion, have continued to be exploited clinically, however the presence of other undesirable effects (e.g. depression of respiration, tolerance/dependence, effects on mood) provided the stimulus to seek analogues that were selective in producing analgesia. Thus a semi-synthetic diacetylated analogue of morphine was introduced in the 19th century in the mistaken belief that this compound (heroin) had those desired properties (Fig. 17b and c). More radical changes to the morphinan nucleus were subsequently explored in various synthetic programmes, in many early cases resulting in the development of low efficacy partial agonist.

1.10.6 Human tachykinin receptors

The tachykinins were first identified in 1931[286]. However, realization of the therapeutic potential of antagonists that block their action has only taken place over the last decade. Tachykinin receptor antagonists have been implicated in various conditions such as depression/anxiety, pain, airway disease, incontinence, nausea and bowel disorders. The tachykinins are the products of two genes, preprotachykinin I which produces substance P (SP) and neurokinin (NK)A and preprotachykinin II which produces NKB*. In 1986 the research community classified the tachykinin receptors – also called neurokinin receptors (NKRs) – into 3 subtypes, NK_1, NK_2 and NK_3 receptors. They have been further identified in the 1990s by cloning and molecular characterization, and correlated with preferential binding to SP, NKA and NKB, respectively[288-290]. Their extracellular N-terminus and extracellular loops 2 and 3 display considerable variation across species, whereas transmembrane regions II and VII and cytoplasmic loop 1 are highly conserved.

It is now well established that tachykinins activate NKRs by coupling to G_q/G_{11} proteins, leading to PLC activation, inositol 1,4,5-triphosphate (I_3) formation and an

* Tachykinin peptides are characterized by a conserved carboxy-terminal pentapeptide amide consisting of -Phe-X-Gly-Leu-Met-NH_2, where X is either an aromatic residue (Phe or Tyr for SP) or a branched aliphatic residue (Val or Ile for NKA and NKB)[287]. Most tachykinins are deca- or undecapeptides but their lengths range between 9 and 42 amino acid residues.

increase in intracellular calcium. In certain systems, stimulation of cyclic AMP (cAMP) production via $G_s\alpha$ is an alternate signalling transduction pathway[291].

One of the earliest examples of advanced development of the tachykinin antagonist class was in the field of depression and anxiety following pioneering work in a number of laboratories and especially those of Merck & Co. Both the limbic system and the mesencephalic brain stem express high levels of SP-like immunoreactivity supporting their role in anxiety and depression. This is further evidenced by the anxiogenic effect of NK_1 or NK_2 agonists when administered into the CNS and the observation that SP levels are altered in experimental models of stress, anxiety and depression. On the basis of this data first generation NK_1 receptor antagonists such as CP96345 were investigated for anxiolytic activity. Of groundbreaking importance, MK-869 (aprepitant) became the first NK_1 antagonist to demonstrate therapeutic activity in patients with a cohort of depressed patients displaying significant improvement in both the level of depression and anxiety[292]. In addition, recent evidence suggests the clinical efficacy of two distinct NK_3 receptor antagonists, osanetant and talnetant[293,294], for the treatment of schizophrenia.

Chapter 2

Aims and Scopes of this Thesis

The aim of this thesis was to over-express and to purify different GPCRs from the MePNet collection for structural studies.

Chapter 3 briefly presents the materials and general methods used throughout this work. It includes standard techniques for cloning and expression in *Pichia pastoris*, purification and crystallization methods, as well as radioligand binding techniques.

Chapter 4 deals with the expression of the human dopamine D_2 receptor in flask and medium-cell density fermentor cultures for the purpose of conducting purification trials. Special attention was put into improving the reproducibility of expression in terms of total and functional expression levels.

Chapter 5 investigates the amenability of the GPCR fusion constructs to various chromatographic purification strategies. We also assess the function of membrane-bound and detergent-solubilized receptors in terms of capacity to binding ligands. Finally, we introduce purified GPCRs in three-dimensional crystallization trials, after having checked their oligomerization state by dynamic light scattering and electronic microscopy.

In Chapter 6 and 7, we generated new fusion constructs, i.e. GPCR–Gα and OmpA–GPCR fusion proteins, with the hope of increasing stability and subsequent efficiency of purification.

Two (fairly) preliminary draft papers are presented in Chapters 4 and 6 while another one, presented in Chapter 5, was recently submitted to Protein Expression and Purification (Elsevier Publishing Group).

Chapter 3

Materials & Methods

3.1 Materials

Cf. Chapters 4, 5 & 6

3.2 Molecular Biology

3.2.1 DNAs and expression vectors

The different GPCR encoding genes were obtained from the MePNet collection [human serotonin $5HT_{1B}$ receptor (MePNet #2), human α_{2B}-adrenergic receptor (#16), rat α_{2C}-adrenergic receptor (#18), human adenosine A_{2A} receptor (#20), human cannabinoid receptor type-2 (#37), human dopamine D_2 receptor long isoform (#43), human neurokinin-1 and -3 receptors (#72, #76), rat neurokinin-2 receptor (#75), human neuropeptide Y receptor type-1 (#79), human delta- and kappa-opioid receptors (#83, #85) and mesau α_{1B}-adrenergic receptor (#105)]. The plasmidic DNAs coding for the G proteins alpha oA, alpha s long, alpha s short, alpha q and alpha q(Q209L) (constitutively active) were purchased from the UMR cDNA Resource Center (cat. Number #GN0OA0000, #GNA0SL0000, #GNA0SS0000, #GNA0Q00000 and #GNA0Q000C0, respectively). The plasmid pET3b-OmpA(1-171)-K107Y was a generous gift from Prof. Dr. Georg E. Schulz (Albert-Ludwigs-Universität Freiburg).

The GPCR ORFs were cloned either in a pCR4Blunt-TOPO plasmid (Invitrogen) or in a modified pPIC9K vector. This pPIC9K_MePNet2 expression vector was specifically engineered for the MePNet project[295,296], it bears the GPCR ORFs cloned in-frame downstream the pheromone α-preprosequence secretion signal from *Saccharomyces*

cerevisiae, a FLAG tag, a decahistidine tag and a TEV cleavage site, a second TEV cleavage site upstream the GPCR cloning site, a biotinylation domain of the transcarboxylase from *Propionibacterium Shermanii*[297] and the TAGTAG termination sequence.

The pPIC9KF vector was derived from the pPIC9K_MePNet2 vector in which the sequence of the biotinylation domain was replaced by a *Spe*I/*Afl*II cloning cassette.

The pPICZG expression vector was engineered from the pPICZ plasmid (Invitrogen) where the *Eco*RI/*Xho*I fragment was replaced by an insert bearing a c-Myc tag sequence followed by *Spe*I/*Afl*II cloning sites.

3.2.2 Manipulating DNA (modification, amplification and purification)

Standard restriction, modification and ligation procedures were applied according to the manufacturer's recommendations (Fermentas Life Sciences). When appropriate, PCR amplifications were performed in standard conditions using a PCR master mix containing specific primers (Sigma-Genosys) and a proofreading PrimeSTAR HS DNA polymerase from Takara. For DNA propagation, heat-chock transformation of a chemically competent *E. coli* TOP10 strain was carried out according to the protocol from Invitrogen and prepared following the instructions of the Nucleospin purification kit from Macherey-Nagel. DNA concentration was measured either semi-quantitatively by comparing the intensity of ethidium bromide fluorescence against that of commercially available DNA marker standards (GeneRuler™ 1kb DNA Ladder, Fermentas), or quantitatively, by measuring optical density values at 260 nm (OD_{260}) on a UV spectrophotometer (Pharmacia).

3.2.3 Cloning of the pPICZG-Gα vectors, pPIC9KF-GPCR:Gα and pPIC9K-OmpA:GPCR

The G protein alpha ORFs were PCR-amplified using specific primers with adapters introducing a unique *Spe*I and *Afl*II restriction sites at the 5' and 3' ends of the gene, respectively. The amplified DNAs were cloned into a pCR4Blunt TOPO vector and sequence checked. After enzymatic restriction, the *Spe*I/*Afl*II fragments were then subcloned into either the *Spe*I/*Afl*II cloning sites of the pPIC9KF-GPCR or pPICZG vectors resulting in the pPIC9KF-GPCR:Gα and pPICZG-Gα constructs (see Fig. 3.1 and Table 3.1 for the GPCR:Gα fusion combinations). Similarly, OmpA:GPCR fusions (see Fig. 3.1 and Table 3.2) were PCR-amplified and sequence checked before being introduced into the *Bam*HI/*Spe*I cloning sites of the pPIC9K_MePNet2 vector leading to the pPIC9K-OmpA:GPCR constructs.

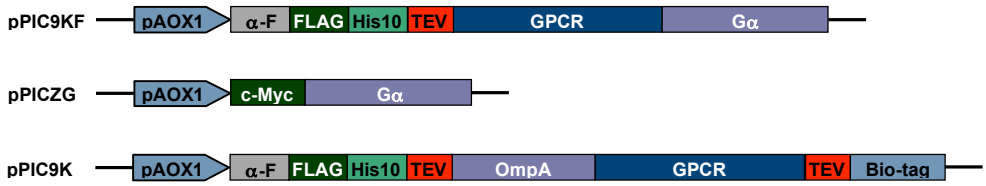

Figure 3.1. Schematic representation of the pPICZG-Gα, pPIC9KF-GPCR:Gα and pPIC9K-OmpA:GPCR expression vector constructs.

Receptor	Gα subunit	GPCR:Gα fusion protein
AA2AR_HUMAN	s long	AA2AR:$G_S\alpha_L$
AA2AR_HUMAN	s short	AA2AR:$G_S\alpha_S$
DRD2_HUMAN	oA	DRD2:$G_{oA}\alpha$
NK2R_RAT	q	NK2R:$G_q\alpha$
NK2R_RAT	q(Q209L)	NK2R:$G_{q(Q209L)}\alpha$

Table 3.1. GPCR:Gα fusion combinations

Receptor	OmpA	OmpA:GPCR fusion protein
DRD2_HUMAN	OmpA(1-171)-K107Y	OmpA:DRD2
CNR2_HUMAN	OmpA(1-171)-K107Y	OmpA:CNR2

Table 3.2. OmpA:GPCR fusion combinations

3.2.4 Transforming yeast strain SMD1163

Transformation of yeast cells was carried out according to the protocol in Higgins and Cregg[298] as documented below.

3.2.4.1 Preparing yeast competent cells

Competent cells were prepared from an overnight culture of SMD1163 (*his4*, *pep4*, *prb1*) (Invitrogen) in YPG medium [1% (w/v) yeast extract, 2% (w/v) peptone, 2% (w/v) glucose] grown at 30 °C. An aliquot was diluted in fresh medium and allowed to reach an OD_{600} ~1 after 2-4 generations. Cells were harvested and resuspended in 100 ml YPG supplemented with 165 mM Hepes pH 8.0 and 20 mM dithiothreitol (DTT), and incubated for 15 min at 30 °C. The cell suspension was transferred onto ice and completed to a final volume of 500 ml with ice-cold sterile deionized water. The cells were pelleted and washed with water, followed by 20 ml 1 M sorbitol and resuspended in 500 µl 1 M sorbitol.

3.2.4.2 Preparing DNA

10 μg of expression vector was linearized with 25 U of *Pme*I in 200 μl reaction volume for 2 h or overnight at 37 °C. Protein extraction was performed using 400 μl of ice-cold 1:1 phenol:chloroform. The sample was centrifuged at 14,000 *g* at room temperature. The aqueous phase was isolated and mixed thoroughly with 400 μl of chloroform then centrifuged again. The aqueous phase was collected by careful pipetting. DNA was precipitated by the addition of 1 ml 100% isopropanol supplemented with 50 μl 3 M sodium acetate pH 4.8. Samples were incubated at room temperature for an hour before being spun down at 14,000 *g* for 1 h at 4 °C. The DNA pellet was washed once with 100 μl 70% ethanol. The pellet was allowed to dry at room temperature before resuspending in 15 μl nuclease-free water.

3.2.4.3 Yeast electroporation

15 μl of linearized DNA was mixed with 40 or 80 μl of competent cells and allowed to incubate on ice for 1 h. The cell-DNA suspension was transferred to a pre-cooled electroporation cuvette. An electric pulse was applied across the cuvette in an electroporator (Eppendorf) with the following values: voltage 1500 V, capacitor 10 μF, resistor 600 Ω. Samples were immediately resuspended in 1 ml ice-cold 1 M sorbitol and allowed to recover for 1 h at 30 °C. Cells were pelleted and resuspended in 500 μl 1 M sorbitol. 2x250 μl was plated on MD plates [1.34% (w/v) yeast nitrogen base without amino acids, 2% (w/v) dextrose, 1.5% (w/v) agar] and incubated for 3 days at 30 °C to isolate histidine auxotrophs.

3.2.4.4 Geneticin resistance screening

His^+ recombinant clones were harvested from the MD plates and resuspended in 2 ml YPG. 10- to 1000-fold serial dilutions were set up and the OD_{600} values measured. 10^5 cells/plate (1 OD_{600} unit ~$5x10^7$ cells/ml) were plated on YPG plates supplemented with 0.1 and 0.25 mg/ml geneticin. Plates were incubated for 3 days at 30 °C.

3.2.4.5 Small-scale expression screening

8 colonies from each YPG plate (0.1 and 0.25 mg/ml geneticin) were used to inoculate 5 ml of BMGY each and incubated overnight at 30 °C. An aliquot from each culture was used to re-inoculate 10 ml of fresh BMGY (OD_{600} ~0.25). The cultures were incubated for a further 4-5 h at 30 °C (OD_{600} ~1) and centrifuged at 3,000 *g* for 10 min. The cell pellet was washed

with 40 ml of sterile deionized water and resuspended in 5 ml of BMMY. Cell cultures were incubated for 18 h at 30 °C.

The cells were collected by centrifugation and resuspended in ice-cold breaking buffer to a final volume of 500 µl. An equal volume of pre-cooled acid-washed glass beads (Sigma-Aldrich) was added to each cell suspension. The samples were vortexed at 1,000 rpm for 1 h. The glass beads and cell debris were removed by centrifugation at 3,000 *g* for 10 min. The glass beads were washed with 500 µl of breaking buffer and the supernatant fractions were pooled.

The pooled fraction was centrifuged at 100,000 *g* for 30 min and the membrane pellet was resuspended in binding buffer [50 mM Tris-HCl pH 7.4, 100 mM NaCl] and kept on ice for analysis (radioligand binding assay & Western-blot immunodetection).

3.3 Yeast culture (shake flask & bioreactor)

Cf. Chapters 4 & 5

3.4 Membrane preparation

Cf. Chapters 4, 5 & 6

3.5 Cholesterol enrichment of membranes

Cf. Chapter 6

3.6 *In vitro* biotinylation

Cf. Chapter 5

3.7 Colorimetric measurement of protein concentration

Samples were diluted either 10- or 100-fold to an approximate working range of 0.25-1.5 mg/ml. The BCA assay was used according to the manufacturer's instructions to estimate protein concentration. Briefly, 2 ml of working reagent was added to 100 µl of each sample and incubated for 30 min in a 60 °C water bath. BSA was diluted in deionized water to plot a standard curve with point values, 0, 0.025, 0.125, 0.25, 0.5, 0.75, 1.0, 1.5 and 2.0 mg/ml. Following incubation, samples were allowed to cool to room temperature before measuring absorbance at 562 nm.

3.8 SDS-PAGE, Western-blotting and immunodetection

Protein samples were diluted in NuPAGE LDS sample buffer (Invitrogen) before running on a NuPAGE 4-12% gradient Bis-Tris gel with MES buffer (Invitrogen). Purified receptor was either stained with Coomassie brillant blue G-250 (Serva) or silver nitrate while *Pichia* membranes (*ca.* 10 μg) were electrophoretically transferred overnight for Western-blot analysis onto a nitrocellulose filter following the standard procedure[299]. Briefly, after electroblotting at the constant current of 30 mA per gel in transfer buffer (2.5 mM Tris, 19 mM glycine, 0.02% SDS, 20% methanol), the membrane was blocked with 8% lowfat milk powder in PBST [10 mM Na_2HPO_4, 1.8 mM K_2HPO_4, pH 7.4, 140 mM NaCl, 2.7 mM KCl, 0.02% Tween 80, (w/v) 1% BSA] for 1 h at room temperature and washed three times for 5 min with PBST. Further, membrane was incubated with either M2 anti-FLAG antibody (diluted 1:8,000 in PBST) or anti-c-Myc antibody (diluted 1:600 in PBST), washed again three times for 5 min with PBST, and incubated with sheep anti-mouse IgG-HRP conjugated antibody (diluted 1:10,000 in PBST). The immunoblot bands were visualized using an enhanced chemiluminescence reagant (SuperSignal West Pico Kit, Pierce) according to the manufacturer's protocol. Alkaline phosphatase-linked streptavidin was also used with a precipitating substrate, BCIP/NBT (5-bromo-4-chloro-3-indolyl phosphate/nitroblue tetrazolium), to detect C-terminal biotinylation (Bio-tag) of recombinant receptors.

3.9 Dot-blot immunodetection

Dot-blot assays were performed in a 96-well plate format using a Bio-Dot microfiltration system (Bio-Rad), as previously described[300]. Briefly, *Pichia* membranes (*ca.* 1 μg) were diluted in 100 μl of Laemmli buffer and absorbed onto a PVDF membrane by gravity-flow. The filter was then washed three times with 200 μl of PBS per well by applying a constant vacuum flow. Dot-blots were then treated in the same way as Western transfers for receptor detection.

3.10 Radioligand binding assays – membrane-bound & purified receptors

Receptor	Radioligand	Cold ligand (conc.)	Binding Buffer
ADA2B_HUMAN	[^{3}H]rauwolscine	yohimbine (100 μM)	50 mM Tris (pH 7.4), 5 mM $MgCl_2$, 1 mM EDTA, 0.1% BSA
AA2AR_HUMAN	[^{3}H]ZM241385	ZM241385 (10 μM)	50 mM Tris (pH 7.4), 5 mM $MgCl_2$, 1 mM EDTA, 0.1% BSA
CNR2_HUMAN	[^{3}H]CP55940	CP55940 (50 μM)	50 mM Tris (pH 7.4), 5 mM $MgCl_2$, 1 mM EDTA, 0.1% BSA
DRD2_HUMAN	[^{3}H]spiperone	(+)-butaclamol (10 μM)	25 mM Hepes (pH 7.4), 200 mM NaCl, 1 mM EDTA, 0.1% BSA
NK2R_RAT	[^{3}H]SR48968	SR48968 (100 μM)	25 mM Hepes (pH 7.4), 200 mM NaCl, 1 mM EDTA, 0.1% BSA

Table 3.3. Radioligand binding conditions for GPCRs expressed in *P. pastoris*.

Single-point and saturation binding assays were conducted as previously described[295]. The binding conditions used are summarized in Table 3.3. In each case, either 10 μg of membrane protein or 0.01-0.1 μg of purified receptor was used per 200 μl reaction, and the radioligand was used at ≥10x its theoretical *Kd* (dissociation constant). The binding reaction was allowed to reach equilibrium by incubation at 25 °C for 2 h. The reaction was terminated by rapid filtration either through GF/B Whatman filter paper presoaked in 0.3% polyethylenimine (Sigma-Aldrich) using a Brandel cell harvester, or 96-well UniFilter GF/B plates (Perkin Elmer) using a vacuum manifold (Millipore). Filters were washed with 3x5 ml ice-cold 50 mM Tris-HCl pH 7.4 and incubated with Ultima Gold MV scintillation fluid (Perkin Elmer) overnight. The LS 6500 (Beckman Coulter) and TopCount NXT (Perkin Elmer) systems were used to analyse samples prepared with the Brandel and Millipore filtration units, respectively.

3.11 [^{35}S]GTPγS binding assays

Cf. Chapter 6

3.12 Purification

Unless otherwise stated, all steps were performed at 4 °C.

3.12.1 Solubilization

The membrane suspension was diluted in solubilization buffer [50 mM Hepes-NaOH pH 7.4, 500 mM NaCl, 20% (w/v) glycerol, ligand, complete EDTA-free protease inhibitor cocktail (PI) tablets] supplemented with either 1% (w/v) n-dodecyl-β-D-maltopyranoside (DDM) or n-decyl-β-D-maltopyranoside (DM) to a final protein concentration of 1-5 mg/ml. In some cases, cholesteryl hemisuccinate (CHS) was added to a final concentration of 0.1%-0.2% (w/v). The suspension was incubated for 1 h with stirring followed by centrifugation at 100,000 *g* for 1 h to pellet insolubilized material.

3.12.2 Immobilized metal affinity chromatography

Binding, wash and elution steps were carried out in batch. 1 ml TALON resin (Clontech) per 100 mg of membrane protein was added to the crude protein solution and imidazole (5 M stock solution, pH 7.5) was supplemented to a final concentration of 20 mM. The suspension was incubated for ≥3 h with stirring before centrifugation at 1,500 *g* for

5 min. The supernatant (flow-through) was collected and the resin was washed with ≥30 resin bed volume (CV) of purification buffer [50 mM Hepes-NaOH pH 7.4, 250 mM NaCl, 0.05% DDM, 10% (w/v) glycerol, ligand, PI] supplemented with 20 mM imidazole. Bound protein was eluted with 3-5 washes of 1 resin bed volume of purification buffer supplemented with 300 mM imidazole. In some cases, CHS was included in the purification buffer at a concentration of 0.01% (w/v).

For subsequent purification steps, where noted, elution samples were pooled and buffer exchanged ≥1,000-fold with an appropriate buffer in a stirred cell pressure concentrator with a 50 kDa MWCO (Millipore).

3.12.3 Immobilized monomeric avidin affinity chromatography

Purification was carried out at room temperature to improve the kinetics of binding and elution. Pooled IMAC elution fraction was exchanged with avidin column buffer [20 mM Tris-HCl pH 8.0, 100 mM NaCl, 0.05% DDM, 0.01% CHS, 10% (w/v) glycerol, ligand, PI]. 5 ml immobilized monomeric avidin resin (Pierce) was packed in a 20 ml drip column (Bio-Rad) by gravity-flow. The column was prepared by passing 5 CV of 100 mM glycine pH 2.8, followed by 5 CV of avidin column buffer supplemented with 20 mM d-biotin to block irreversible binding sites. The column was then equilibrated with 5 CV of avidin column buffer. Sample was applied to the column and allowed to bind for 15 min. The column was then washed with 6 CV of avidin column buffer and bound protein was eluted using 10 CV of avidin column buffer supplemented with 20 mM d-biotin.

3.12.4 Anti-FLAG M2 affinity chromatography (batch)

Pooled IMAC elution fraction was incubated overnight with 1-2 ml of anti-FLAG M2 affinity gel prepared according to the manufacturer's instructions. After extensive washing (~20 CV), the bound receptor was eluted with purification start buffer containing 100 µg/ml FLAG peptide.

3.12.5 Purification of streptavidin and TEV protease

Cf. Chapter 5

3.12.6 Preparation of streptavidin-coated agarose beads

Cf. Chapter 5

3.12.7 Streptavidin-based affinity chromatography

Cf. Chapter 5

3.12.8 Deglycosylation

Pooled streptavidin-based affinity chromatography elution fraction was exchanged with purification buffer. PNGase F (New England Biolabs) was included at 50 U/mg protein and incubated at room temperature for 1 h with agitation.

3.12.9 Size exclusion chromatography

Pooled streptavidin-based affinity chromatography elution fraction was exchanged with gel filtration buffer [50 mM Tris-HCl pH 8.0, 150 mM NaCl, 0.05% DDM, 0.01% CHS, 10% (w/v) glycerol, ligand, PI]. The protein sample was further concentrated in a centrifugal concentrator with a 50 kDa MWCO (Vivaspin). 200-500 µl of sample was loaded onto a Superose 6 column (GE Healthcare) pre-equilibrated with 3 CV buffer on an ÄKTA FPLC system (GE Healthcare). Absorbance was measured at 280 nm. 1 ml fractions were collected over 2-3 CV at 0.2 ml/min.

3.13 Dynamic light scattering

Dynamic light scattering (DLS) measurements were performed using a DynaPro MS/X instrument (Protein Solutions). Protein samples were centrifuged at 15,000 *g* for 10 min and analyzed in the range of 10-50 µg/ml in 25 mM Tris-HCl (pH 7.5), 150 mM NaCl, 0.05% DDM or DM. Data were examined using Dynamics V6 software.

3.14 Electronic microscopy

The protein sample was diluted below 50 µg/ml in 25 mM Tris-HCl (pH 7.5), 150 mM NaCl, 0.05% DDM or DM. 5 µl of this suspension was applied on a glow discharged electron microscopy grid coated with a thin carbon film. Excess sample solution was washed off with water, and the sample was negatively stained with 2% (w/v) uranyl acetate. Grids were observed with a FEI CM120 electron microscope operating at 100 kV. Images were recorded using a Gatan CCD camera of 1024x1024 pixels.

3.15 MALDI-TOF mass spectrometry

Cf. Chapter 5

3.16 Three-dimensional crystallization trials

Purified receptor samples were concentrated up to 3-4 mg/ml and then used for 3D crystallization screening in 200 nl drops using a Cartesian Honeybee robot. Commercially available crystallization kits (Nextal MBClass I & II Suites) were used and two different temperatures (4 °C and 18 °C) were tested.

Chapter 4

Large-Scale Expression of GPCRs

Large-Scale Expression of Functional Human Dopamine D_2 Receptor in *Pichia pastoris* Bioreactor Cultures

Cédric Fiez-Vandal[1*], Adrien Gras[2*], Franc Pattus[1], So Iwata[2], Renaud Wagner[1], Bernadette Byrne[2+]

[1]LC1-UMR 7175, Institut Gilbert Laustriat, ESBS, Bd Sébastien Brandt, BP 10413, 67412 Illkirch Cedex, France
[2]Membrane Protein Crystallography Research Group, Division of Molecular Biosciences, Imperial College London, South Kensington, London, SW7 2AZ, UK

[*]These authors contributed equally to the work presented in this manuscript.

[+]To whom correspondence should be addressed:
Dr. Bernadette Byrne
Fax: +44 20 7594 3004
E-mail: b.byrne@imperial.ac.uk

INTRODUCTION

G protein-coupled receptors (GPCRs) form a large superfamily of cell-surface receptors that mediate cellular responses to a wide range of biologically active molecules including hormones, neurotransmitters and drugs. Indeed half of all currently available pharmaceuticals act through GPCRs (Hopkins and Groom 2002; Klabunde and Hessler 2002). The relative physiological importance of these proteins makes them a key target for drug discovery programmes. Our understanding of the precise mechanism of action of these important proteins is limited by a lack of high-resolution structural data. One limiting factor to structural studies of GPCRs has, until recently, been low expression levels (Tate and Grisshammer 1996). With the exception of rhodopsin, all GPCRs are expressed at very low levels endogenously, thus requiring the development of recombinant overexpression systems. Careful expression vector design, GPCR codon-optimisation (Chelikani et al. 2006) and high throughput approaches used to identify GPCRs with the highest expression levels in different expression systems (Lundstrom et al. 2006), are among the methods that have been used to produce sufficiently high levels of functional GPCRs suitable for structural studies.

A high degree of success has been achieved when using the expression host *Pichia pastoris* for the production of membrane proteins, most notably the rat membrane protein K^+ channel. This latter was subsequently crystallised and it successfully yielded a high resolution structure (Long et al. 2005). *Pichia* has several advantages over other systems for the production of GPCRs. It is easy to manipulate, has high production levels and is relatively inexpensive. In addition, *Pichia* has the ability to glycosylate expressed receptors, albeit in a modified form compared to higher eukaryotes, which is essential for the proper functioning and membrane targeting of many receptors. Much effort has been applied to the optimisation of *Pichia* expression systems specifically for GPCR production (Weiss et al. 1995; Weiss et al. 1998a; Weiss et al. 1998b; Feng et al. 2002; Sarramegna et al. 2002a; Sarramegna et al. 2002b; de Jong et al. 2004; Grünewald et al. 2004; Kim et al. 2005; Sarramegna et al. 2005; André et al. 2006; Fraser 2006; Shukla et al. 2007). The basic system uses a pPIC9K vector (Invitrogen) where GPCR expression is under the control of the strong methanol inducible AOX1 promoter. Protease deficient expression strains, such as the SMD1163 strain, and the use of the α-factor leader sequence have improved receptor expression levels (Weiss et al. 1995; Weiss et al. 1998a). Modifications to the growth media including addition of histidine, dimethyl sulfoxide, which has been shown to facilitate phospholipids biosynthesis and membrane proliferation in yeast (Murata et al. 2003) and receptor specific ligands have been

systematically analysed and shown to increase the expression levels of 20 different GPCRs in *Pichia* (André et al. 2006).

An additional advantage to the use of *Pichia* compared to many other expression systems is that it readily adapts to large-scale fermentative growth in bioreactors (Cereghino et al. 2002). Bioreactors allow precise regulation of the aeration, pH and addition of carbon source, which in turn allows the cultures to grow to ultra-high cell densities maximising expression of the target protein. However optimisation of standard protocols is usually necessary for specific targets. One particular issue is the amount of methanol supplemented for induction. Indeed, very high levels of methanol can induce cytotoxic effects which reduce expression. Methanol sensors, which detect the level of unmetabolised methanol have been key to reducing these cytotoxic effects. Another important issue to be considered is the osmotic stress induced during high cell density culturing which is known to be responsible for adaptative cell response mechanisms, such as changes in the membrane lipid content (Mattanovich et al. 2004). This may not be desirable in the process of membrane protein production and medium cell density culturing approach appear more attractive. Finally, several parameters, such as temperature adjustment and addition of chemical chaperones, that have been shown to significantly improve the yield of functional GPCRs expressed in shake flasks (André et al, 2006) also need to be investigated.

Using a previously described vector system (André et al. 2006) for expression we have developed a large-scale fermentation protocol which produces significantly higher levels of functional receptor than the equivalent volume of culture in a shaker flask. The levels achieved for a test receptor, the human dopamine D_2, are among the highest reported for heterologously expressed GPCRs. This fermentation protocol should be applicable to the large-scale expression of most GPCRs in *Pichia*.

MATERIALS & METHODS

Materials

Yeast nitrogen base and yeast extract were purchased from Difco, peptone and L-histidine from Sigma-Aldrich, dimethyl sulfoxide (DMSO) from Acros Organics. Complete EDTA-free protease inhibitor cocktail (PI) tablets were purchased from Roche. The bicinchoninic acid assay (BCA) kit was from Pierce. Metoclopramide and (+)-butaclamol hydrochloride were purchased from Sigma-Aldrich; ^{3}H-labeled spiperone was from Tocris. Scintillation cocktail (Ultima Gold MV) was obtained from PerkinElmer. Nitrocellulose

membrane was from Millipore and GF/B filters were from Whatman. The mouse M2 anti-FLAG antibody was from Sigma-Aldrich and the sheep anti-mouse IgG-horseradish peroxidase (HRP) conjugate from GE Healthcare. All other chemicals were obtained from Sigma-Aldrich.

Strain

The protease-deficient *Pichia pastoris* strain SMD1163[pPIC9K-DRD2] from the MePNet collection (Lundstrom et al. 2006) was used for heterologous expression.

Glycerol stocks of SMD1163 recombinant cells were plated on YPG agar plates and incubated overnight at 30 °C. The cells were used to inoculate a 2 L baffled flask containing 400 ml of BMGY medium [100 mM potassium phosphate pH 6.0, 1% (w/v) yeast extract, 2% (w/v) peptone, 1.34% (w/v) yeast nitrogen base without amino acids, 0.00004% (w/v) biotin, 1% (w/v) glycerol] and incubated overnight at 30 °C to an OD_{600} of 3-5. This starter culture was then diluted in 500 ml BMGY medium in 2 L baffled flasks and grown for 6-8 h to an OD_{600} of 4-5. The cells were spun down at 3,000 *g* for 20 min and the cell pellet was resuspended in 500 ml BMMY [similar to BMGY with the following changes: phosphate buffer at pH 8.0, 2.5% (v/v) dimethyl sulfoxide, 0.04% (w/v) histidine, and 0.5% (v/v) methanol instead of 1% glycerol] supplemented with 10 μM metoclopramide (DRD2 antagonist). The culture was incubated for 18 h at 18 °C and then harvested by centrifugation.

Expression in fermentor

Glycerol stocks of SMD1163 recombinant cells were plated on YPG agar plates and incubated for 2-3 days at 30 °C. The cells were used to inoculate a 1 L baffled flask containing 200 ml of MGY medium [100 mM potassium phosphate pH 6.0, 1.34% (w/v) yeast nitrogen base without amino acids, 0.00004% (w/v) biotin, 1% (w/v) glycerol] and incubated overnight at 30 °C to OD_{600} ~20. The cells were spun down at 3,000 *g* for 20 min and the cell pellet was washed with 40 ml of sterile deionised water before being resuspended in 20 ml of MGY. This was used to inoculate 2 L of FM22 [4.3% (w/v) monobasic potassium phosphate, 0.5% (w/v) ammonium sulfate, 0.1% (w/v) calcium sulphate, 1.43% (w/v) potassium sulphate, 1.17% (w/v) magnesium sulfate, 2% (w/v) glycerol] supplemented with 2 ml of PMT4 [0.2% (w/v) copper sulphate, 0.008% (w/v) sodium iodide, 0.3% (w/v) manganese sulphate, 0.02% (w/v) sodium molybdate, 0.002% boric acid, 0.05% (w/v) calcium sulphate, 0.05% (w/v) cobalt chloride, 0.7% (w/v) zinc chloride, 2.2% (w/v) iron sulphate, 0.02% (w/v) biotin and 1 ml/L sulphuric acid] in a 3 L single wall Applikon

bioreactor vessel, operated by an ADI 1010 Bio controller connected to a PC running BioXpert software version 1.20 (Applikon Biotechnology). Agitation was set at 1000 rpm, pH maintained at 5 with 30% (v/v) ammonium hydroxide, and dissolved oxygen (DO_2) control at 35% for the duration of the culture growth. During growth phase, the culture was grown until the glycerol was exhausted, which was indicated by the so-called "oxygen spike". The culture was then supplemented with 50% (w/v) glycerol for 3-4 h at a rate of 0.15 ml/min until OD_{600} reached ~100-120. The glycerol feed was stopped and the culture allowed to consume the remaining glycerol. 30 min following complete glycerol consumption, the temperature of the culture was either kept constant at 30 °C or lowered to 20 °C, 18 °C or 16 °C. Depending on the different induction conditions evaluated in this study, other additives such as 5% (v/v) DMSO, 0.04% (w/v) histidine and 10 μM metoclopramide were added. To initiate methanol adaptation, the methanol level was raised to 0.05% (v/v) by direct injection of 100% methanol supplemented with 4 ml/L PMT4. The methanol level was further raised step-wise to 0.1, 0.2, 0.3 and 0.5%. During induction, the concentration of methanol in the culture vessel was maintained by a methanol feed pump (Gilson minipuls 3). Induction was carried out for 18-20 h and the cells were harvested by centrifugation. The setup required for cultivation in a BioBench 20 L bioreactor (Applikon Biotechnology) was similar to that for 3 L fermentors, but was only scaled up in volume. The main difference is that the amount of medium, methanol and base used was increased. The initial and final volumes were calculated just as with the 3 L fermentation, only on a larger scale. The feeding strategy also remained the same.

Membrane preparation

Cells from small-scale cultures or time course samples were resuspended in ice-cold breaking buffer [50 mM Hepes-NaOH pH 7.4, 100 mM NaCl, 10% (w/v) glycerol, 2 mM EDTA, 1 mM PMSF, ligand, PI], and broken by vortexing with glass beads (8x1 min). The beads were removed from the cell suspension by passing the mixture through a chromatography column (Poly-Prep Column, Bio-Rad). Cell debris, including intact cells, were removed by a low speed spin (3,000 *g*) for 10 min. The supernatant was retained, and membranes isolated by centrifugation at 100,000 *g* for 30 min. Each membrane pellet was re-dissolved in a membrane buffer [50 mM Hepes-NaOH pH 7.4, 100 mM NaCl, 10% (w/v) glycerol] and flash frozen in liquid nitrogen for storage. Cells from large-scale cultures were resuspended in ice-cold breaking buffer before being passed twice through a cell breaker (Constant Systems) at 30 Kpsi. The cell suspension was centrifuged at 3,000 *g* for 10 min to

pellet unlysed cells and cell debris. The supernatant was centrifuged at 100,000 *g* for 1 h to collect the membranes. As a wash step, the membrane pellet was resuspended in breaking buffer in a homogenizer and pelleted by ultracentrifugation. The membrane pellet was then resuspended in membrane buffer and stored at -80 °C. Protein concentrations were determined by bicinchoninic acid (BCA) assay using bovine serum albumin as standard (Smith et al. 1985).

Radioligand binding assays

All radioligand binding assays were carried out using the DRD2 antagonist [^{3}H]spiperone in binding buffer [25 mM Hepes-NaOH pH 7.4, 200 mM NaCl, 1 mM EDTA, 1 mg/ml BSA]. Single-point binding assays on yeast membrane-bound receptor contained 5 μg of protein in a final volume of 200 μl. Binding was performed by incubating a saturating concentration of radioligand (10 nM) with receptor for 2 h at 25 °C. Non-specific binding was determined in the presence of 10 μM (+)-butaclamol. Following incubation, bound and free radioligands were separated by sucking the suspension onto Whatman GF/B filters pre-soaked in 0.3% polyethylenimine under vacuum using a Brandel cell harvester. The filters were washed three times with ice-cold wash buffer (50 mM Tris-HCl pH 7.4), and the filter discs counted for tritium using a LS 6500 (Beckman Coulter) system. All measurements with membrane-bound DRD2 were made in triplicates. Binding data were analyzed by non-linear least squares fitting using the computer package GraphPad Prism.

Western-blotting and immunodetection

Pichia membranes (*ca.* 10 μg) were diluted in NuPAGE LDS sample buffer (Invitrogen) before running on a 12% NuPAGE Bis-Tris gel with MES buffer (Invitrogen). They were subsequently electrophoretically transferred overnight for Western-blot analysis onto a nitrocellulose filter following the standard procedure (Towbin et al. 1992). Briefly, after electroblotting at the constant current of 30 mA per gel in transfer buffer (2.5 mM Tris, 19 mM glycine, 0.02% SDS, 20% methanol), the membrane was blocked with 8% lowfat milk powder in PBST [10 mM Na_2HPO_4, 1.8 mM K_2HPO_4, pH 7.4, 140 mM NaCl, 2.7 mM KCl, 0.02% Tween 80, 1% (w/v) BSA] for 1 h at room temperature and washed three times for 5 min with PBST. The membrane was then incubated with M2 anti-FLAG antibody (diluted 1:8,000 in PBST), washed again three times for 5 min with PBST, and incubated with sheep anti-mouse IgG-HRP conjugated antibody (diluted 1:10,000 in PBST). The immunoblot

bands were visualized using an enhanced chemiluminescence reagant (SuperSignal West Pico Kit, Pierce) according to the manufacturer's protocol.

RESULTS & DISCUSSION

Prior to the commencement of this work, the recombinant expression of functional DRD2 (B_{max} = 4.7 pmol/mg) in *P. pastoris* had been established by our group within the MePNet consortium (André et al. 2006). The transformed SMD1163 cells obtained had been selected for high total protein expression measured by semi-quantitative Western-blotting. By using optimized expression conditions (André et al. 2006), the production level achieved was close to 8.5 picomoles (pmol) bound ligand per milligram total membrane protein from flask cultures. The wet cell weight was approximately 10 mg/L, providing sufficient biomass to begin purification studies.

However, variable aeration as well as the inability to measure or control many expression conditions, such as pH, glycerol and methanol levels, during the course of culture growth result in batch-to-batch variation. The use of medium cell density fermentors should help to overcome these problems. Cultures can be grown to much higher cell density while still maintaining proper aeration and nutrition through glycerol/methanol feed lines. The inclusion of pH and dissolved oxygen probes allow for feedback-based maintenance of the expression conditions, which is particularly important during the methanol adaptation and induction phases. The increase in produced biomass and the potential for greater reproducibility in protein expression should facilitate more efficient purification and crystallization trials.

Hence, in order to scale-up expression and to facilitate greater batch-to-batch reproducibility, DRD2 clone was first grown in 2 L fermentor cultures by using standard expression conditions (FM22/PMT4, 30 °C, 18-h induction time). The culture parameters were tracked during growth and induction (Fig. 1). Slight pH increases were noted at various points during fermentation. The dissolved oxygen level in the cultures during glycerol batch and glycerol fed-batch phases decreased as cell density (OD_{600}) increased. Towards the end of the glycerol and methanol fed-batch stages, the ammonia pump was triggered to inject ammonia in order to maintain a pH at a set point of 5 in the culture. During the methanol fed-batch stages, DO_2 level in the cultures fluctuated at ~35 %. OD_{600} readings taken at various time points during induction increased linearly to a final value of ~120 at the end of induction. Wet cell weight achieved in fermentors was approximately 80 g/L.

We then managed to increase the yield of functional expressed DRD2 by using optimized conditions (FM22/PMT4, 5% (v/v) DMSO, 0.04% (w/v) histidine, 10 μM metoclopramide, 30 °C, 18-h induction time). Different time course points were submitted to Western-blot analysis and [^{3}H]spiperone binding assays and compared to those taken from the first fermentation trials in standard conditions. As shown in Figure 2, we improve the overall receptor fonctionality by adding, among others, chemical (DMSO) and pharmacological (metoclopramide, a DRD2 antagonist) chaperones to the growth media. Less amounts of D2DR were produced by using optimized conditions, but the receptor was found to be more functional (3.5 pmol/mg *vs.* 0.9 pmol/mg) after 18 hours of induction.

Decreasing the temperature of induction was shown to increase recombinant GPCRs' functionality when expressed in yeast (André et al. 2006). It is thought that the insertion of the transmembrane helices, in particular for this case in which the lipidic environment of the yeast differs from the native human host (Gimpl and Fahrenholz 2000) is facilitated at lower temperature. Several fermentation cultures were then performed in optimized conditions while shifting the induction temperature to 20 °C, 18 °C or 16 °C. Figure 6.3 summarized the [^{3}H]spiperone binding assay results of both standard (30 °C) and optimized expression conditions (30 °C, 20 °C, 18 °C, 16 °C). The highest production of functional receptor was obtained in optimized conditions at 18 °C (16.6 pmol/mg). Surprisingly, a considerable drop in the yield of functional DRD2 (5.5 pmol/mg) was observed when the temperatrure of induction was decreased to 16 °C . By these means, we were able to scale-up DRD2 production in bioreactors while simultaneously improving receptor functionality by roughly a two-fold factor compared to shake flask cultures (16.6 pmol/mg *vs.* 8.5 pmol/mg).

By using these promising optimized expression conditions in a 20 liters vessel fermentor (Applikon), we managed to produce 1.2 kg of wet weigh cells, which represents 20 mg of total membrane protein and 15 mg of fully active DRD2 (10 pmol/mg)! This large-scale expression of DRD2 will allow us to use the same batch over a long period of time, which is ideal when working with the aim of solving a GPCR structure.

ACKNOWLEDGMENTS

We thank James Mansfield for technical assistance. This research was funded by the Membrane Protein Network (MePNet), the European Membrane Protein Consortium (E-MeP), and the French government (Association Nationale de la Recherche Technique).

REFERENCES

André, N., Cherouati, N., Prual, C., Steffan, T., Zeder-Lutz, G., Magnin, T., Pattus, F., Michel, H., Wagner, R., and Reinhart, C. 2006. Enhancing functional production of G protein-coupled receptors in *Pichia pastoris* to levels required for structural studies via a single expression screen. *Protein Science* **15:** 1115-1126.

Cereghino, G.P.L., Cereghino, J.L., Ilgen, C., and Cregg, J.M. 2002. Production of recombinant proteins in fermenter cultures of the yeast *Pichia pastoris*. *Current Opinion in Biotechnology* **13:** 329-332.

Chelikani, P., Reeves, P.J., Rajbhandary, U.L., and Khorana, H.G. 2006. The synthesis and high-level expression of a β_2-adrenergic receptor gene in a tetracycline-inducible stable mammalian cell line. *Protein Science* **15:** 1433-1440.

de Jong, L.A.A., Grünewald, S., Franke, J.P., Uges, D.R.A., and Bischoff, R. 2004. Purification and characterization of the recombinant human dopamine D_{2S} receptor from *Pichia pastoris*. *Protein Expression and Purification* **33:** 176-184.

Feng, W., Cai, J., Pierce, W.M., and Song, Z.-H. 2002. Expression of CB_2 cannabinoid receptor in *Pichia pastoris*. *Protein Expression and Purification* **26:** 496-505.

Fraser, N.J. 2006. Expression and functional purification of a glycosylation deficient version of the human adenosine 2A receptor for structural studies. *Protein Expression and Purification* **49:** 129-137.

Gimpl, G., and Fahrenholz, F. 2000. Human oxytocin receptors in cholesterol-rich *vs.* cholesterol-poor microdomains of the plasma membrane. *European Journal of Biochemistry* **267:** 2483-2497.

Grünewald, S., Haase, W., Molsberger, E., Michel, H., and Reiländer, H. 2004. Production of the human D_{2S} receptor in the methylotrophic yeast *P. pastoris*. *Receptors and Channels* **10:** 37-50.

Hopkins, A.L., and Groom, C.R. 2002. The druggable genome. *Nature Reviews: Drug Discovery* **1:** 727-730.

Kim, T.-K., Zhang, R., Feng, W., Cai, J., Pierce, W., and Song, Z.-H. 2005. Expression and characterization of human CB_1 cannabinoid receptor in methylotrophic yeast *Pichia pastoris*. *Protein Expression and Purification* **40:** 60-70.

Klabunde, T., and Hessler, G. 2002. Drug design strategies for targeting G protein-coupled receptors. *ChemBioChem* **3:** 928-944.

Long, S.B., Campbell, E.B., and McKinnon, R. 2005. Crystal structure of a mammalian voltage-dependent *Shaker* family K^+ channel. *Science* **309:** 897-903.

Lundstrom, K., Wagner, R., Reinhart, C., Desmyter, A., Cherouati, N., Magnin, T., Zeder-Lutz, G., Courtot, M., Prual, C., André, N., et al. 2006. Structural genomics on membrane proteins: comparison of more than 100 GPCRs in 3 expression systems. *Journal of Structural and Functional Genomics* **7:** 77-91.

Mattanovich, D., Gasser, B., Hohenblum, H., and Sauer, M. 2004. Stress in recombinant protein producing yeasts. *Journal of Biotechnology* **113:** 121-135.

Murata, Y., Watanabe, T., Sato, M., Momose, Y., Nakahara, T., Oka, S.-i., and Iwahashi, H. 2003. Dimethyl sulfoxide exposure facilitates phospholipid biosynthesis and cellular membrane proliferation in yeast cells. *Journal of Biological Chemistry* **278:** 33185-33193.

Sarramegna, V., Demange, P., Milon, A., and Talmont, F. 2002a. Optimizing functional versus total expression of the human μ-opioid receptor in *Pichia pastoris*. *Protein Expression and Purification* **24:** 212-220.

Sarramegna, V., Muller, I., Mousseau, G., Froment, C., Monsarrat, B., Milon, A., and Talmont, F. 2005. Solubilization, purification, and mass spectrometry analysis of the

human mu-opioid receptor expressed in *Pichia pastoris*. *Protein Expression and Purification* **43:** 85-93.

Sarramegna, V., Talmont, F., Seree de Roch, M., Milon, A., and Demange, P. 2002b. Green fluorescent protein as a reporter of human μ-opioid receptor overexpression and localization in the methylotrophic yeast *Pichia pastoris*. *Journal of Biotechnology* **99:** 23-39.

Shukla, A.K., Haase, W., Reinhart, C., and Michel, H. 2007. Heterologous expression and characterization of the recombinant bradykinin B_2 receptor using the methylotrophic yeast *Pichia pastoris*. *Protein Expression and Purification* **55:** 1-8.

Smith, P.K., Krohn, R.I., Hermanson, G.T., Mallia, A.K., Gartner, F.H., Provenzano, M.D., Fujimoto, E.K., Goeke, N.M., Olson, B.J., and Klenk, D.C. 1985. Measurement of protein using bicinchoninic acid. *Analytical Biochemistry* **150:** 76-85.

Tate, C.G., and Grisshammer, R. 1996. Heterologous expression of G protein-coupled receptors. *Trends in Biotechnology* **14:** 426-430.

Towbin, H., Staehelin, T., and Gordon, J. 1992. Electrophoretic transfer of proteins from polyacrylamide gels to nitrocellulose sheets: procedure and some applications. *Biotechnology* **24:** 145-149.

Weiss, H.M., Haase, W., Michel, H., and Reiländer, H. 1995. Expression of functional mouse $5HT_{5A}$ serotonin receptor in the methylotrophic yeast *Pichia pastoris*: pharmacological characterization and localization. *FEBS Letters* **377:** 451-456.

Weiss, H.M., Haase, W., Michel, H., and Reiländer, H. 1998a. Comparative biochemical and pharmacological characterization of the mouse $5HT_{5A}$ 5-hydroxytryptamine receptor and the human β_2-adrenergic receptor produced in the methylotrophic yeast *Pichia pastoris*. *Biochemical Journal* **330:** 1137-1147.

Weiss, H.M., Haase, W., and Reiländer, H. 1998b. Expression of an integral membrane protein, the $5HT_{5A}$ receptor. *Methods in Molecular Biology* **103:** 227-239.

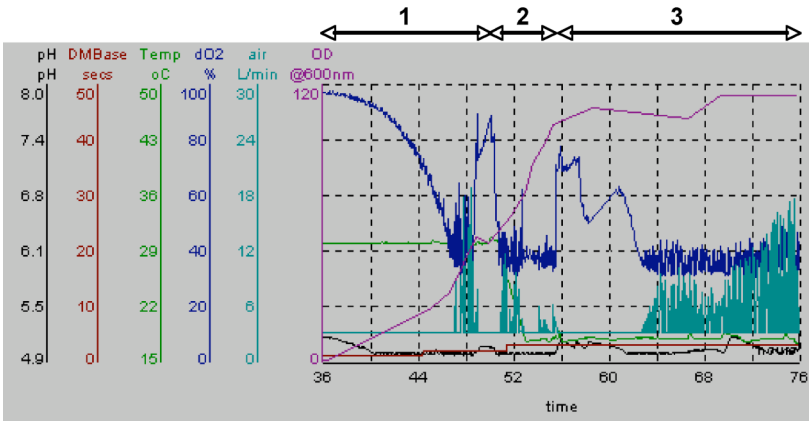

Figure 1. Graphical representation of the progression of different fermentation culture parameters during the glycerol batch (**1**), glycerol fed-batch (**2**) and methanol fed-batch (**3**) stages of DRD2 expression in *Pichia pastoris*. Temperature was maintained at 30 °C and 18 °C for growth and induction, respectively. pH and DO_2 minimum set-points were set to 5 and 35%, respectively.

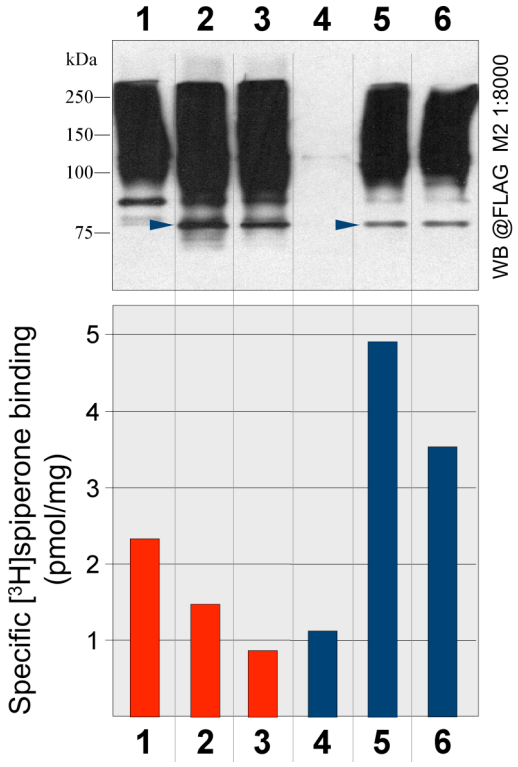

Figure 2. upper panel, Immunoblot analysis of membrane proteins prepared from recombinant *P. pastoris* cells expressing DRD2 at different timecourse points. *Pichia* membranes were separated by SDS-PAGE, transferred to a nitrocellulose filter, and probed using the M2 anti-FLAG antibody as described in Chapter 3. DRD2 is indicated by an arrow.

Molecular mass markers (kDa) are shown on the left side. Each lane was loaded with 10 μg of membrane protein. **lower panel**, [^{3}H]Spiperone (10 nM) binding assays on DRD2.

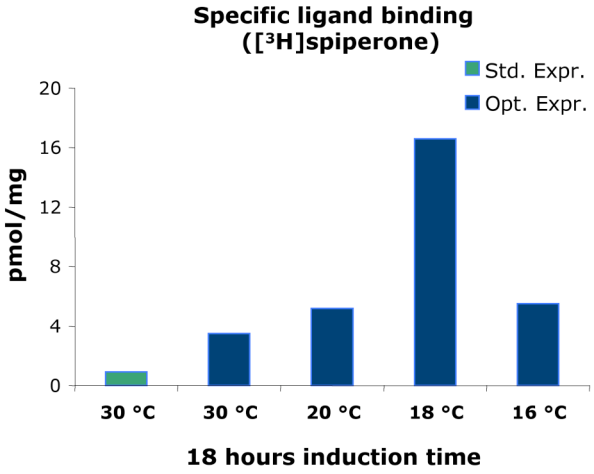

Figure 3. Production level for DRD2 in various conditions. In a first fermentation experiment, cells were grown in FM22/PMT4 at 30 °C, 18-h induction time (standard expression conditions). Further, cultures were conducted by supplementing the medium with 5% DMSO, 0.04% histidine and antagonist (metoclopramide at 100x K_d). Under these optimized expression conditions, temperature was either kept constant at 30 °C or schifted to 20 °C, 18 °C or 16 °C during induction. The binding values for standard expression conditions (Std. Expr.) and optimized expression conditions (Opt. Expr.) were calculated from single point measurements using 10x K_d for the [^{3}H]spiperone.

Chapter 5

Production & Purification of GPCRs

5.1 Production & Purification trials on DRD2, ADA2B and AA2AR

5.1.1 Expression construct

All the receptor constructs bear the coding region for α-mating factor prepro-peptide of *Saccharomyces cerevisiae* (shortly: α-factor) fused to the N-terminal domain of the receptor coding sequence. The α-factor is used as a secretion signal for soluble proteins and therefore should drive the expressed receptor to the cell membrane. A protease cleavage site was inserted between the α-factor and the receptor, which is recognized by *P. pastoris* Kex2 protease so as to provide efficient α-factor cleavage. Different affinity tags were appended to both receptor termini in order to provide easy detection and purification of expressed receptor protein. Octapeptide FLAG epitope (with amino acid sequence DYKDDDDK) and a decahistidine tag were introduced at the N-terminus, for subsequent use in immunological detection and receptor purification on FLAG-M2 antibody matrix and IMAC resins, respectively. A Bio-tag, 9.7 kDa biotinylation domain of *Propionibacterium shermanii* transcarboxylase[297] was appended to the C-terminus. This domain enabled receptor purification on monomeric avidin resin/home-made streptavidine-coated beads and detection with alkaline phosphatase-linked streptavidin. The tags were separated from the receptor coding region by a tobacco etch virus (TEV) protease cleavage site (Fig. 5.1).

Figure 5.1. Schematic representation of the expression vector construct used in expression and purification trials. The GPCR open reading frame is flanked by the α-factor, FLAG tag, decahistidine tag and TEV site at the 5' end, and a TEV site followed by a biotinylation tag sequence at the 3' end. Expression is under the control of the AOX1 promoter.

5.1.2 Production of recombinant receptors

Pichia cultures were grown either in shake flasks or in a bioreactor (see previous chapter); membranes were prepared* (after 18 hours of induction with methanol) and subjected to Western-blot analysis and radioligand binding assays.

5.1.2.1 Western-blot analysis

Western-blot with M2 anti-FLAG antibody was performed to check the expression of recombinant receptors. As shown in Figure 5.2, one major band in the size range between 65 and 75 kDa was seen in membranes from *P. pastoris* cells expressing DRD2, AA2AR or ADA2B. This corresponds well with the calculated size of the recombinant fusion protein in each case. For ADA2B, an upper second band was seen and would correspond to either a myristoylated/palmitoylated or phosphorylated receptor. Signals also often appeared as smears, suggesting either protein aggregation or extensive glycosylation.

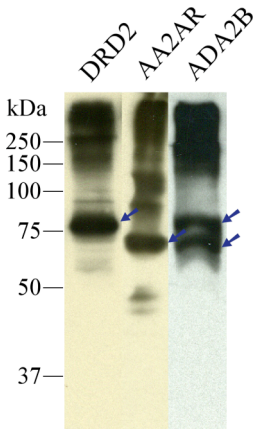

Figure 5.2. Immunoblot of membrane proteins prepared from *P. pastoris* cells harvested from fermentor (DRD2) and shake flask (AA2AR, ADA2B) cultures. Immobilized samples of crude membrane proteins were probed with monoclonal antibody against the FLAG epitope. Each lane was loaded with 10 μg of membrane protein.

5.1.2.2 Radioligand binding assays

In order to check the functionality of recombinant receptors and to calculate the total amount of functional receptors in membranes, saturation binding experiments using [^{3}H]ligands were performed. [^{3}H]spiperone binding was saturable and revealed a B_{max} value of ~12 pmol recombinant DRD2 per mg membrane protein. A high affinity binding of

* Cell lysis resulted in a significant amount of cell debris (~1/4 sample volume), which was removed from the sample by low speed centrifugation. Isolation of the membrane fraction by ultracentrifugation typically yielded 200-250 mg of membrane protein per 2 L flask culture, and ~20 g per 15 L fermentor culture, estimated by BCA.

[^{3}H]spiperone to the recombinant receptor was observed with a K_d value of 0.17 nM. Similar results were obtained for ADA2B (~14 pmol/mg, K_d = 20 nM) and AA2AR (~38 pmol/mg, K_d = 0.45 nM) by using [^{3}H]rauwolscine and [^{3}H]ZM241385, respectively.

5.1.3 Purification of DRD2

Several purification procedures were attempted on the dopamine D_2 receptor (DRD2) expressed in *Pichia* membranes, including different affinity chromatography resins (IMAC matrix, avidin agarose resin, anti-FLAG M2 affinity gel, home-made streptavidine-coated beads), ion exchange chromatography and gel filtration columns (SP Sepharose Fast Flow, Mono S, Resource S, Superose 6). I present here only the most relevant trials and those which were the most successful.

5.1.3.1 Purification of DRD2 – immobilized metal affinity chromatography

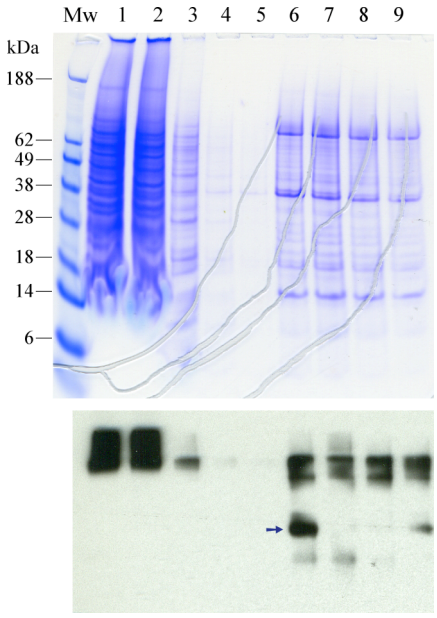

Figure 5.3. SDS-PAGE analysis of initial Co^{2+}-IMAC purification of DRD2 prepared in fermentor cultures. Upper panel: Coomassie-stained 4-12% gradient polyacrylamide gel showing moderate amounts of elution contaminants. Lower panel: Western-blot using M2 anti-FLAG antibody with ECL plus detection. A major ~75 kDa species is detected and indicated with a blue arrow. Lane contents: (**1**) solubilized material from *P. pastoris* membranes; (**2**) flow-through fraction; (**3-5**) wash fractions; (**6-9**) elution fractions; (**Mw**) SeeBlue molecular weight marker, values in kDa.

In order to test which metal ion was the most suitable for receptor purification, in terms of highest receptor purity and least aggregation, two-commercially available metal-coupled matrices were tested for comparison, Ni^{2+} coupled to nitrilotriacetic

acid-agarose (Ni-NTA) and Cobalt-based Talon resin (Co^{2+} coupled to Sepharose). Of the two, Talon matrix yielded better results (data not shown).

An immobilized Co^{2+} affinity chromatography purification step was thus performed with solubilized material from fermentor cultures. The results were analyzed by SDS-PAGE and immunoblot analysis against the N-terminal FLAG epitope (Fig. 5.3). Analysis revealed a large proportion of a ~75 kDa species in the elution fractions (blue arrow in Fig. 5.3). This is thought to correspond to the Kex2-processed receptor. Approximately 8 mg of total protein was recovered from 600 mg of membrane protein in this step.

5.1.3.2 Purification of DRD2 – immobilized monomeric avidin chromatography

Native streptavidin exists as a tetrameric protein composed of four identical subunits. It binds biotin specifically and almost irreversibly. The immobilization of monomeric avidin results in a support with a much lower biotin-binding affinity, which in theory, enables recovery of bound biotinylated protein under mild elution condition. Analysis of the concentrated pooled elution fractions by SDS-PAGE revealed the presence of a ~75 kDa band (Fig. 5.4). Immunodetection confirmed that this band corresponds to the species detected by M2 anti-FLAG antibody in the pooled Co^{2+}-IMAC elution fraction. However, the band was very faint, and judging by the intensities of the Coomassie-stained bands before and after avidin purification, it is obvious that a large proportion of the target protein is lost in the flow-through fraction and that eluted receptor seems to be aggregated. 0.1 mg of protein was recovered from 8 mg of load sample in this step.

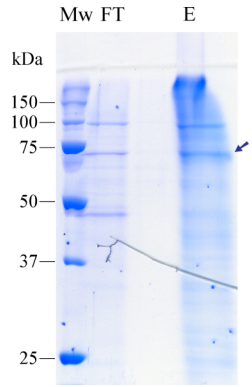

Figure 5.4. SDS-PAGE analysis of the immobilized monomeric avidin elution fraction of D2DR. The Coomassie-stained gel of the concentrated pooled elution fraction revealed the presence of a 75 kDa band, possibly the same species detected by Western-blotting with M2 anti-FLAG antiboby in the Co^{2+}-IMAC elutions (blue arrow). (**Mw**) Precision Plus Protein Standards molecular weight marker, values in kDa.

5.1.3.3 Purification of DRD2 – M2 anti-FLAG antibody matrix

Alternatively, the pooled Co^{2+}-IMAC elution fraction was applied to an anti-FLAG M2 antibody resin. Elution under mild conditions with competing free FLAG peptide was employed, so as not to perturb the receptor's native conformation. Eluate analysis on a silver-stained gel showed a tiny monomeric receptor band at ~75 kDa and massive aggregates at higher molecular weight (data not shown).

5.1.3.4 Purification of DRD2 – streptavidin-based affinity chromatography

As the previous purification trials on DRD2 lead to high aggregation and low yields, we developed an alternative purification procedure which relies on (i) the high affinity capture of solubilized receptors on streptavidin (SAV) coupled to agarose beads and (ii) the subsequent release of the native receptor by using the tobacco etch virus (TEV) protease. As shown in Figure 5.5, this method allowed the purification of DRD2 without massive aggregation. Identities of monomer and dimer bands (~50 and 100 kDa, respectively) were checked by MALDI-TOF mass spectrometry, and corresponded to the unfused DRD2 after cleavage of both N- and C-terminal tags by TEV protease. Starting from 100 mg membrane protein, approximately 50 μg receptor was recovered. However, in our hands, [^{3}H]spiperone ligand binding assays revealed that purified DRD2 was not functional, even when cholesteryl hemisuccinate (CHS) was added in solubilization and purification buffers.

This one-step purification method in batch was the first to allow the purification of reasonable amounts of DRD2, which was until now very difficult to isolate. We thus decided to apply it to several other GPCRs from the MePNet collection.

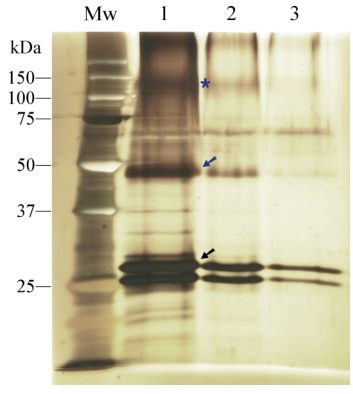

Figure 5.5. SDS-PAGE analysis of streptavidin-based affinity chromatography of D2DR by silver-stained 4-12% gradient polyacrylamide gel. Lane contents: (**1-3**) elution fractions; (**Mw**) Precision Plus Protein Standards molecular weight marker, values in kDa; blue arrow, DRD2 monomers; blue asterix, DRD2 dimers; black arrow, TEV protease.

5.1.3.5 Purification of DRD2 – deglycosylation

There are three putative glycosylation sites in DRD2, two at the N-terminus (N^5 and N^{17}), and one in the third intracellular domain (N^{243}). These sites were predicted based on conserved N-linked glycosylation motif (Asn-X-Ser/Thr). In order to evaluate the extent of glycosylation of the receptor, the pooled SAV-based affinity chromatography elution fraction of DRD2 was treated with PNGase F. As shown in Figure 5.6, the recombinant receptor band was shifted to lower molecular weight size upon enzymatic deglycosylation. This result reveals that the recombinant DRD2 produced in *P. pastoris* was glycosylated.

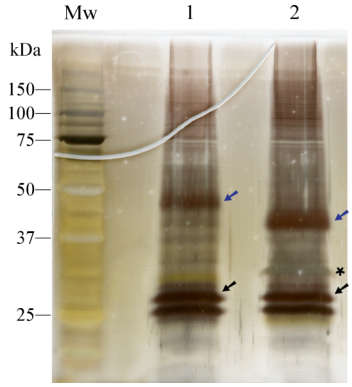

Figure 5.6. SDS-PAGE analysis of PNGase F-treated pooled SAV-based affinity chromatography elution fraction of DRD2 by silver-stained 4-12% gradient polyacrylamide gel. Treatment with PNGase F (lane **2**) resulted in band shift to lower molecular weights. (**Mw**) Precision Plus Protein Standards molecular weight marker, values in kDa; blue arrows, DRD2; black arrows, TEV protease; asterix, PNGase F.

5.1.3.6 Purification of DRD2 – dialysis removal of TEV protease

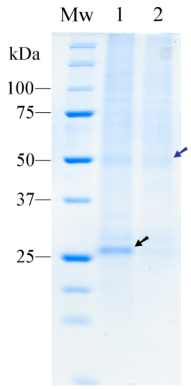

Figure 5.7. SDS-PAGE analysis of streptavidin-based affinity chromatography of DRD2 and subsequent TEV removal by dialysis (50,000 kDa MWCO). The Coomassie-stained 4-12% gradient polyacrylamide gel suggests complete TEV removal. Lane contents: (**1**) 10x concentrated pooled elution fraction, pre-dialyzed sample; (**2**) post-dialyzed sample; (**Mw**) Precision Plus Protein Standards molecular weight marker, values in kDa; blue arrow, DRD2; black arrow, TEV protease.

In order to remove TEV protease, purified DRD2 was dialyzed 18 h at 4 °C against several changes of purification buffer using a Spectra/Por Float-A-Lyzer with a molecular weight cutoff (MWCO) of 50,000 Da (Pierce). The Coomassie-stained SDS-PAGE gel of pre- and post-dialyzed sample suggested complete TEV removal (Fig. 5.7).

5.1.4 Purification of ADA2B

5.1.4.1 Purification of ADA2B – streptavidin-based affinity chromatography

ADA2B, which is not glycosylated, was successfully purified by using streptavidin-coated beads in batch. The purification yield was much higher than for DRD2 (~200 μg receptor was recovered, starting from 100 mg membrane protein) and roughly 2% of the receptor was found to be fully active (~400 pmol/mg was obtained by using [^{3}H]rauwolscine ligand binding assay). As shown in Figure 5.8, the two bands previously observed by Western-blot immunodetection of *Pichia* membrane-bound ADA2B (Fig. 5.2), were also seen after purification, with a shift of ~20-25 kDa corresponding to the cleavage of N- and C-ter tags. It was thought that these bands corresponded to a modified and unmodified ADA2B, which was indeed confirmed by MALDI-TOF mass spectrometry. However, no palmitoylation or myristoylation signature was detected.

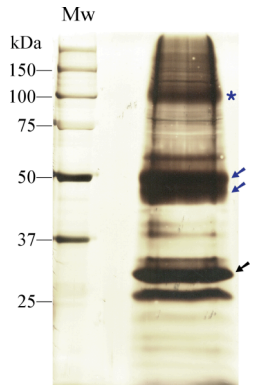

Figure 5.8. SDS-PAGE analysis of streptavidin-based affinity chromatography of ADA2B by silver-stained 4-12% gradient polyacrylamide gel. Lane content: 10x concentrated pooled elution fraction; (**Mw**) Precision Plus Protein Standards molecular weight marker, values in kDa; blue arrows, ADA2B monomers; blue asterix, ADA2B dimers; black arrow, TEV protease.

5.1.4.2 Purification of ADA2B – dialysis removal of TEV protease

As for DRD2, TEV protease was removed from the purified ADA2B by extensive dialysis. However, a large amount of the purified receptor was lost during this step, suggesting that ADA2B was adsorbed on dialysis membrane (Fig. 5.9).

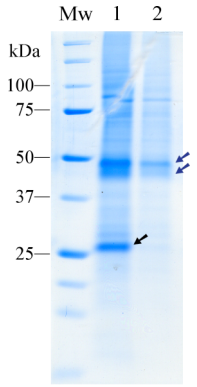

Figure 5.9. SDS-PAGE analysis of streptavidin-based affinity chromatography of ADA2B and subsequent TEV removal by dialysis (50,000 kDa MWCO). The Coomassie-stained 4-12% gradient polyacrylamide gel suggests complete TEV removal. Lane contents: (**1**) 10x concentrated pooled elution fraction, pre-dialyzed sample; (**2**) post-dialyzed sample; (**Mw**) Precision Plus Protein Standards molecular weight marker, values in kDa; blue arrows, ADA2B; black arrow, TEV protease.

5.1.4.3 Purification of ADA2B – size exclusion chromatography

In order to check the homogeneity of the purified receptor as well as to remove the TEV protease, the eluate from streptavidin-coated beads was analyzed by gel filtration on a Superose 6 column using an ÄKTA FPLC system. The chromatogram, substantiated by SDS-PAGE analysis of the fractions, revealed the target receptor eluting just after the void volume (**A**), suggestive of higher order oligomerization. A sharp peak (**C**) was detected after the main broad peak containing ADA2B (**B**) and corresponded to the TEV protease (Fig. 5.10).

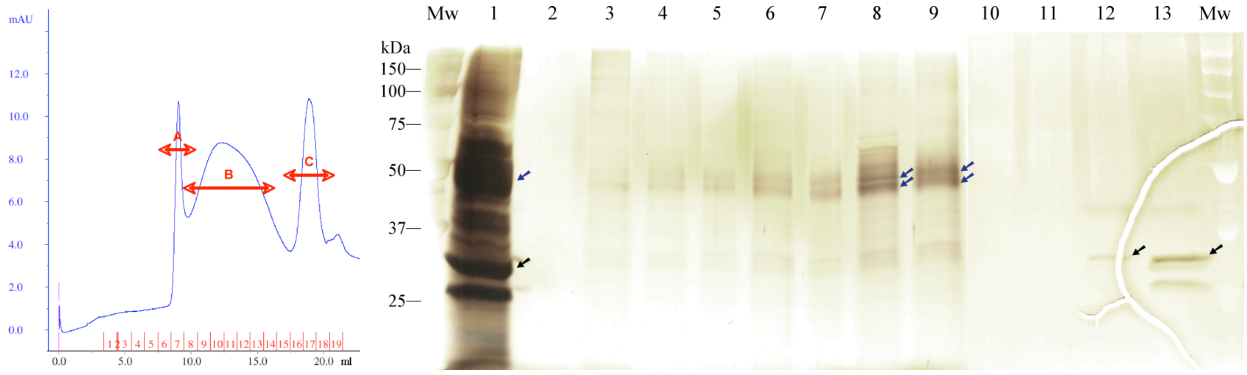

Figure 5.10. Purification of ADA2B by size-exclusion chromatography. Superose 6 HR 10/30 chromatogram (left) recorded at 280 nm on an ÄKTA FPLC system, and SDS-PAGE analysis of selected elution fractions (right) using silver-stain. The elution profile revealed an initial broad peak (**B**) arriving after the void volume (**A**), suggestive of higher order oligomerization. SDS-PAGE lane contents: (**1**) load sample; (**2-3**) void volume; (**4-11**) ADA2B; (**12-13**) TEV protease (**C**). (**Mw**) Precision Plus Protein Standards molecular weight marker, values in kDa; blue arrows, ADA2B; black arrows, TEV protease.

5.1.5 Purification of AA2AR

5.1.5.1 Purification of AA2AR – streptavidin-based affinity chromatography

AA2AR was purified by using streptavidin-coated beads in batch. Starting from 100 mg membrane protein, ~400 μg receptor was recovered (Fig. 5.11), and roughly 1-2% of the receptor was found to be fully active (~300 pmol/mg was obtaining by using [^{3}H]ZM241385 ligand binding assay).

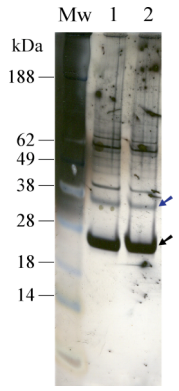

Figure 5.11. SDS-PAGE analysis of streptavidin-based affinity chromatography of AA2AR by silver-stained 4-12% gradient polyacrylamide gel. Lane contents: (**1-2**) elution fractions; (**Mw**) SeeBlue molecular weight marker, values in kDa; blue arrow, AA2AR; black arrow, TEV protease.

5.1.5.2 Purification of AA2AR – size exclusion chromatography

Purified AA2AR was further analyzed by gel filtration on a Superose 6 prep grade column. SDS-PAGE analysis of the fractions revealed that a large amount of AA2A eluted in the void volume (**A**) as well as in a broad peak just after the void volume (**B**), suggestive of aggregation and higher order oligomerization, respectively (Fig. 5.12).

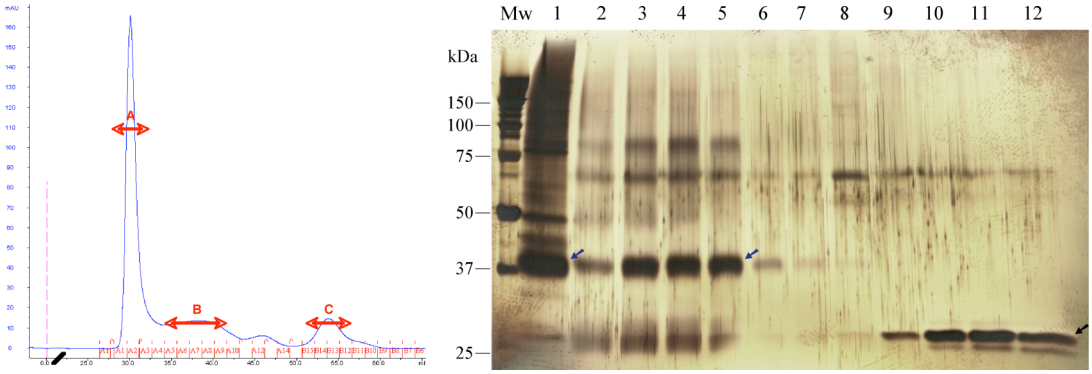

Figure 5.12. Purification of AA2AR by size-exclusion chromatography. Superose 6 prep grade chromatogram (left) recorded at 280 nm on an ÄKTA FPLC system, and SDS-PAGE analysis of selected elution fractions (right) using silver-stain. The elution profile revealed a broad peak (**B**) arriving after the void volume (**A**), suggestive of aggregation and higher order oligomerization. SDS-PAGE lane contents: (**1**) void volume; (**2-8**) AA2AR; (**9-12**) TEV protease (**C**). (**Mw**) Precision Plus Protein Standards molecular weight marker, values in kDa; blue arrows, AA2AR; black arrow, TEV protease.

5.2 Purification of several other GPCRs from the MePNet collection

We applied this single step streptavidin-based affinity method to several other GPCRs from the MePNet collection, namely the human serotonin $5HT_{1B}$ receptor (MePNet #2), the rat α_{2C}-adrenergic receptor (#18), the human cannabinoid receptor type-2 (#37), the human neurokinin-1 and -3 receptors (#72, #76), the human neuropeptide Y receptor type-1 (#79), the human delta- and kappa-opioid receptors (#83, #85) and the mesau α_{1B}-adrenergic receptor (#105). Purification results are presented in the following submitted paper (see further Chapter 5, pages 90-107): A Novel and Effective Single Step Method for the Rapid Purification of G Protein-Coupled Receptors.

5.3 Dynamic light scattering and electronic microscopy experiments

Dynamic light scattering (DLS) and electronic microscopy experiments were carried out to assess the oligomerization state of ADA2B and CNR2, purified by streptavidin-based affinity chromatography and gel filtration. In both cases, DLS of diluted proteins to 10-50 μg/ml revealed polydisperse structures (~16% polydispersity) of sizes ranging from 2-3 nm. Electron micrographs of negatively stained ADA2B and CNR2 particles exhibit homogenous oligomeric structures (tetramers? hexamers?), indicating high sample quality (Fig. 5.13).

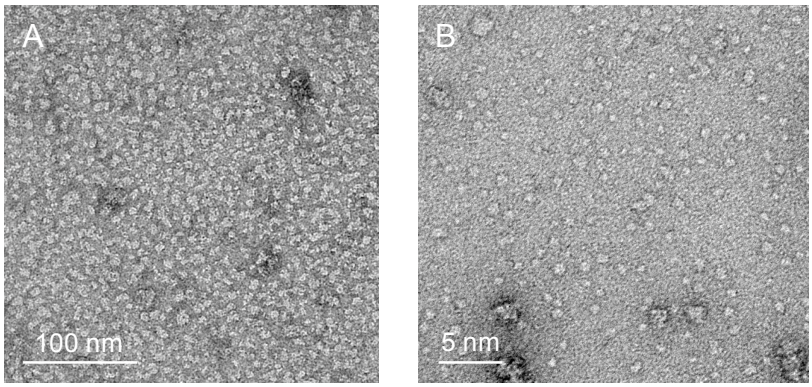

Figure 5.13. Electron micrographs of negatively stained purified ADA2B (**A**) and CNR2 (**B**) particles in 0.05% DDM. The scale bars correspond to 100 nm for ADA2B and to 50 nm for CNR2.

5.4 Three-dimensional crystallization trials of DRD2, ADA2B, AA2AR and CNR2

Purified DRD2, ADA2B, AA2AR and CNR2 were used for 3D crystallization attempts. Some crystalline structures were observed; however, these were too small to verify either by mass spectrometric analysis or by X-ray beam. It has not been possible so far to

reproduce these crystals under the same conditions. Further crystallization screening is ongoing to obtain reproducible and bigger crystals.

5.5 Discussion & Future work

The solubilization conditions used in this study (50 mM Hepes-NaOH pH 7.4, 500 mM NaCl, 20% glycerol, ligand, 1% DDM or DM ± 0.1%-0.2% CHS, PI; 2-5 mg/ml membrane protein; 1 h incubation at 4 °C) demonstrate the ability in extracting sufficient target protein from the membrane for purification trials. Sugar-like detergents such as DDM or DM were chosen from our previous solubilization-screening tests, involving various detergent classes (e.g. maltosides, glucosides, FOS-Choline series, LDAO, digitonine, CHAPS) and coupled with Western-blot immunodetection and ligand binding studies (Nadia Cherouati, Ph.D. thesis[301]).

For flexible proteins such as GPCRs, it is important to maintain a saturating concentration of ligands in the buffers in order to increase receptor stability[302,303]. For this purpose, the receptors were expressed and purified in the presence of high affinity antagonists (except when we planned to measure [^{3}H]ligand binding on purified fractions). However, inverse agonists should be preferred to agonists or antagonists. Whereas antagonists merely occupy the ligand-binding pocket promoting competitive binding without activating the GPCR, the interaction with inverse agonist is thought to result in the reversible locking of the protein conformation in an inactive state, conferring rigidity to the structure[304]. For instance, to overcome the structural flexibility of the human β_2AR and to facilitate its crystallization, Brian Kobilka managed to purify the receptor in the presence of the β-blocker carazolol, an inverse agonist[2-4]. However, in the case of the GPCRs investigated in this study, no inverse agonists have been either characterized or commercially available.

Results from flask and fermentor cultures indicated that streptavidin-based affinity chromatography followed by gel filtration was a promising method for the purification of several biotin-tagged GPCRs, in the absence of major contaminants as detected by Coomassie or silver staining.

Concerning the yield of purified functional receptors, some technical issues need to be addressed. Because it is thought that some receptors may pass through filter paper presoaked in 0.3% polyethylenimine during filtration, leading to low and unreproducible binding results, saturation and single-point ligand-binding assays on liposome-reconstituted receptors may be investigated, as well as scintillation proximity assays (SPA) or binding on streptavidine-

agarose bound receptors. By using this latter technique, preliminary results pointed out that CNR2 was indeed 42% active (10.2 nmol/mg).

For purified receptors with such binding results, immobilized ligand affinity chromatographic separation* can serve as a useful purification method, ensuring that only active protein is isolated, thereby decreasing sample heterogeneity.

Considering the results of dynamic light scattering and electronic microscopy, it seems that purified GPCRs are not fully aggregated at low concentration. It is then highly probable that decreasing the protein concentration of the load sample might reduce aggregation during size exclusion chromatography.

However, the tendency of the GPCRs produced in yeast to aggregate and to form high-order oligomers when concentrated represents a serious obstacle in obtaining homogeneous protein preparation, and efforts were made during this work to find a solution to this problem.

Aggregates can be formed as a result of receptor oxidation, since GPCRs possess free cysteines in their polypeptide chain. To avoid oxidation of thiol groups, 0.5-2 mM DTT was used in some cases as a reducing agent during purification. However, no significative difference in the receptor aggregation patterns was observed when purification was performed in the presence and absence of DTT (data not shown).

Another cause for receptor aggregation could be delipidation. Since it has been shown that some GPCRs undergoe total delipidation during solubilization with DDM[310], providing external lipids seemed like a reasonable solution. Purification in the presence of long-chain lipids (0.1 mg/ml 3:1:1 POPC:POPE:POPG†) or cholesteryl hemisuccinate (CHS) – a water-soluble derivative of cholesterol – was attempted, hoping that it would have a protective role against receptor aggregation. Unfortunately, these lipids didn't give any positive results in stabilizing the receptor in its native form (data not shown). In addition, the inclusion of CHS during solubilization has proven to hinder various steps downstream; in particular, those involving buffer exchange or concentration. It is thought that the size of the detergent-protein micelle increases dramatically with the incorporation of CHS, and its presence increases the

* Ligand affinity chromatography exploits a target receptor's affinity for its ligand. This interaction is often highly selective and has proven useful in the purification of a number of GPCRs, including the dopamine D_2 receptor[305], the β_2-adrenoreceptor[306,307] and the muscarinic acetylcholine receptors[308,309]. The coupling of small molecules to a resin support is easily achieved by exploiting the esterification reaction between NHS-activated resins, such as Sepharose (GE Healthcare) and Affigel (Bio-Rad), and primary amino groups.

† 1-Palmitoyl-2-Oleoyl-sn-Glycero-3-Phosphocholine, 1-Palmitoyl-2-Oleoyl-sn-Glycero-3-Phosphoethanolamine, and 1-Palmitoyl-2-Oleoyl-sn-Glycero-3-[Phospho-rac-(1-glycerol)]

tendency to obtain large detergent-CHS mixed micelles, which collectively clog membrane filters.

A complex of GPCR-β-arrestin* may also be useful to prevent receptor aggregation during concentration. Purified ADA2B and CNR2 were recently mixed with a purified phosphorylation-independent β-arrestin-1 mutant[311,312] in a molar ratio of 1:10 and incubated at room temperature for 2 hours. Studies are ongoing to examine the stability of such complexes by analytical gel filtration.

Further experiments in this direction are required, in order to identify a mixture of substances or protein partners (e.g. G proteins, GRKs, venom peptide toxins, antibodies), which can stabilize GPCRs or aid in resolving the receptor aggregates once they form.

* β-arrestin is a soluble protein that binds to the agonist activated GPCRs and blocks the G protein coupling. This results in downregulation of G protein dependant signalling pathways mediated via GPCRs.

A Novel and Effective Single Step Method for the Rapid Purification of G Protein-Coupled Receptors

Thierry Magnin[*1+], Cédric Fiez-Vandal[*1], Noëlle Potier[2], Aline Coquard[1], Isabelle Leray[1], Tania Steffan[1], Christel Logez[1], Fatima Alkhalfioui[1], Franc Pattus[1] and Renaud Wagner[*1]

[1]LC1-UMR 7175, Institut Gilbert Laustriat, ESBS, Bd Sébastien Brandt, BP 10413, 67412 Illkirch Cedex, France
[2]LC3-UMR 7177, Institut de Chimie, ISIS, 8, Allée Gaspard Monge, 67083 Strasbourg, France

[*]These authors contributed equally to the work presented in this manuscript.

[+]To whom correspondence should be addressed:
Dr. Thierry Magnin
Fax: +33 39 0244 829
E-mail: magnin@esbs.u-strasbg.fr

G protein-coupled receptors (GPCRs) constitute the largest family of membrane receptors and are of major therapeutic importance. Structure determination of G protein-coupled receptors and other applications require milligram quantities of purified receptor proteins on a regular basis. Recombinant GPCRs fused to a heterologous biotinylation domain were produced in the yeast Pichia pastoris. We describe an efficient method for their rapid purification that relies on the capture of these receptors with streptavidin immobilized on agarose beads, and their subsequent release by enzymatic digestion with TEV protease. This method has been applied to several GPCRs belonging to the class A rhodopsin-like subfamily, leading to high yields of purified proteins; it represents a method of choice for biochemical and biophysical studies when large quantities of purified GPCRs are needed.

Author Keywords: G protein-coupled receptor; *Pichia pastoris*; Streptavidin-based affinity chromatography; Cannabinoid receptor type-2; Radioligand binding

INTRODUCTION

Considerable research is ongoing in the area of membrane protein structure and function, and in recent years many efforts have been, in particular, focused on G protein-coupled receptors (GPCRs). These proteins share a conserved architecture based on seven

transmembrane segments; they are the key players of signal transduction and constitute the major group of drug targets for the pharmaceutical industry, with already more than half of modern drugs and almost 25% of the top 200 best-selling drugs targeting them (Fredriksson et al. 2003). Despite these crucial biological implications, very little is known about the detailed molecular mechanisms by which these membrane proteins recognize their extra-cellular stimuli and transmit the associated messages. The speed of discovery of novel GPCR-active drugs is hampered by the lack of structural information about these proteins, which is reflected by the fact that, to date, only rhodopsin, the rod-cell GPCR involved in dim light vision, and the β_2-adrenergic receptor, which plays an important role in cardiovascular physiology, have been crystallized and their structures solved at 2.2 and 2.4 Å, respectively (Okada et al. 2004; Cherezov et al. 2007).

For several protein families, including most of helical membrane proteins and in particular GPCRs, structural studies are still limited by low expression levels in heterologous systems and/or by difficulties in obtaining pure, homogeneous protein preparations (Lacapère et al. 2007).

During the last decade, the methylotrophic yeast *Pichia pastoris* has been increasingly used for heterologous GPCR expression (Weiss et al. 1998b; Sarramegna et al. 2003; Fraser 2006; Noguchi and Satow 2006). This yeast is particularly suitable for these applications, combining multiple advantages: (i) the relatively low costs related to protein expression; (ii) the availability of protease deficient *P. pastoris* strains; (iii) the presence of a well-defined strong promoter (i.e. the alcohol oxidase promoter) for efficient over-expression; (iv) the eukaryotic nature of post-translational modifications that lack extensive glycosylation; (v) the addressing of proteins to the plasma membrane due to the presence of targeting sequences; (vi) the feasibility of large-scale fermentation culturing when substantial quantities of material are needed.

We are currently using the *P. pastoris* system to express a dozen of GPCRs. Expression of these proteins has been optimized in a previous work (André et al. 2006), but their purification presented several problems: despite the relatively good levels of expression, GPCRs expressed in *P. pastoris* were very difficult to purify to homogeneity and in large quantities. Only time-consuming purification schemes consisting of numerous purification steps that included affinity immobilization on expensive resins such as M2 anti-FLAG agarose, eventually gave protein preparations of sufficient quality. Several GPCRs, such as the human cannabinoid receptor type-2 (CNR2_HUMAN), the kappa-opioid receptor (OPRK_HUMAN) and the α_{2B}-adrenergic receptor (ADA2B_HUMAN) were purified. The

state of purity of the proteins was reasonably good, but the yields remained quite low: a 2 liters culture gave only 10 to 100 µg of purified proteins with heavy losses occurring at each purification step. From previous dot-blot experiments, we estimated that, depending on the receptor, 1-5 mg of protein were present in the membranes from a 2 liters culture. These proteins were efficiently solubilized from their membranes with yields of up to 60-80% (data not shown). Therefore, we focused on improving the efficiency of the purification procedure to further enhance the yields of purified proteins.

We have developed a rapid, single step, generic purification procedure for GPCRs expressed in *P. pastoris*. This method relies on the presence of a C-terminal biotinylation domain in the recombinant proteins, allowing the high affinity capture of solubilized proteins on streptavidin (SAV) coupled to agarose beads. We also used the highly specific tobacco etch virus (TEV) protease for the removal of both N- and C-terminal tags and the concomitant release of the native protein. Scale-up of this purification protocol will allow large quantities of receptors to be purified, thus enabling three-dimensional crystallization attempts and other biophysical approaches.

EXPERIMENTAL PROCEDURES

Strains and plasmids

Pichia pastoris strains expressing different GPCRs were obtained as previously described (André et al. 2006). The plasmid for tobacco etch virus (TEV) protease overexpression in *Escherichia coli* was obtained from Gunter Stier (EMBL Heidelberg, Germany). The plasmid for streptavidin overexpression in *Escherichia coli* was obtained from Prof. Paulo Arosio (University of Brescia, Italy) (Gallizia et al. 1998).

Growth of *P. pastoris* and protein expression

Cells were grown overnight in BMGY (1% yeast extract; 1% peptone; 1.34% yeast nitrogen base; 1% glycerol; 0.00004% biotin; 100 mM potassium phosphate pH 6.0). Next day, the cells were diluted in BMGY and grown to an OD_{600} of 10. The culture was centrifuged and the pellet resuspended in the same volume of BMMY (1% yeast extract; 1% peptone; 1.34% yeast nitrogen base; 0.5% methanol; 0.00004% biotin; 100 mM potassium phosphate pH 6.0; 2.5% DMSO; 0.4 mg/ml histidine) for the induction of protein production. After 18 hours at 23 °C, the cells were spun down, washed with PBS (phosphate buffer saline:

20 mM sodium phosphate pH 7.4; 2 mM KCl; 150 mM NaCl) and either used immediately or frozen at -80 °C.

Preparation of the cell membranes

All procedures were performed on ice. The cells were resuspended in cold lysis buffer (50 mM sodium phosphate pH 7.4; 100 mM NaCl; 5% glycerol; 5 mM EDTA; 1 mM PMSF). Cells were broken with glass beads (0.5 mm; 3 x 20 s), using a MP Biomedicals fast prep device. Cell debris and unbroken cells were removed by centrifugation at 5,000 *g* for 10 min and the turbid supernatant containing cell membranes was ultracentrifuged at 150,000 *g* for 45 min. The resulting pellets were resuspended in membrane buffer (50 mM Tris pH 8.0; 120 mM NaCl; 10% glycerol; 1 mM PMSF) and ultracentrifuged again. The membrane pellets were resuspended in membrane buffer, flash frozen in liquid nitrogen and stored at -80 °C. Protein concentrations were determined by bicinchoninic acid assay (Pierce) using bovine serum albumin as standard.

Western-blotting and immunodetection

Chemiluminescent Western-blotting detection reagents were from Pierce. Mouse monoclonal M2 anti-FLAG antibody was from Sigma-Aldrich. Peroxidase-linked anti mouse IgG was purchased from GE Healthcare. Alkaline phosphatase-linked streptavidin and the corresponding substrate tablets (NBT/BCIP) were purchased from Sigma-Aldrich. Proteins were separated by SDS-PAGE (10% gel) and visualized with Coomassie blue or transferred overnight at 30 V to a nitrocellulose membrane. The membrane was developed either with the M2 anti-FLAG antibody or with alkaline phosphatase-conjugated streptavidin.

***In vitro* biotinylation**

Membranes (50 µg) were mixed with 10 mM ATP, 10 mM MgOAc, 50 µM biotin, 50 mM bicine buffer (pH 8.3) with or without 12,500 units of biotin-protein ligase (BirA; Genecopoeia). The suspensions were incubated at 30 °C for 40 min, then submitted to SDS-PAGE and Western-blotting. Biotinylated proteins were detected as described above.

Solubilization

Detergents were obtained from Anatrace except for CHAPS (Euromedex). Membranes were diluted to obtain a protein concentration of 1 mg/ml in the solubilization buffer (final concentrations: 50 mM Hepes-NaOH pH 7.4, 500 mM NaCl, 20% (w/v) glycerol). Then the

detergent n-dodecyl-β-D-maltopyranoside (DDM) was added to a final concentration of 1% and the solution was stirred at room temperature for 1 h. After ultracentrifugation (150,000 *g*, 45 min), the supernatant was directly used for purification.

Purification with streptavidin beads

The supernatant obtained after solubilization was mixed with streptavidin-coated beads (see below) at various ratios. This preparation was kept overnight at 4 °C with orbital shaking; then the suspension was centrifuged at 1,000 *g* for 5 min, the supernatant was removed and the beads were incubated for one hour at 30 °C in solubilization buffer supplemented with 0.1% DDM and endoglycosidase (PNGase F, 1,000 units). The beads were then sequentially washed with (i) solubilization buffer supplemented with 1% CHAPS, (ii) solubilization buffer supplemented with 0.1% DDM (iii) solubilization buffer supplemented with NaCl (1.5 M final concentration) and 0.1% DDM, (iv) solubilization buffer supplemented with 1 M NaSCN and 0.1% DDM, (v) three times with solubilization buffer supplemented with 2 mM DTT and 0.1% DDM (TEV buffer). All washing steps were performed at room temperature with gentle orbital shaking. Immobilized receptor were then cleaved off their tags and therefore released from the beads by addition of TEV protease (1 µg of protease for 20 mg of starting membrane proteins) and shaking at 25 °C for 0.5-16 hours.

Preparation of streptavidin, streptavidin-coated agarose beads and TEV protease

Streptavidin was overproduced in *Escherichia coli* and purified as previously described (Gallizia et al. 1998). The protein was dialyzed against 0.1 M $NaHCO_3$ pH 8.3 containing 0.5 M NaCl and then concentrated on a Vivaspin concentrator (30 kDa MWCO). The protein (0.8 mg/ml final concentration) was then coupled to cyanogen bromide-activated sepharose 4B (Sigma-Aldrich) according to the manufacturer's instructions, except that the sepharose beads were pre-hydrolyzed for 2 hours at pH 8.3 before adding streptavidin. The beads were kept at 4 °C in PBS supplemented with 0.02% sodium azide (four volumes of PBS/azide added to one volume of wet beads), and no decrease in the GPCR capture efficiency was noticed after 6 months of storage. In some experiments, used streptavidin beads were recycled by denaturation with 8 M guanidine-HCl in 50 mM citrate pH 3.0 followed by renaturation with a decreasing guanidine concentration gradient. The capacity of these recycled beads to immobilize receptors was decreased by 40-60%, when compared with unused beads.

TEV protease was overexpressed in *E. Coli* BL21(DE3)pLysS (overnight induction in LB at 23 °C with 0.5 mM IPTG) and then purified on an IMAC column (HisTrap, GE Healthcare) followed by a desalting step and a cation exchange chromatography at pH 6.1 on a Mono S column (GE Healthcare). After elution with a 0-1.0 M NaCl gradient, protease containing fractions, which eluted at 750 mM NaCl, were aliquoted and stored at -80 °C.

Radioligand binding assays

Binding assays were performed as previously described (André et al. 2006), using 10 nM tritiated ligands CP55940 and rauwolscine for CNR2_HUMAN and ADA2B_HUMAN, respectively. The binding buffer used for the CNR2 receptor contained 50 mM Tris-HCl pH 7.4, 2.5 mM EDTA, 5 mM $MgCl_2$ and 0.5 mg/ml bovine serum albumin.

MALDI-TOF mass spectrometry

SDS-PAGE separated protein bands were excised from the gel and the proteins were digested according to the Shevchenko protocol (Jensen et al. 1999). The gel plugs were washed three times with 100 µl of 25 mM ammonium hydrogen carbonate (NH_4HCO_3) and 100 µl of acetonitrile. The cysteine residues were reduced by 50 µl of 10 mM dithiothreitol at 56 °C and alkylated by 50 µl of 55 mM iodoacetamide. After dehydration with acetonitrile, the proteins were cleaved with 15 µl of a 12.5 ng/µl solution of proteomics grade trypsin (Sigma-Aldrich) in 25 mM NH_4HCO_3. The digestion was performed overnight at room temperature. The resulting peptides were extracted with a 65% acetonitrile solution containing 5% acid formic and 0.05% SDS for 1 h. MALDI-TOF mass measurements were carried out on an AutoFlex II TOF/TOF (Bruker Daltonik GmbH, Bremen, Germany) operating in positive reflectron mode. The samples were prepared by standard dried droplet preparation on stainless steel MALDI targets using α-cyano-4-hydroxycinnamic acid as matrix. The samples were washed twice with 5% formic acid. External calibration of MALDI mass spectra was carried out using singly charged monoisotopic peaks of a mixture of bradykinin 1-7 (m/z=757.400), human angiotensin II (m/z=1046.542), human angiotensin I (m/z=1296.685), substance P (m/z=1347.735), bombesin (m/z=1619.822), ACTH 1-17 (m/z=2093.087) and ACTH 18-39 (m/z=2465.199). Monoisotopic peptide masses were automatically annotated using Flexanalysis 3.0.

RESULTS

GPCRs were overexpressed in *P. pastoris* as previously described (André et al. 2006). The recombinant proteins comprise an N-terminal α-factor signal sequence from *Saccharomyces cerevisiae* followed by a FLAG tag, a decahistidine tag, a tobacco etch virus (TEV) protease site, the GPCR open reading frame, a second TEV site, and finally the *Propionibacterium shermanii* biotinylation domain at the C-terminus.

Our earlier purification schemes relied on the presence of the N-terminal decahistidine and FLAG tags, but this strategy gave unsatisfactory results because of the poor specificity and efficiency of these tags. In these recombinant proteins, the C-terminal transcarboxylase biotinylation domain had been added mainly to detect the protein throughout the purification steps and to maintain its stability (Grünewald et al. 2004; Lundstrom et al. 2006). As an alternative to the first purification strategy, we decided to take advantage of the biotinylation domain to efficiently capture the GPCRs on SAV-agarose beads. The protein is immobilized on the beads through high affinity interaction, and can undergo subsequent washing treatment and might also be reconditioned. The final step relies on exploiting the TEV protease sites flanking the receptor to release the purified protein from the beads (Figure 1).

In vivo biotinylation of recombinant GPCRs expressed in *Pichia pastoris*

A prerequisite for the development of such a purification method is that the receptors are efficiently biotinylated *in vivo*. Several studies conducted on membrane proteins fused with biotinylation tags and expressed in *P. pastoris* have shown that this yeast indeed possesses a biotin ligase (ortholog of the *Escherichia coli* BirA protein), which biotinylates not only several low abundance *Pichia* proteins but also heterologous proteins (Weiss et al. 1998a; Julien et al. 2000).

Thus, we first verified that the *Pichia* strains used in this study effectively contained a biotin ligase activity and that the level of *in vivo* biotinylation was sufficient to directly undertake purification on streptavidin-agarose. For this purpose, yeast cells overexpressing four different GPCRs were grown in induction conditions. Then, membrane proteins were extracted, submitted to SDS-PAGE and transferred to a nitrocellulose membrane prior to the detection of biotinylated proteins with alkaline phosphatase-linked streptavidin. Figure 2A (lanes 1-4) shows that all four receptors tested, respectively ADA2B_HUMAN, CNR2_HUMAN, OPRK_HUMAN, and NK3R_HUMAN are biotinylated in *P. pastoris*. The sizes of the detected proteins are in good agreement with those expected for ADA2B (observed Mr: 65 kDa) and CNR2 (55 kDa), taking into account the size contribution of the

N- and C-terminal tags. For OPRK (85 kDa) and NK3R (100 kDa), the observed sizes are higher than expected. This is likely to be due to a lack of processing of the N-terminal α-factor signal sequence by internal Kex2 endopeptidase of *P. pastoris*. The same probably applies to the additional ~85 kDa doublet observed for the ADA2B receptor (Figure 2A, lanes 1 and 5). This absence of signal sequence processing was reported for the mouse $5HT_{5A}$ receptor also expressed in *P. pastoris* (Weiss et al. 1998a).

When the membranes were treated with exogenously added biotin-protein ligase (BirA), only a slight increase in the level of biotinylation could be observed (Figure 2A, compare lanes 1-4 and 5-8), indicating that, *in vivo*, the biotinylation of the proteins was almost complete. Figure 2B shows the same receptors detected with an M2 anti-FLAG monoclonal antibody; the bands observed are essentially the same as those detected with streptavidin-phosphatase. Taken together, these results indicate that both the N- and C-terminal parts of the proteins are intact since they are detected by the anti-FLAG antibody and streptavidin-phosphatase, respectively. Dimers and higher-order oligomers are also detected, especially for CNR2 and OPRK (Figure 2A, lanes 2, 3, 6 and 7; Figure 2B, lanes 2 and 3). Such SDS-resistant dimers/higher-order oligomers have been reported for an ever-increasing number of GPCRs (Javitch 2004).

These results along with the efficient *in vivo* biotinylation of these receptors prompted us to perform further purification tests. With the aim of developing a generic method (see Figure 1), the human peripheral cannabinoid receptor (CNR2_HUMAN) was used as a prototypical GPCR.

CNR2_HUMAN capture onto streptavidin-coated beads and its release by TEV protease

Membrane proteins (1 mg/ml) containing CNR2_HUMAN were solubilized with 1% DDM (n-dodecyl-β-D-maltopyranoside) and then mixed with SAV-agarose beads. Commercial beads were tested in preliminary experiments, but the results were not as good as with our in-house made SAV beads prepared as described in the Experimental section. The difference is most likely due to the different levels of substitution of the agarose beads with SAV: the pre-hydrolysis of the beads which we included prior to streptavidin coupling most probably leads to a lower density of SAV on the beads and thus reduces the steric hindrance problems that could be associated with a higher SAV density.

After solubilization, receptors were captured on SAV-coated beads in a batch mode. Surprisingly, very small quantities of the receptors bound to the beads within the first hours, although the streptavidin-biotin interaction is the strongest non-covalent biological interaction

(Ka = 10^{15} M^{-1}) between a protein and its ligand known to date. The bond formation between SAV and biotin is normally rapid and essentially non-reversible, suggesting that most probably, in our case, steric hindrance due to the interaction of the biotinylated C-terminal part of the tagged GPCR with neighbouring parts of the protein prevented the rapid capture of biotin by SAV. However, the quantity of bound protein increased with time, and an overnight contact at 4 °C proved to be optimum. Longer incubation times, even at higher temperatures (20-37 °C), did not increase the yield (data not shown). The optimal amount of home-made SAV-agarose resin necessary for the purification, starting from 20 mg of membrane proteins, was calculated to be 1.2 ml of resin. Increasing the resin quantity did not improve the yield of purified protein but actually slightly increased the amount of contaminants.

After capture of CNR2 on SAV, the beads were incubated in presence of an endoglycosidase (PNGase F). They were further extensively washed to remove non-specific contaminants. Several washing buffers were tested, including high and low pH buffers, high detergent and high salt buffers. The best results in terms of final receptor purity consisted in sequential washes with buffers containing (i) 1% CHAPS for removal of contaminants interacting through hydrophobic bonds, (ii) 1.5 M NaCl for contaminants bound through hydrophilic interactions and in some cases (iii) the chaotropic agent NaSCN (1.0 M) for very strongly bound contaminants. Then, the beads were equilibrated in TEV buffer containing 2 mM DTT which is an essential component to maintain the functionality of the TEV protease over long periods of time. The TEV protease cleaves off the receptors from the SAV-coated beads to which the receptors are bound by their C-terminal biotinylated tag, and also releases the N-terminal tags from the receptors. After addition of the protease, a time-course was performed to estimate the optimal incubation time: Figure 3 shows that the cleaved receptor can be detected after one hour of incubation (lane 2). Its quantity increased from 1 to 3 hours (lanes 1-4). However, the maximum amount of receptor was obtained either after 3 hours (lane 4) or after overnight incubation (lane 5). Two bands can be seen, the main one at 36 kDa and a more hazy band at ~40 kDa. Both were identified as the cannabinoid receptor by mass spectrometry (see below). The 40 kDa band most likely represents a post-translationally modified version of the receptor.

Several purified GPCRs

The one step purification method described above was tested out on several other GPCRs belonging to the rhodopsin-related class A subfamily. Figure 4 shows the results obtained with five of these receptors, the human neurokinin-3 receptor (NK3R_HUMAN,

theoretical molecular weight 52 kDa), the human neuropeptide Y receptor type-1 (P2RY1_HUMAN, 42 kDa), the human kappa-opioid receptor (OPRK_HUMAN, 43 kDa), the human histamine H_1 receptor (HRH1_HUMAN, 56 kDa), the human α_{2B}-adrenergic receptor (ADA2B_HUMAN, 50 kDa). All of these receptors were obtained in a relatively pure state (Figure 4). NK3R (lane 1) and ADA2B (lane 5) migrate at the expected molecular weights, but P2RY1 (lane 2), OPRK (lane 3) and HRH1 (lane 4) migrate slightly faster than expected (34, 37 and 50 kDa, respectively). This behavior is relatively frequent with membrane proteins and particularly among GPCRs (Gan et al. 2006). They may bind more SDS than other proteins of similar size, due to a higher level of hydrophobicity, and thus migrate faster during SDS-PAGE.

In order to confirm the identities of the purified receptors, the SDS-PAGE bands of purified OPRK, CNR2 and ADA2B were excised and submitted to in-gel digestion followed by MALDI TOF mass fingerprinting. As shown in Table 1, a total of 4, 8 and 11 peptides were identified for OPRK, CNR2, and ADA2B, respectively. Their masses were in concordance with the calculated molecular masses of theoretical tryptic peptides derived either from the cytoplasmic loops or from the N- and C-terminal domains. These analyses provided an unambiguous confirmation of the identities of the purified receptors. In the case of the CNR2 receptor, that gives two bands on SDS-PAGE (Figure 3), both bands gave a similar pattern, thus confirming that the upper band likely represents a post-translationally modified version of the receptor.

Ligand binding capacity of purified CNR2 and ADA2B receptors

Binding assays were realized for two purified SAV-agarose bound receptors, CNR2_HUMAN and ADA2B_HUMAN, using specific ^{3}H-labelled ligands (CP 55940 and rauwolscine, respectively). Two purification conditions were tested, the first including 0.1% DDM in all buffers, the second with 0.1% DDM and 0.02% cholesteryl hemisuccinate (CHS), a well-known GPCR stabilizer. For CNR2, the binding level was 9 nmol/mg in the first condition and 10.5 nmol/mg in the second, corresponding respectively to 36% and 42% of active receptors in the preparation. For the ADA2B receptor, the values were much lower: 0 and 0.2 nmol/mg in the two conditions tested, respectively, corresponding to only 0 and 1% of active receptors.

Purification yields

The yields obtained for several receptors are displayed in Table 2. They were mainly determined by two methods. The first consisted of protein measurements made after the removal of the TEV protein and the N-terminal free tags over a gel filtration column (Superose 12, GE Healthcare). The second was obtained by comparing the band intensities of purified receptors on a Coomassie blue stained gel with known quantities of BSA loaded on the same gels. The yields vary between 0.05 and 0.9 mg of purified receptor per liter of culture. Since several liters of *P. pastoris* culture can be easily handled and processed, especially using the easy purification method we describe here, most of the receptors are available in sufficient quantities for biophysical studies or for other studies requiring large amounts of purified proteins. A few receptors could not be purified, e.g. the human serotonin $5HT_{1B}$ receptor (5HT1B_HUMAN) or only purified in low amounts, e.g. the human proteinase-activated receptor 1 precursor (PAR1_HUMAN), the mesau α_{1B}-adrenergic receptor (ADA1B_MESAU), the human neurokinin-1 receptor (NK1R_HUMAN), and the rat α_{2C}-adrenergic receptor (ADA2C_RAT). In addition, the human neurokinin-2 receptor (NK2R_HUMAN) could only be purified as a low molecular weight, breakdown product, due to the presence of a cryptic TEV site in its sequence, as was the case for the human neurotensin receptor (White et al. 2004).

DISCUSSION

The GPCRs are the largest protein family known to date, comprised of an estimated 600-1000 members involved in various types of stimulus-response pathways, ranging from intercellular communication pathways to determination of physiological senses. GPCRs are involved in a wide range of disorders, including allergies, cardiovascular dysfunction, depression, obesity, cancer, pain, diabetes, and various central nervous system disorders. The GPCR family of receptors is well established as the premier target family for drug development: about half of the drugs on the market today are targeted towards GPCRs. Thus, taking into consideration the pharmacological importance of GPCRs, it is crucial to be able to produce pure and functional GPCRs on a custom basis to assist in the development of new GPCR targeting drugs.

Methods in use for GPCR purification from mammalian, insect, yeast or bacterial cells usually include numerous, lengthy, high-cost purification steps (Klammt et al. 2007b; Lacapère et al. 2007). Recent advances have been made with cell-free translational systems and the results obtained seem to be promising. However, the number of GPCRs expressed in

this way is still low and the experiments are still costly and require a lot of development and optimization (Ishihara et al. 2005; Klammt et al. 2007a; Klammt et al. 2007b).

Purification methods for membrane proteins that use the avidin-biotin interaction have been developed in a few cases (Jidenko et al. 2006; Krepkiy et al. 2006). Usually, monomeric avidin bound to agarose has been used, but some problems, mainly concerning elution of the proteins, have been frequently reported (Jidenko et al. 2006). The streptavidin-biotin is not generally used because of the very high strength of this interaction, making it virtually impossible to elute the protein of interest in mild conditions. We turned this drawback to our advantage by actually conserving the N-terminal tags in position on the streptavidin protein and exploiting TEV elution to liberate the protein of interest. The strength of the streptavidin-biotin interaction also allows, when necessary, the use of harsh washing conditions such as very high or low pH, or high concentrations of denaturants such as urea or guanidine.

The method described here is highly efficient and allows the rapid purification of GPCRs: the purification itself can be performed within 18 hours, and only three days are necessary to obtain the purified protein from a starter culture. Preliminary tests can be performed, when a new GPCR or a mutated GPCR is being studied, with only 20-50 mg of membrane proteins, thus limiting the amount of handwork needed. The costs involved are very low because of the use of the yeast *Pichia pastoris*, but also because no expensive purification resins or apparatuses are needed, since the method relies on the sole streptavidin-agarose resin and batch method.

The method allows easy exchange of buffers, salts and detergents, as well as addition of stabilizing additives early in the purification process, or only at the last step involving elution by TEV. In our hands, no strong inhibition of the TEV protease could be observed, whatever the additives (specific ligands and/or CHS) or detergents used. In a previous study, the protease was shown to be inhibited by several detergents, however, the detergent concentrations used were much higher, at least by an order of magnitude, than the concentrations used in our study (Mohanty et al. 2003).

For most GPCRs used in this study, substantial amounts of tag-free proteins have been purified in quantities and at purity levels sufficient to initiate structural studies. Among the receptors tested, one could not be purified and a few were obtained only in low amounts. Most of these refractory receptors were nevertheless expressed and biotinylated to levels comparable to receptors purified with good yields, indicating that the problem most probably lies in the organization of the C-terminal part of the proteins, where the biotin moiety could

be hindered. A possible remedy would be to add a linker between the GPCR and the biotinylation domain, thus rendering the biotin able to interact with SAV.

Besides structural studies, a possible application of the method would be to use streptavidin-agarose bound receptors to go "fishing" for receptor-interacting proteins in soluble/membrane extracts of various types of cells or tissues, in the presence or absence of added ligands. We recently obtained preliminary results showing that β-arrestin-1, a protein involved in GPCR internalization, can be retrieved with SAV-agarose-bound CNR2 receptor from an *Escherichia coli* extract containing arrestin expressed in low amounts (results not shown). The method described here would allow (i) a direct biochemical confirmation of interactions detected by other methods such as immunoprecipitation, (ii) the identification of novel interacting partners, and (iii) the possibility to release the GPCR-interacting partner-complexes with the TEV protease and to realize a biochemical study of such complexes.

ACKNOWLEDGMENTS

We are grateful to Rim Benmaamar for carefully reading the manuscript. This study was funded by the European Membrane Protein Consortium (E-MeP).

REFERENCES

André, N., Cherouati, N., Prual, C., Steffan, T., Zeder-Lutz, G., Magnin, T., Pattus, F., Michel, H., Wagner, R., and Reinhart, C. 2006. Enhancing functional production of G protein-coupled receptors in *Pichia pastoris* to levels required for structural studies via a single expression screen. *Protein Science* **15:** 1115-1126.

Cherezov, V., Rosenbaum, D.M., Hanson, M.A., Rasmussen, S.G.F., Thian, F.S., Kobilka, T.S., Choi, H.-J., Kuhn, P., Weis, W.I., Kobilka, B.K., et al. 2007. High-resolution crystal structure of an engineered human β_2-adrenergic G protein-coupled receptor. *Science* **318:** 1258-1265.

Fraser, N.J. 2006. Expression and functional purification of a glycosylation deficient version of the human adenosine 2A receptor for structural studies. *Protein Expression and Purification* **49:** 129-137.

Fredriksson, R., Lagerström, M.C., Lundin, L.-G., and Schiöth, H.B. 2003. The G protein-coupled receptors in the human genome form five main families. Phylogenetic analysis, paralogon groups, and fingerprints. *Molecular Pharmacology* **63:** 1256-1272.

Gallizia, A., de Lalla, C., Nardone, E., Santambrogio, P., Brandazza, A., Sidoli, A., and Arosio, P. 1998. Production of a soluble and functional recombinant streptavidin in *Escherichia coli*. *Protein Expression and Purification* **14:** 192-196.

Gan, L., Alexander, J.M., Wittelsberger, A., Thomas, B., and Rosenblatt, M. 2006. Large-scale purification and characterization of human parathyroid hormone-1 receptor stably expressed in HEK293S GnTI$^-$ cells. *Protein Expression and Purification* **47:** 296-302.

Grünewald, S., Haase, W., Molsberger, E., Michel, H., and Reiländer, H. 2004. Production of the human D_{2S} receptor in the methylotrophic yeast *P. pastoris*. *Receptors and Channels* **10:** 37-50.

Ishihara, G., Goto, M., Saeki, M., Ito, K., Hori, T., Kigawa, T., Shirouzu, M., and Yokoyama, S. 2005. Expression of G protein-coupled receptors in a cell-free translational system using detergents and thioredoxin-fusion vectors. *Protein Expression and Purification* **41:** 27-37.

Javitch, J.A. 2004. The ants go marching two by two: oligomeric structure of G protein-coupled receptors. *Molecular Pharmacology* **66:** 1077-1082.

Jensen, O.N., Wilm, M., Shevchenko, A., and Mann, M. 1999. Peptide sequencing of 2-DE gel-isolated proteins by nanoelectrospray tandem mass spectrometry. *Methods in Molecular Biology* **112:** 571-588.

Jidenko, M., Lenoir, G., Fuentes, J.M., le Maire, M., and Jaxel, C. 2006. Expression in yeast and purification of a membrane protein, SERCA1a, using a biotinylated acceptor domain. *Protein Expression and Purification* **48:** 32-42.

Julien, M., Kajiji, S., Kaback, R.H., and Gros, P. 2000. Simple purification of highly active biotinylated P-glycoprotein: enantiomer-specific modulation of drug-stimulated ATPase activity. *Biochemistry* **39:** 75-85.

Klammt, C., Schwarz, D., Eifler, N., Engel, A., Piehler, J., Haase, W., Hahn, S., Dötsch, V., and Bernhard, F. 2007a. Reprint of "Cell-free production of G protein-coupled receptors for functional and structural studies" [J. Struct. Biol. 158 (2007) 482-493]. *Journal of Structural Biology* **159:** 194-205.

Klammt, C., Srivastava, A., Eifler, N., Junge, F., Beyermann, M., Schwarz, D., Michel, H., Doetsch, V., and Bernhard, F. 2007b. Functional analysis of cell-free-produced human endothelin B receptor reveals transmembrane segment 1 as an essential area for ET-1 binding and homodimer formation. *FEBS Journal* **274:** 3257-3269.

Krepkiy, D., Wong, K., Gawrisch, K., and Yeliseev, A. 2006. Bacterial expression of functional, biotinylated peripheral cannabinoid receptor CB_2. *Protein Expression and Purification* **49:** 60-70.

Lacapère, J.-J., Pebay-Peyroula, E., Neumann, J.-M., and Etchebest, C. 2007. Determining membrane protein structures: still a challenge. *Trends in Biochemical Sciences* **32:** 259-270.

Lundstrom, K., Wagner, R., Reinhart, C., Desmyter, A., Cherouati, N., Magnin, T., Zeder-Lutz, G., Courtot, M., Prual, C., André, N., et al. 2006. Structural genomics on membrane proteins: comparison of more than 100 GPCRs in 3 expression systems. *Journal of Structural and Functional Genomics* **7:** 77-91.

Mohanty, A.K., Simmons, C.R., and Wiener, M.C. 2003. Inhibition of tobacco etch virus protease activity by detergents. *Protein Expression and Purification* **27:** 109-114.

Noguchi, S., and Satow, Y. 2006. Purification of human β_2-adrenergic receptor expressed in methylotrophic yeast *Pichia pastoris*. *Journal of Biochemistry* **140:** 799-804.

Okada, T., Sugihara, M., Bondar, A.-N., Elstner, M., Entel, P., and Buss, V. 2004. The retinal conformation and its environment in rhodopsin in light of a new 2.2 Å crystal structure. *Journal of Molecular Biology* **342:** 571-583.

Sarramegna, V., Talmont, F., Demange, P., and Milon, A. 2003. Heterologous expression of G protein-coupled receptors: comparison of expression systems from the standpoint of large-scale production and purification. *Cellular and Molecular Life Sciences (CMLS)* **60:** 1529-1546.

Weiss, H.M., Haase, W., Michel, H., and Reiländer, H. 1998a. Comparative biochemical and pharmacological characterization of the mouse $5HT_{5A}$ 5-hydroxytryptamine receptor

and the human β_2-adrenergic receptor produced in the methylotrophic yeast *Pichia pastoris*. *Biochemical Journal* **330:** 1137-1147.

Weiss, H.M., Haase, W., and Reiländer, H. 1998b. Expression of an integral membrane protein, the $5HT_{5A}$ receptor. *Methods in Molecular Biology* **103:** 227-239.

White, J.F., Trinh, L.B., Shiloach, J., and Grisshammer, R. 2004. Automated large-scale purification of a G protein-coupled receptor for neurotensin. *FEBS Letters* **564:** 289-293.

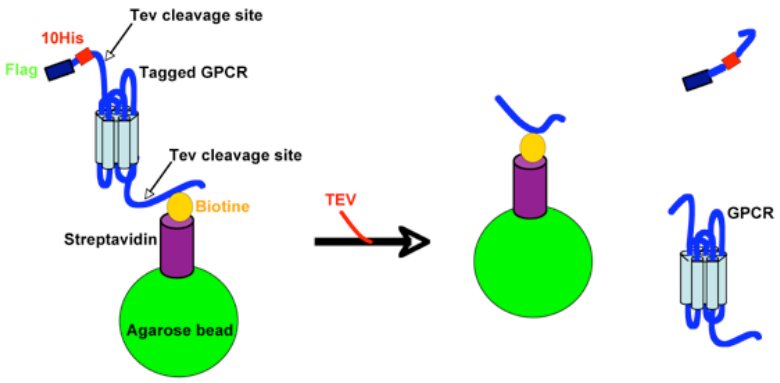

Figure 1. Schematic representation of the method

A solubilized receptor is captured on immobilized streptavidin. The TEV protease then cleaves the N- and C-terminal tags, thus releasing the receptor and the N-terminal tag. The C-terminal tag remains bound to streptavidin.

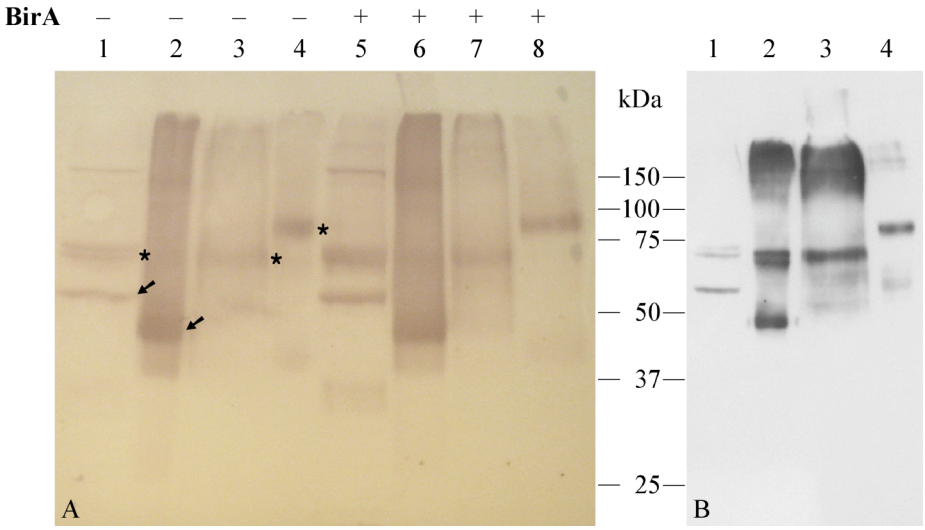

Figure 2. **Detection of four GPCRs expressed in *Pichia pastoris***

Membrane proteins were subjected to SDS-PAGE, and transferred to nitrocellulose. The receptors were detected with (A) alkaline phosphatase-linked streptavidin or (B) M2 anti-FLAG monoclonal antibody. Lanes 1 and 5: ADA2B_HUMAN; lanes 2 and 6: CNR2_HUMAN; lanes 3 and 7: OPRK_HUMAN; lanes 4 and 8: NK3R_HUMAN. Membranes from lanes 5 to 8 were subjected to *in vitro* biotinylation with the BirA protein-biotin ligase prior to SDS-PAGE. *Arrows point to receptor bands at the expected size. Receptors for which the signal sequence was not processed, leading to molecular masses higher than expected, are indicated by an asterix.*

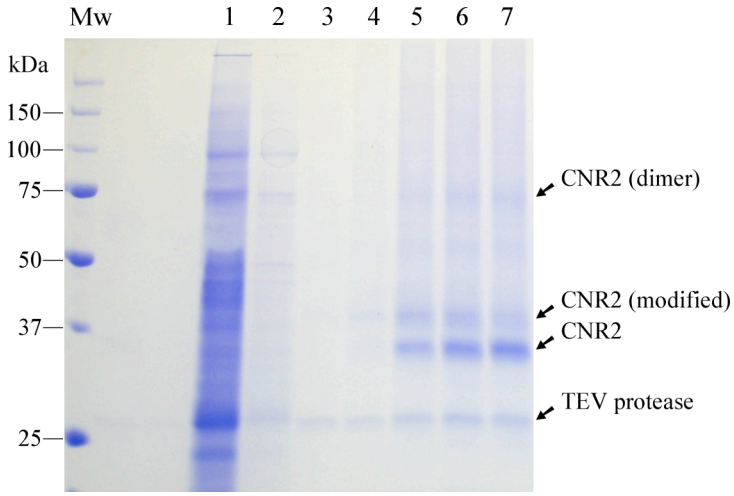

Figure 3. Time course of CNR2 release by the TEV protease

CNR2 was solubilized, bound to streptavidin-agarose beads; the beads were washed, and samples were taken and denatured with SDS sample buffer at different time points after addition of the TEV protease. Lane 1: solubilized proteins; lane 2: time 0 after addition of the TEV protease; lane 3: 1 hour after addition; lane 4: 2 hours; lane 5: 3 hours; lane 6: 14 hours (overnight).

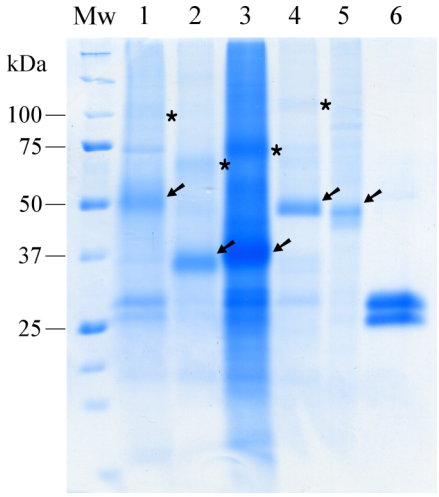

Figure 4. **Several purified GPCRs**

Proteins purified with streptavidin-coated beads were separated by SDS-PAGE and stained with Coomassie blue. Lane 1: NK3R_HUMAN; lane 2: P2Y1_HUMAN; lane 3: OPRK_HUMAN; lane 4: HRH1_HUMAN; lane 5: ADA2B_HUMAN; lane 6: TEV protease control. Arrows point to GPCR monomers and asterix indicate GPCR dimers.

Receptor	Measured masses	Sequence
OPRK	1086.536	157-165
	1176.577	362-371
	1389.618	340-349
	1431.763	360-371
CNR2	758.386	229-235
	971.483	345-352
	1045.551	229-237
	1243.616	322-333
	1333.612	307-317
	1542.740	215-228
	2075.997	334-352
	2109.026	14-32
ADA2B	854.459	58-65
	980.569	23-30
	1055.676	140-150
	1186.689	254-264
	1320.670	163-174
	1342.804	254-265
	1395.967	241-263
	1722.032	175-191
	1822.928	158-174
	2202.289	117-139
	2441.589	126-150

Table 1. Tryptic fragments observed by MS

Tryptic fragments were obtained and analyzed by MALDI mass spectrometry, as described in the Experimental Procedures section, for the following receptors: OPRK_HUMAN, CNR2_HUMAN and ADA2B_HUMAN.

Receptor	Yield (mg)
CNR2_HUMAN	0.90
NK1R_HUMAN	0.05
NK3R_HUMAN	0.40
ADA2B_HUMAN	0.20
ADA1B_MESAU	0.10
HRH1_HUMAN	0.50
D2DR_HUMAN	0.05
P2Y1_HUMAN	0.50
OPRD_HUMAN	0.70
OPRK_HUMAN	0.80

Table 2. Purification yields for 10 GPCRs

The yields are expressed in mg of purified GPCR, obtained from 1 liter of induced culture.

Chapter 6

GPCR–Gα fusion proteins

6.1 Introduction

Strosberg's group[313] was the first to construct and express a GPCR–Gα fusion protein. In their seminal paper, Bertin *et al.*[313] showed that a fusion protein of the β_2AR and $G_s\alpha_S$ was more efficient in stabilizing high-affinity agonist-binding and stimulating adenylate cyclase when expressed in $G_s\alpha$-deficient S49 *cyc*$^-$ lymphoma cells than non-fused β_2AR expressed in S49 wild-type cells. These data were tantalizing in view of the fact that, in S49 wild-type cells, there is an ~100-fold molar excess of $G_s\alpha$ relative to β_2AR[314], whereas in the fusion protein, there is only a 1:1 stoichiometry of the signalling partners.

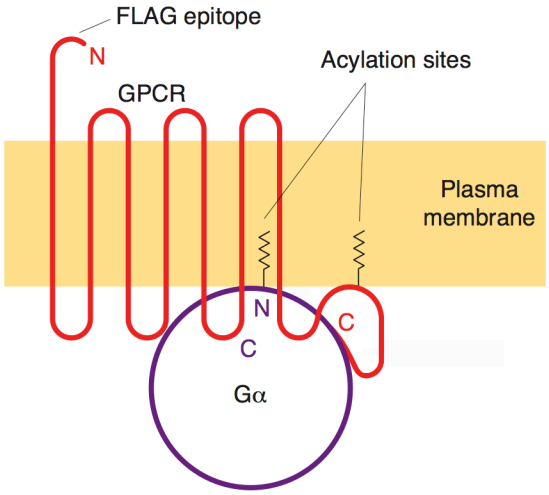

Figure 6.1. Assumed two-dimensional topology of GPCR–Gα fusion proteins in the plasma membrane. The GPCR portion of the fusion protein is shown in red, the G protein α-subunit in purple. N and C in red and purple designate the locations of the N- and C-termini of GPCR and Gα, respectively. GPCRs are C-terminally palmitoylated and G protein α-subunits are N-terminally myristoylated or palmitoylated, or both. Acylation tethers the proteins to the membrane. The FLAG epitope allows immunological detection of fusion proteins with monoclonal antibodies. (Adapted from Seifert *et al.*, 1999)

Fusion proteins are generated by linking the GPCR C-terminus, which is located intracellularly, to the N-terminus of Gα[313,315-325]. This is achieved by fusing the open reading frame of the two proteins using DNA restriction enzyme and polymerase chain reaction

(PCR)-based techniques. Figure 6.1 illustrates the two-dimensional topology of GPCR–Gα fusion proteins in the plasma membrane. In most GPCRs, the second and third intracellular loops are crucial for G protein coupling[326-329], although the first intracellular loop and the C-terminus can also be involved[330-332]. With respect to Gα, the extreme C-terminus is essential for receptor coupling[329,333]. Thus, the GPCR C-terminus must bend backwards towards the membrane and GPCR core in order to allow interaction of the non-constrained C-terminus of Gα with the cytosolic domains of the GPCR.

The most salient properties of GPCR–Gα fusion proteins are: (i) the defined 1:1 stoichiometry of the signalling partners; (ii) the close physical proximity of the signalling partners, and (iii) the tight tethering of Gα to the membrane.

The fusion protein technique has been applied successfully to a number of mammalian GPCRs, i.e. the β_2-adrenoreceptor[313,315,316,323-325,334-336], α_{2A}-adrenoreceptor[318-322,337,338], adenosine A_1 receptor[339,340], $5HT_{1A}$ receptor[341,342], type 1 and 4 opioid receptors[336], dopamine D_1 receptor[336], *N*-formyl peptide receptor[343,344], nociceptin receptor[345], M_2 muscarinic acetylcholine receptor[346] and α-factor receptor (Ste2) from yeast[317]. With respect to Gα, the short ($G_s\alpha_S$) and long ($G_s\alpha_L$) splice variants of $G_s\alpha$[313,315,316,323-325,334-336], the G_i/G_o-proteins $G_i\alpha_1$, $G_i\alpha_2$, $G_i\alpha_3$, and $G_o\alpha_1$[318-322,336-346] and the yeast G protein Gpa[317] have been fused to, and shown to functionally interact with, GPCR partners.

These data show that the fusion protein approach can be applied to many GPCRs and G protein α-subunits.

In addition, Rosenbaum and co-workers recently stressed in their seminal paper[3] the next challenge for the GPCR research community: "A full understanding of the structural basis of GPCR activation will require a high-resolution structure of a complex between a receptor with an agonist bound and its G protein, as well as methods to assess the dynamics of their interaction."

Hence, to improve GPCR stability and to facilitate their purification as well as their crystallisation (by increasing polar surface area), I thought it would be interesting to express different GPCR–Gα fusion proteins in *Pichia pastoris*.

6.2 Results & Discussion

Three different GPCRs from the MePNet collection, namely the human adenosine A_{2A} receptor (AA2AR), the dopamine D_2 receptor (D2DR), and the rat neurokinin-2 receptor (NK2R), were fused to the short and long $G_s\alpha$, $G_{oA}\alpha$, and $G_q\alpha$ or $G_{q(Q209L)}\alpha$, respectively. All

these fusion proteins were successfully expressed in *Pichia pastoris* at their expected size, i.e. 110-120 kDa, as shown in Figure 6.2 and 6.3 (upper panel).

Single-point radioligands binding assays also showed that these fusion proteins were able to bind antagonists (Fig. 6.3, lower panel).

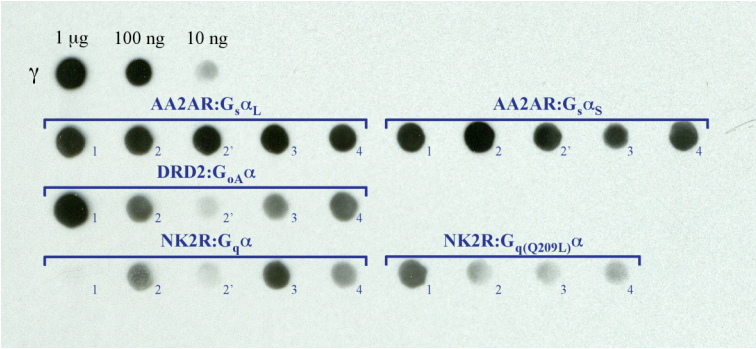

Figure 6.2. Dot-blot experiments on *P. pastoris* clones expressing different GPCR:Gα fusion proteins. Top row (γ): concentration range of β_2AR membranes (25 pmol/mg). Immunoblot analysis was performed using the M2 anti-FLAG antibody as described in Chapter 3.

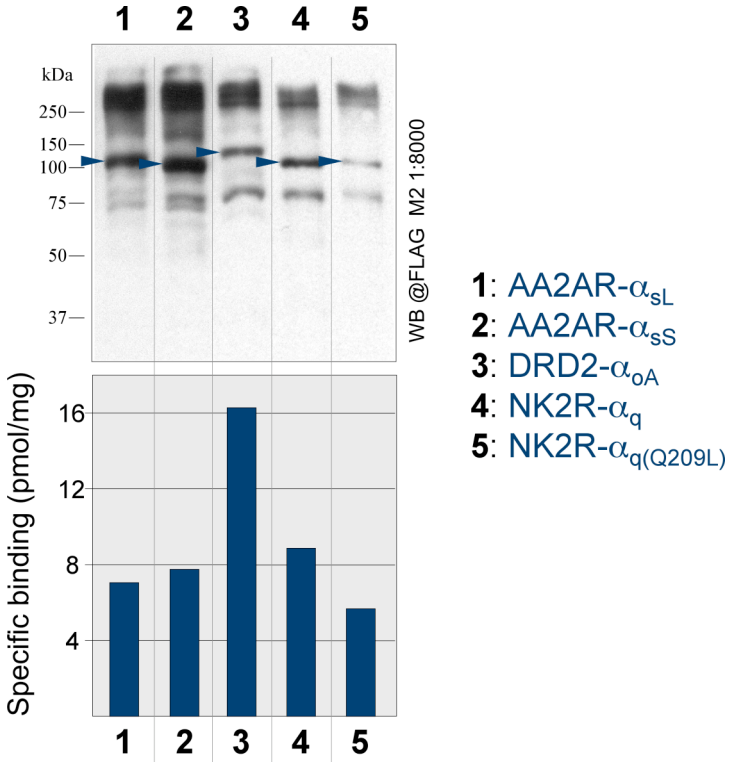

Figure 6.3. upper panel, Immunoblot analysis of membrane proteins prepared from recombinant *P. pastoris* cells expressing different GPCR:Gα fusion proteins. *Pichia* membranes were separated by SDS-PAGE, transferred to a nitrocellulose filter, and probed using the M2 anti-FLAG antibody as described in Chapter 3. Fusion proteins are indicated by arrows. Molecular mass markers (kDa) are shown on the left side. Each lane was loaded with 10 µg of membrane protein. **lower panel**, Saturation radioligand binding assays on AA2AR-$\alpha_{sL/S}$, DRD2-α_{oA}, NK2R-$\alpha_{q/q(Q209L)}$ by using [^{3}H]ZM241385 (10 nM), [^{3}H]spiperone (10 nM) and [^{3}H]SR48698 (20 nM), respectively.

However, only agonist-stimulated binding of [^{35}S]Guanosine-5′-*O*-(3-thio)triphosphate binding assays ([^{35}S]GTPγS) would assess the functionality of such fusions. For this purpose, and to have further insights onto the DRD2:$G_{oA}\alpha$ and AA2AR:$G_s\alpha$ fusion proteins, we initiated collaboration with Prof. Philip G. Strange (School of Pharmacy, University of Reading, UK), who has been working on the function of the human dopamine D_2 receptor since the early 1980s. Highlights of his research include purification of the dopamine D_2 receptor from brain in 1988[305], showing that antipsychotic drugs are inverse agonists at the D_2 receptor in 1997[45], and that the D_2 receptor is a functional dimer in 2001[347]. A fairly preliminary draft presents the results obtained on the DRD2:$G_{oA}\alpha$ fusion protein (see further Chapter 6, pages 114-128). Ongoing studies also show promising results for the AA2AR:$G_s\alpha$ fusion protein; in particular we retrieve, as it was the case for the D_2-α_o fusion, a clear response to agonists and a B_{max} value 8-10-fold higher than for the receptor expressed alone. As the estimated quantities of receptor in the membranes are roughly the same for the receptor and the corresponding fusion, we can assume that fusing a Gα subunit to its corresponding GPCR seems to enhance GPCR functionality when expressed in *Pichia pastoris*. With such B_{max} values, i.e. ~100-200 pmol/mg, it could be conceivable to think of a purification process that would involve a ligand affinity chromatography as a second or third step. By doing this, it will allow to purify a GPCR fusion protein to homogeneity, which is an important factor in obtaining well-diffracting crystals. Despite the quite disappointing results obtained by the first purification trials using IMAC resins in batch (data not shown), we should go further in this direction.

AA2AR and DRD2 were also co-expressed in *Pichia pastoris* with their Gα subunits ($G_s\alpha$ and $G_{oA}\alpha$, respectively). As for GPCR–Gα fusions, the basic premise was to enhance stability of the expressed receptors. Gα subunits were detected in both cytosolic and membrane fractions (Fig. 6.4a). However, in the case of *Pichia* membranes co-expressing DRD2 and palmitoylated Gα, no response to dopamine was detected by Philip G. Strange (Fig. 6.4b), suggesting different stoichiometric expression patterns and/or insertion of the two partners in different membrane compartiments.

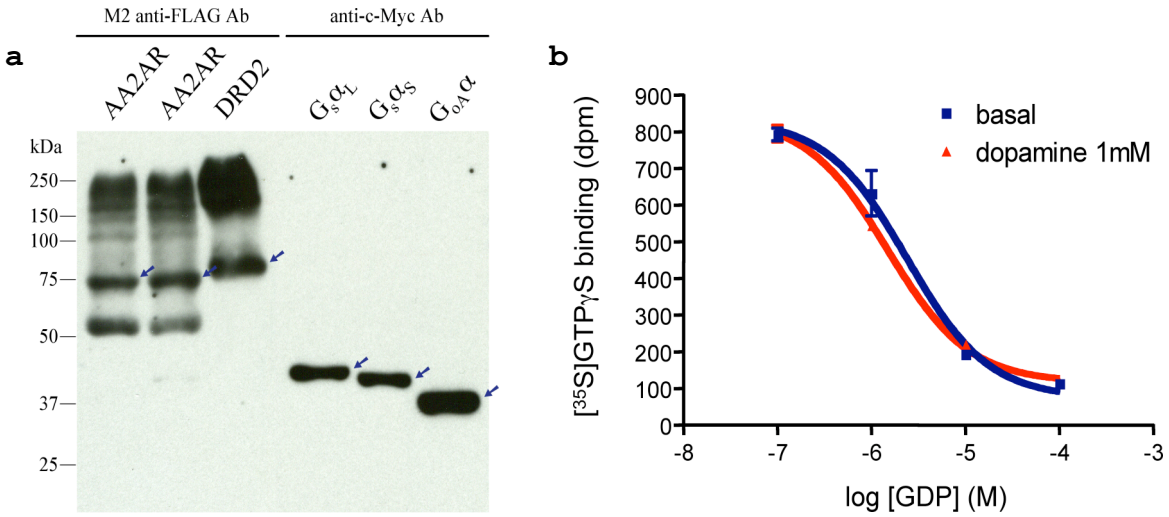

Figure 6.4. a, Immunoblot analysis of membrane proteins prepared from recombinant *P. pastoris* cells co-expressing either AA2AR/$G_s\alpha_{L/S}$ or DRD2/$G_{oA}\alpha$. *Pichia* membranes were separated by SDS-PAGE, transferred to a nitrocellulose filter, and probed using either the M2 anti-FLAG antibody (for FLAG-tagged GPCRs) or anti-c-Myc antibody (for c-Myc-tagged α subunits) as described in Chapter 3. AA2AR, DRD2, $G_s\alpha_{L/S}$ and $G_{oA}\alpha$ are indicated by arrows. Molecular mass markers (kDa) are shown on the left side. Each lane was loaded with 10 μg of membrane protein. **b**, Effect of dopamine on [^{35}S]GTPγS binding to membranes co-expressing DRD2/$G_{oA}\alpha$.

Pharmacological analysis of a Dopamine D_2:$G_o\alpha$ Fusion Protein Expressed in *Pichia pastoris*

Cédric Fiez-Vandal[*2], Tara Mills[*1], Hong Lin[1], Elodie Kara[1], Renaud Wagner[2] and Philip G. Strange[1+]

[1]School of Pharmacy, University of Reading, PO Box 228, Whiteknights, Reading, RG6 6AJ, UK

[2]LC1-UMR 7175, Institut Gilbert Laustriat, ESBS, Bd Sébastien Brandt, BP 10413, 67412 Illkirch Cedex, France

[*]These authors contributed equally to the work presented in this manuscript.

[+]To whom correspondence should be addressed:
Prof. Philip G. Strange
Tel: +44 11 8378 6537
E-mail: p.g.strange@reading.ac.uk

Author Keywords: D_2 dopamine receptor; G protein-coupled receptor; Fusion protein; *Pichia pastoris*; [^{3}H]Spiperone binding; [^{35}S]Guanosine-5′-*O*-(3-thio)triphosphate binding

Abbreviations: D_2, dopamine D_2 receptor; D_2-α_o, dopamine D_2 receptor:$G_o\alpha$ fusion protein; GPCR, G protein-coupled receptor; GTPγS, Guanosine-5′-*O*-(3-thio)triphosphate ; NMDG, N-methyl-D-glucamine

INTRODUCTION

The G protein-coupled receptors (GPCRs) constitute a large super-family of proteins involved in the detection of many kinds of signalling molecules (e.g. hormones, neurotransmitters). Signalling depends on the interaction of a GPCR with a G protein and alteration of the activity of intracellular effector molecules such as adenylate cyclase and phospholipase C. There is increasing evidence that GPCRs themselves may form oligomers although the importance of these oligomers for signalling is still under debate (Milligan,

2007). Also there has been recent evidence that GPCRs and their G proteins may stay associated during signalling (Gales et al., 2006).

In order to study the signalling processes more clearly we have expressed GPCRs in well-defined heterologous expression systems. The GPCR we have studied most in this context is the D_2 dopamine receptor. This is an important site for the physiological actions of dopamine as well as a key target for drug action (e.g. anti-parkinsonian drugs, antipsychotic drugs). We have expressed this receptor in both Sf9 insect cells using the baculovirus expression system and in *Schizosaccharomyces pombe* (Gazi et al., 2003; Presland and Strange, 1998). Although we were able to use these systems to obtain some interesting data, the expression levels were not very high for this receptor and we sought another system. GPCRs have been expressed at high levels in the yeast *Pichia pastoris* and the receptors appear to be expressed with fidelity (Fraser, 2006). In this study, we report the expression of the D_2 dopamine receptor at high levels in *P. pastoris* and the characterisation of the expressed receptor.

MATERIALS & METHODS

Materials

[^{35}S]GTPγS (~37 TBq.mmol^{-1}) and [^{3}H]spiperone (~600 GBq.mmol^{-1}) were purchased from Amersham Biosciences (Buckinghamshire, UK). [^{3}H]nemonapride (83-85 Ci/mmol) was purchased from NEN (Boston, MA). Optiphase HiSafe-3 scintillation fluid was purchased from Perkin-Elmer Life Sciences (Cambridge, UK). Dopamine, bromocriptine, AJ-76 and UH-232 were purchased from Tocris (Bristol, UK). N-methyl-D-glucamine, p-tyramine and (-)-3-PPP were purchased from Sigma-Aldrich (Dorset, UK).

The G protein alpha oA ($G_{oA}\alpha$) cDNA was purchased from the UMR cDNA Resource Center (clone ID: GNA0OA0000), the pCR4Blunt TOPO vector was from Invitrogen, the modified pPIC9K vector containing the DRD2_HUMAN cDNA was obtained from the MePNet consortium (Lundstrom et al. 2006) and the pPICZG was derived from the pPICZA (Invitrogen). Plasmids were propagated in a TOP10 *E. coli* strain (Invitrogen) and prepared using the Nucleospin purification kit (Macherey-Nagel). Restriction, modification and ligation enzymes were purchased from Fermentas Life Sciences, whereas the PrimeSTAR HS DNA polymerase used for PCR amplification was from Takara and oligonucleotides from Sigma-Genosys.

The protease-deficient *Pichia pastoris* strain SMD1163 (*his4*, *pep4*, *prb1*) (Invitrogen) and SMD1163[pPIC9K-DRD2] from the MePNet collection were used for transformation and heterologous expression. Yeast nitrogen base and yeast extract were purchased from Difco, peptone and L-histidine from Sigma-Aldrich, zeocine from Invitrogen and dimethyl sulfoxide (DMSO) from Acros Organics. Complete EDTA-free protease inhibitor cocktail (PI) tablets were purchased from Roche, cholesterol and methyl-β-cyclodextrin (MβCD) were from Sigma-Aldrich. The bicinchoninic acid assay (BCA) kit was from Pierce and the Amplex Red cholesterol assay kit from Invitrogen. Nitrocellulose membrane was purchased from Millipore, the mouse M2 anti-FLAG and the rabbit anti-c-Myc monoclonal antibodies were from Sigma-Aldrich and the sheep anti-mouse IgG-horseradish peroxidase (HRP) conjugate from GE Healthcare. All other chemicals were obtained from Sigma-Aldrich.

Cloning of the pPIC9KF-DRD2:$G_{oA}\alpha$ and pPICZG-$G_{oA}\alpha$ vectors

The G protein alpha oA ORF was PCR amplified using specific primers with adapters introducing a unique *Spe*I and *Afl*II restriction sites at the 5' and 3' ends of the gene, respectively. The amplified DNA was cloned into a pCR4Blunt TOPO vector and sequence checked. After enzymatic restriction, the *Spe*I/*Afl*II fragment was then subcloned into either the pPIC9KF-DRD2 or pPICZG vectors resulting in the pPIC9KF-DRD2:$G_{oA}\alpha$ and pPICZG-$G_{oA}\alpha$ constructs.

Recombinant yeast clone selection and culturing

Following standard procedures, the pPIC9KF-DRD2:$G_{oA}\alpha$ and pPICZG-$G_{oA}\alpha$ integrative expression vectors were linearized using the *Pme*I restriction enzyme prior to electrotransformation of competent SMD1163 or SMD1163[pPIC9K-DRD2] strains, respectively. In the first case, recombinant SMD1163 clones bearing the pPIC9KF-DRD2:$G_{oA}\alpha$ construct were selected on their His^+ and G418 resistant phenotype as described previously (André et al. 2006). In the latter case, integrant clones bearing both the pPIC9K-DRD2 and the pPICZG-$G_{oA}\alpha$ were selected on YPD agar plates [1% (w/v) yeast extract, 2% (w/v) peptone, 2% (w/v) dextrose, 2% (w/v) agar] supplemented with 0.1 mg/ml zeocine.

Glycerol stocks of SMD1163 recombinant cells were plated on YPG agar plates and incubated overnight at 30 °C. The cells were used to inoculate a 2 L baffled flask containing 400 ml of BMGY medium [100 mM potassium phosphate pH 6.0, 1% (w/v) yeast extract,

2% (w/v) peptone, 1.34% (w/v) yeast nitrogen base without amino acids, 0.00004% (w/v) biotin, 1% (w/v) glycerol] and incubated overnight at 30 °C to an OD_{600} of 3-5. This starter was then diluted in 500 ml BMGY medium in 2 L baffled flasks and grown for 6-8 h to an OD_{600} of 4-5. The cells were spun down at 3,000 *g* for 20 min and the cell pellet was resuspended in 500 ml BMMY [similar to BMGY with the following changes: phosphate buffer at pH 8.0, 2.5% (v/v) dimethyl sulfoxide, 0.04% (w/v) histidine, and 0.5% (v/v) methanol instead of 1% glycerol]. The culture was incubated for 18 h at 18 °C and then harvested by centrifugation.

Membrane preparation

Cells were resuspended in ice-cold breaking buffer [50 mM Hepes-NaOH pH 7.4, 100 mM NaCl, 10% (w/v) glycerol, 2 mM EDTA, 1 mM PMSF, ligand, PI], and broken by vortexing with glass beads (8 x 1 min). The beads were removed from the cell suspension by passing the mixture through a chromatography column (Poly-Prep Column, Bio-Rad). Cell debris, including intact cells, were removed by a low speed spin (3,000 *g*) for 10 min. The supernatant was retained, and membranes isolated by centrifugation at 100,000 *g* for 30 min. Each membrane pellet was re-dissolved in a membrane buffer [50 mM Hepes-NaOH pH 7.4, 100 mM NaCl, 10% (w/v) glycerol] and flash frozen in liquid nitrogen for storage. Protein concentrations were determined by bicinchoninic acid (BCA) assay using bovine serum albumin as standard (Smith et al. 1985).

Cholesterol enrichment of membranes

In some cases, membranes were enriched with cholesterol using a water soluble cholesterol methyl-β-cyclodextrin (MβCD) complex prepared as described previously (Pucadyil and Chattopadhyay 2004), with a few modifications. Stock solutions of the cholesterol-MβCD complex (typically containing 5:30 mM cholesterol:MβCD) were prepared by dissolving the required amounts of cholesterol and MβCD in 50 mM Tris-HCl pH 7.4 by sonication (ten 30 s pulses at 50% amplitude with 30 s rest in between) and by constant shaking at room temperature. Stock solutions were freshly prepared before each experiment. Membranes were incubated overnight with the cholesterol-MβCD complex (final concentration 2.5:15 mM of cholesterol:MβCD) at a protein concentration of 2 mg/ml in 50 mM Tris-HCl pH 7.4 at 4 °C under constant shaking. Membranes were then spun down at 100,000 *g* for 20 min, washed once with 50 mM Tris-HCl pH 7.4 and resuspended in the

same buffer. Cholesterol content in membranes was estimated using the Amplex Red cholesterol assay kit (Amundson and Zhou 1999).

Western-blotting and immunodetection

Pichia membranes (*ca.* 10 μg) were diluted in NuPAGE LDS sample buffer (Invitrogen) before running on a 12% NuPAGE Bis-Tris gel with MES buffer (Invitrogen). They were subsequently electrophoretically transferred overnight for Western-blot analysis onto a nitrocellulose filter following the standard procedure (Towbin et al. 1992). Briefly, after electroblotting the membrane was blocked with 8% lowfat milk powder in PBST [10 mM Na_2HPO_4, 1.8 mM K_2HPO_4, pH 7.4, 140 mM NaCl, 2.7 mM KCl, 0.02% Tween 80, 1% (w/v) BSA] for 1 h at room temperature and washed three times for 5 min with PBST. Further, membrane was incubated with either M2 anti-FLAG antibody (diluted 1:8,000 in PBST) or anti-c-Myc antibody (diluted 1:600 in PBST), washed again three times for 5 min with PBST, and incubated with sheep anti-mouse IgG-HRP conjugated antibody (diluted 1:10,000 in PBST). The immunoblot bands were visualized using an enhanced chemiluminescence reagant (SuperSignal West Pico Kit, Pierce) according to the manufacturer's protocol.

Radioligand binding assays

Cell membranes (25 μg) were incubated in triplicate with [^{3}H]spiperone (~0.25 nM) and competing drugs in Hepes buffer [20 mM Hepes, 1 mM EGTA, 1 mM EDTA, 10 mM $MgCl_2$, 100 mM NaCl or 100 mM N-methyl-D-glucamine (NMDG, to maintain ionic strength in the absence of sodium ions (Nunnari et al., 1987)); pH 7.4 (using HCl) containing 0.1 mM dithiothreitol] in a final volume of 1 ml for 3 h at 25 °C. The assay was terminated by rapid filtration (through Whatman GF/C filters) using a Brandel cell harvester followed by four washes with 4 ml ice-cold phosphate-buffered saline (10 mM Na_2HPO_4, 1.8 mM K_2HPO_4, pH 7.4, 140 mM NaCl, 2.7 mM KCl) to remove unbound radioactivity. Filters were soaked in 2 ml of scintillation fluid for at least 6 hours and bound radioactivity was determined by liquid scintillation counting. Non-specific binding of [^{3}H]spiperone was determined in the presence of 3 μM (+)-butaclamol.

[^{35}S]GTPγS binding assays

Cell membranes (25 μg) were incubated in triplicate with ligands for 30 min at 30 °C in 0.9 ml of Hepes buffer containing 1 μM GDP and 100 mM NaCl, NMDG, LiCl, or KCl

where indicated. The assay was initiated by addition of 100 µl of diluted [^{35}S]GTPγS to give a final concentration of 50-100 pM. The assay was incubated for a further 30 min and terminated by rapid filtration as above.

Data analysis

Radioligand binding data were analysed using Prism (GraphPad) and were assumed to conform to a one-binding site model unless a statistically better fit could be obtained using a two-binding site model (P<0.05, F-test). In competition experiments that were fitted best by a one-binding site model, a single IC_{50} value was obtained, whereas in competition experiments that were fitted best by a two-binding site model, two IC_{50} values (for the higher and lower affinity sites) and the % higher affinity sites were obtained. The inhibition constants (K_i from the single IC_{50}, K_h, K_l from the IC_{50} values for the higher and lower affinity sites) were calculated from IC_{50} values, derived from competition binding analyses, using the Cheng-Prusoff equation (Cheng and Prusoff, 1973) as described in (Roberts et al., 2004). This corrects for the concentration of the radioligand ([^{3}H]spiperone) and its dissociation constant at the relevant binding site.

Data from [^{35}S]GTPγS binding experiments were fitted to a sigmoidal concentration/response curve with a Hill coefficient of one which provided the best fit to the data in all cases (P<0.05).

Statistical significance of differences between two data sets (e.g. two sets of pKi values) was determined using one way or two-way analysis of variance (ANOVA) followed by a Bonferroni post-test with significance determined as P<0.05.

RESULTS

Radioligand binding studies

Saturation analyses

Saturation ligand binding analyses on *P. pastoris* membranes expressing the D_2 dopamine receptor and a fusion of the D_2 receptor and the G protein subunit α_o (D_2-α_o) were carried out using two radioligands ([^{3}H]nemonapride and [^{3}H]spiperone) in buffers containing Na^+ and in buffers where Na^+ had been substituted by NMDG. In both cases, both radioligands gave saturable high affinity binding and the data were best-fitted by one-binding site models. For [^{3}H]spiperone, the dissociation constant was slightly increased by the substitution of Na^+ whereas the B_{max} was decreased. For [^{3}H]nemonapride, a similar pattern

was seen but the effects were greater. In the presence or absence of Na^+, the B_{max} values for the two radioligands were different. The B_{max} for expression of D_2-α_o was much higher than for D_2.

Competition analyses

Competition experiments with (+)-butaclamol, dopamine, nemonapride, quinpirole and raclopride were performed versus [^{3}H]spiperone using *P. pastoris* membranes expressing D_2 or D_2-α_o. In all cases, competition data were fitted best by one-binding site models. There was no effect of GTP on dopamine/[^{3}H]spiperone competition.

[^{35}S]GTPγS binding

Stimulation of [^{35}S]GTPγS binding by agonists was evident in membranes of *P. pastoris* expressing D_2-α_o but not in membranes expressing D_2 alone. Data for maximal effect and potency are given in Table 2.

Effects of cholesterol treatment on properties of membranes expressing D_2 receptors

P. pastoris membranes expressing D_2-α_o were treated with cholesterol as described in the Materials and Methods section. This increased the sterol content of the membranes from 2.6 to 10.8 μg/ml for membranes expressing D_2 and from 4.2 to 13.3 μg/ml for membranes expressing D_2-α_o.

In the cholesterol treated membranes, dopamine inhibition of [^{3}H]spiperone binding occurred with a Hill coefficient less than one although the competition curve was sensitive to effects of GTP. In [^{35}S]GTPγS binding experiments, agonist stimulation curves were flattened relative to controls.

DISCUSSION

We have expressed the D_2 dopamine receptor and a D_2-α_o fusion in *P. pastoris* at high levels. The ligand binding properties of the receptor are relatively normal in that competition experiments with a range of ligands show the usual rank order for a D_2 receptor although mostly the dissociation constants indicate reduce affinity.

In [^{35}S]GTPγS binding experiments no stimulation was seen with D_2 but with D_2-α_o stimulation was seen with typical dopamine agonists, although the potencies were reduced compared to mammalian expression systems.

In saturation binding analyses with [^{3}H]spiperone and [^{3}H]nemonapride we observed differences in B_{max} for the two radioligands and effects of Na^+ on the B_{max} values recorded. We have interpreted such effects in the past as evidence for negative cooperativity in an oligomer (Armstrong and Strange, 2001; Vivo et al., 2006).

When *P. pastoris* membranes expressing D_2-α_o were treated with cholesterol we observed a decrease in the Hill coefficient for agonists in both ligand binding and stimulation of [^{35}S]GTPγS binding. This may indicate increased interaction between protomers in a cooperative oligomer.

ACKNOWLEDGMENTS

We thank Juliette Kempf and Tania Steffan for their technical support. This research was funded by the Membrane Protein Network (MePNet) and the European Membrane Protein Consortium (E-MeP).

REFERENCES

Amundson DM and Zhou M (1999) Fluorometric method for the enzymatic determination of cholesterol. *J Biochem Biophys Methods* **38**(1):43-52.

André N, Cherouati N, Prual C, Steffan T, Zeder-Lutz G, Magnin T, Pattus F, Michel H, Wagner R and Reinhart C (2006) Enhancing functional production of G protein-coupled receptors in *Pichia pastoris* to levels required for structural studies via a single expression screen. *Protein Science* **15**(5):1115-1126.

Armstrong D and Strange PG (2001) Dopamine D2 receptor dimer formation: evidence from ligand binding. *J Biol Chem* **276**(25):22621-22629.

Cheng Y and Prusoff WH (1973) Relationship between the inhibition constant (K1) and the concentration of inhibitor which causes 50 per cent inhibition (I50) of an enzymatic reaction. *Biochem Pharmacol* **22**(23):3099-3108.

Fraser NJ (2006) Expression and functional purification of a glycosylation deficient version of the human adenosine 2a receptor for structural studies. *Protein Expr Purif* **49**(1):129-137.

Gales C, Van Durm JJ, Schaak S, Pontier S, Percherancier Y, Audet M, Paris H and Bouvier M (2006) Probing the activation-promoted structural rearrangements in preassembled receptor-G protein complexes. *Nat Struct Mol Biol* **13**(9):778-786.

Gazi L, Nickolls SA and Strange PG (2003) Functional coupling of the human dopamine D2 receptor with G alpha i1, G alpha i2, G alpha i3 and G alpha o G proteins: evidence for agonist regulation of G protein selectivity. *Br J Pharmacol* **138**(5):775-786.

Lowry O, Rosebrough N, Farr A and Randall R (1951) Protein measurement with the folin phenol reagent. *J Biol Chem* **193**:265-275.

Lundstrom K, Wagner R, Reinhart C, Desmyter A, Cherouati N, Magnin T, Zeder-Lutz G, Courtot M, Prual C, André N, Hassaine G, Michel H, Cambillau C and Pattus F (2006) Structural genomics on membrane proteins: comparison of more than 100 GPCRs in 3 expression systems. *Journal of Structural and Functional Genomics* **7**(2):77-91.

Milligan G (2007) A day in the life of a G protein-coupled receptor: the contribution to function of G protein-coupled receptor dimerization. *Br J Pharmacol*.

Nunnari JM, Repaske MG, Brandon S, Cragoe EJ, Jr. and Limbird LE (1987) Regulation of porcine brain alpha 2-adrenergic receptors by Na+,H+ and inhibitors of Na+/H+ exchange. *J Biol Chem* **262**(25):12387-12392.

Presland J and Strange PG (1998) Pharmacological characterisation of the D2 dopamine receptor expressed in the yeast Schizosaccharomyces pombe. *Biochem Pharmacol* **56**(5):577-582.

Pucadyil TJ and Chattopadhyay A (2004) Cholesterol modulates ligand binding and G protein coupling to serotonin$_{1A}$ receptors from bovine hippocampus. *Biochimica et Biophysica Acta (BBA) - Biomembranes* **1663**(1-2):188-200.

Roberts DJ, Lin H and Strange PG (2004) Investigation of the mechanism of agonist and inverse agonist action at D2 dopamine receptors. *Biochem Pharmacol* **67**(9):1657-1665.

Towbin H, Staehelin T and Gordon J (1992) Electrophoretic transfer of proteins from polyacrylamide gels to nitrocellulose sheets: procedure and some applications. *Biotechnology* **24**:145-149.

Vivo M, Lin H and Strange PG (2006) Investigation of cooperativity in the binding of ligands to the D(2) dopamine receptor. *Mol Pharmacol* **69**(1):226-235.

	B_{max} ± sem (pmol/mg protein)			
Radioligand	[^{3}H]spiperone		[^{3}H]nemonapride	
Buffer	Na^+	NMDG	Na^+	NMDG
D_2	11.54±0.48	9.62±0.79	13.36±0.33	7.46±0.44
D_2-α_o fusion	73.73±5.46	79.47±6.62	88.23±4.98	57.32±3.72

	pK_d ± sem (K_d, nM)			
Radioligand	[^{3}H]spiperone		[^{3}H]nemonapride	
Buffer	Na^+	NMDG	Na^+	NMDG
D_2	9.78±0.03 (0.17)	9.49±0.03 (0.32)	10.28±0.05 (0.05)	9.00±0.05 (0.99)
D_2-α_o fusion	9.63±0.06 (0.23)	9.36±0.03 (0.44)	9.89±0.03 (0.13)	8.79±0.02 (1.62)

Table 1. Saturation radioligand binding studies on D_2 dopamine receptors expressed in *P. pastoris*. Saturation binding analyses with either [^{3}H]spiperone or [^{3}H]nemonapride were performed in buffers containing Na^+ or NMDG as described in the Materials and Methods section. Values for B_{max} and pK_d are shown with the sem from 3 experiments.

	pK_i ± sem (K_i)			
	D_2		D_2-α_o fusion	
	Na+	NMDG	Na+	NMDG
(+)-butaclamol	8.92±0.04 (1.2 nM)	8.97± 0.04 (1.1 nM)	8.72±0.05 (1.9 nM)	8.85±0.05 (1.4 nM)
Dopamine	4.72±0.18 (19.1 μM)	4.25±0.02 (56.2 μM)	4.35±0.08 (44.7μM)	4.19±0.05 (64.6μM)
Nemonapride	9.08±0.02 (0.83 nM)	7.54±0.01 (28.8 nM)	8.77±0.04 (1.7 nM)	7.36±0.03 (43.7nM)
Quinpirole	4.79±0.06 (16.2 μM)	4.62±0.02 (24.0 μM)	4.58±0.07 (26.3μM)	4.56±0.06 (27.5 μM)
Raclopride	8.06±0.02 (8.7 nM)	6.07±0.03 (851 nM)	7.68±0.07 (20.9 nM)	5.92±0.06 (1.2 μM)

Table 2. Competition radioligand binding studies on D_2 dopamine receptors expressed in *P. pastoris*. Competition binding analyses versus [^{3}H]spiperone were performed in buffers containing Na^+ or NMDG as described in the Materials and Methods section. Values for pK_i are given with the sem from three experiments.

	control			with cholesterol		
	$logEC_{50}$	Hill slope	n	$logEC_{50}$	Hill slope	n
dopamine	-4,29 ± 0,06	0,77 ± 0,05	7	-3,06 ± 0,24***	0,35 ± 0,03***	3
NPA	-6,46 ± 0,05	1,06 ± 0,07	3	-6,66 ± 0,24	0,54 ± 0,13*	3
aripiprazole	-6,53 ± 0,22	0,78 ± 0,08	7	-6,63 ± 0,1	0,86 ± 0,16	4

Table 3. Agonist stimulation of [^{35}S]GTPγS binding to membranes of *P. pastoris* expressing D_2-α_o: effect of cholesterol treatment. [^{35}S]GTPγS binding experiments were performed using control membranes and membranes treated with cholesterol as described in the Materials and Methods section. The values are expressed as mean ± sem. n represents the number of experiments. An unpaired t-test has been used to compare the values obtained with or without cholesterol. *p<0.05; ***p<0.001

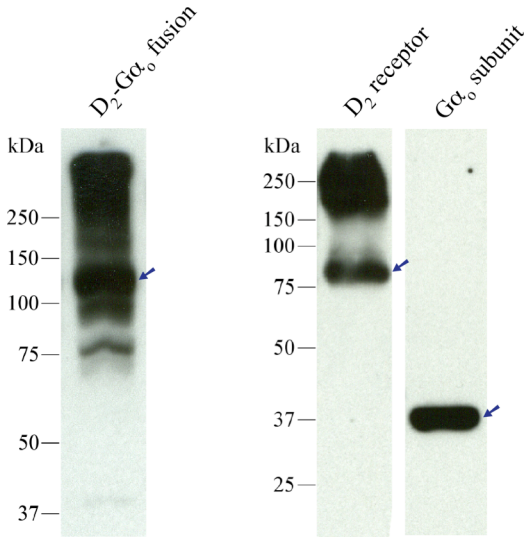

Figure 1. Immunoblot analysis of membrane proteins prepared from recombinant *P. pastoris* cells (SMD1163) either producing the D_2-α_o fusion protein (left) or co-expressing D_2 and α_o subunit (right). *Pichia* membranes were separated by SDS-PAGE, transferred to a nitrocellulose filter, and probed using either the M2 anti-FLAG antibody (for FLAG-tagged D_2-α_o fusion and D_2) or anti-c-Myc antibody (for c-Myc-tagged α_o subunit) as described in the Materials and Methods section. D_2-α_o, D_2 and α_o subunit are indicated by arrows. Molecular mass markers (kDa) are shown on the left side. Each lane was loaded with 10 μg of membrane protein.

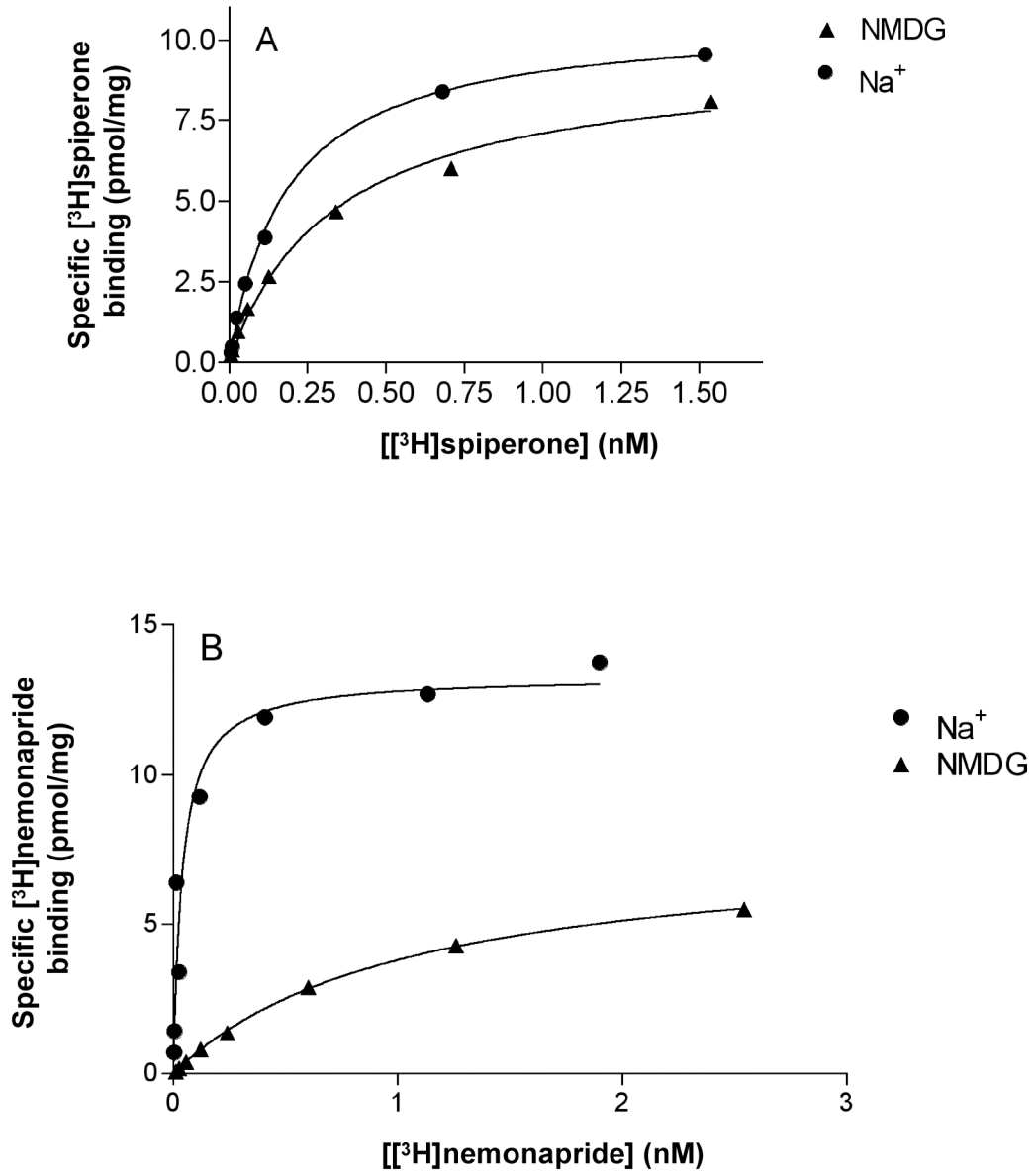

Figure 2. Saturation binding of [^{3}H]spiperone (A) and [^{3}H]nemonapride (B) to membranes of *P. pastoris* expressing D_2 dopamine receptors. Saturation binding analyses were performed in the presence of Na^+ ions or NMDG as described in the Materials and Methods section and the best-fit curves to one binding site models are shown. Data are from representative experiments replicated as indicated in Table 1.

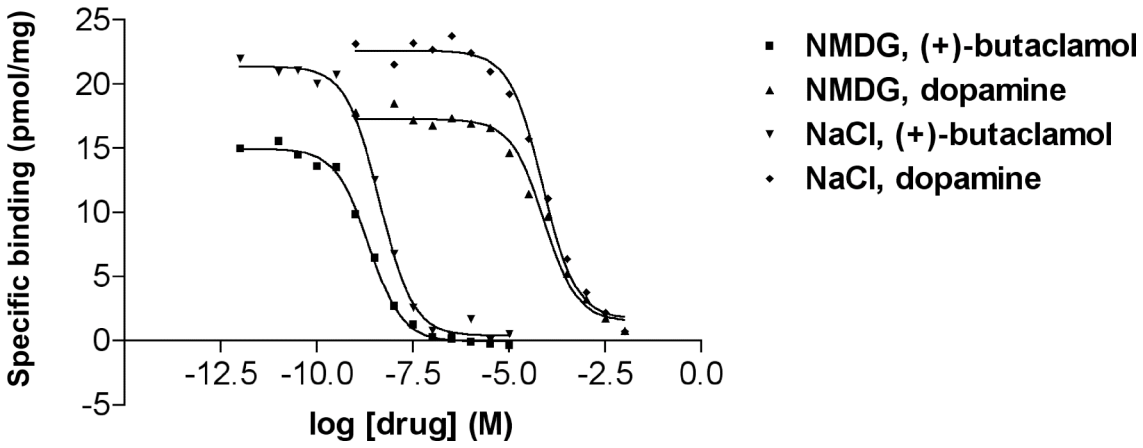

Figure 3. Competition of dopamine and (+)-butaclamol versus [^{3}H]spiperone to membranes of *P. pastoris* expressing D_2-α_o fusion. Competition binding analyses were performed in the presence of Na^+ ions or NMDG as described in the Materials and Methods section and the best-fit curves to one binding site models are shown. Data are from representative experiments replicated as indicated in Table 2.

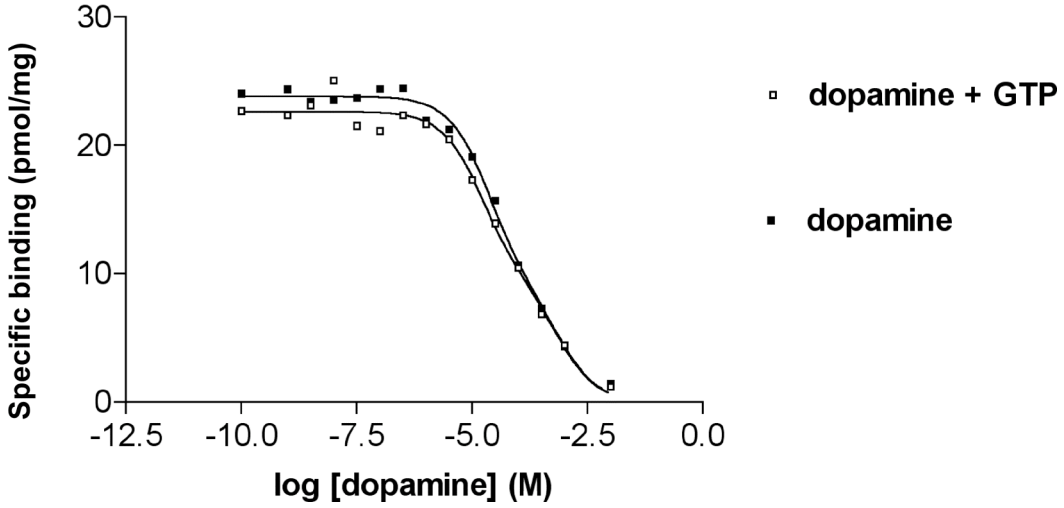

Figure 4. Competition of dopamine versus [^{3}H]spiperone to membranes of *P. pastoris* expressing D_2-α_o fusion treated with cholesterol. Competition binding analyses were performed in the presence of Na^+ ions in the presence or absence of GTP (100 μM) as described in the Materials and Methods section and the best-fit curves to one binding site models are shown.

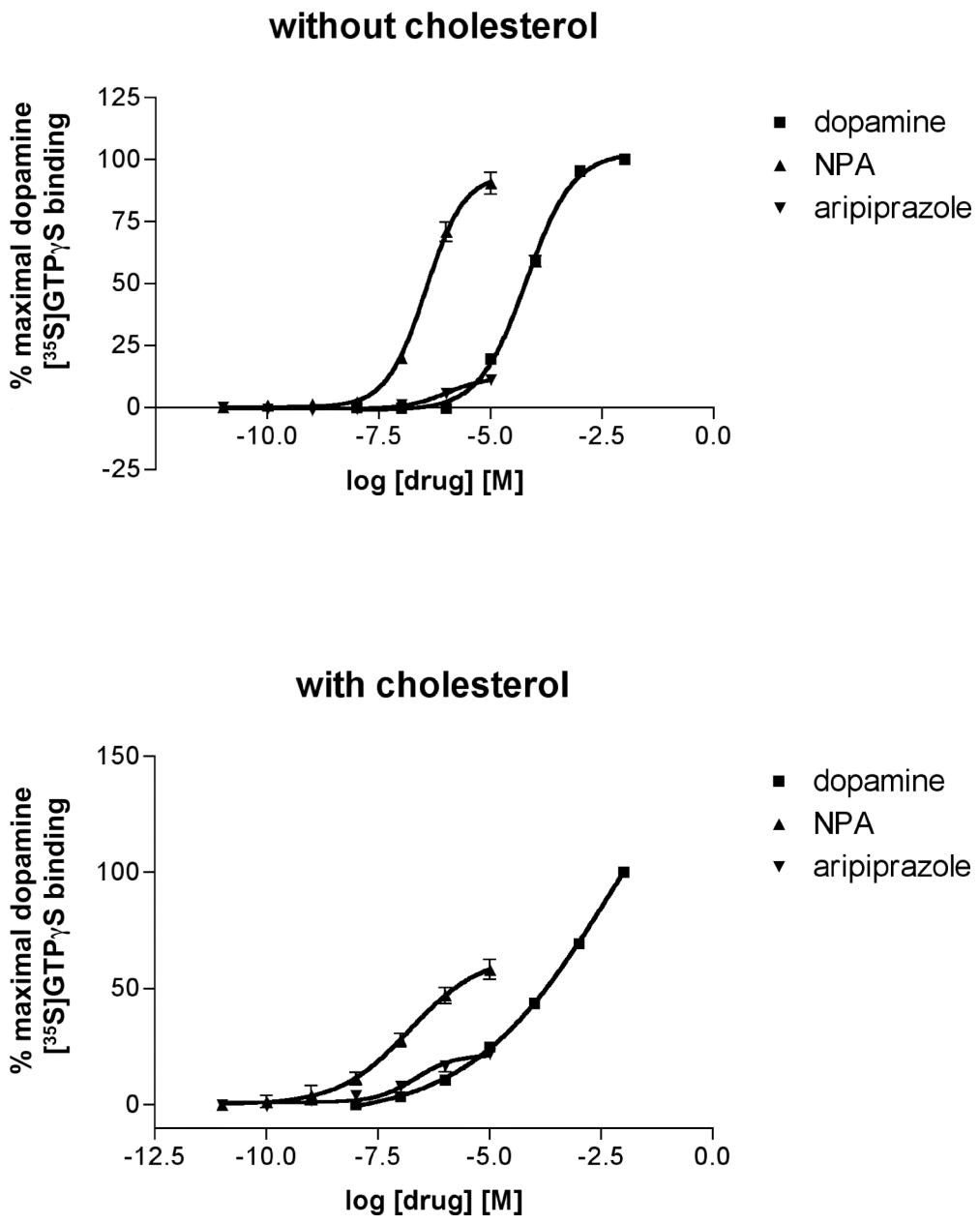

Figure 5. Agonist stimulation of [^{35}S]GTPγS binding to membranes of *P. pastoris* expressing D_2-α_o: effect of cholesterol treatment. [^{35}S]GTPγS binding experiments were performed using control membranes and membranes treated with cholesterol as described in the Materials and Methods section. The data are the mean ± sem of three experiments.

Chapter 7

OmpA–GPCR fusion proteins

7.1 Introduction

Last spring I thought of fusing OmpA, the smallest and also the best-characterized bacterial outer membrane protein, to the N-terminal end of the human dopamine D_2 receptor long isoform (DRD2). Hence, I asked Prof. Dr. Georg E. Schulz (Albert-Ludwigs-Universität Freiburg) for the plasmid carrying the triple mutant OmpA171t last June (without, of course, informing him of what I had in mind!). But before we go any further, allow me to briefly introduce this porin.

The outer membrane protein A from *Escherichia coli* (OmpA) belongs to a large family of homologous bacterial proteins. Apart from being very abundant, OmpA stabilizes the outer membrane[348], participates in bacterial conjugation[349,350], functions as a receptor for bacteriophages[351] and colicines[352], as well as mediates virulence and pathogenicity[353,354]. OmpA has therefore served as an important model for studying membrane protein folding[355,356]. The structure of its membrane domain (OmpA171, residues 1 to 171) had been established at 2.5 Å resolution[357] using an engineered triple mutant (OmpA171t) whose crystal properties had been decisively improved[358]. Residues 1-171 form a regular eight-stranded β-barrel in the outer membrane and their mode of assembly resembles that of a reversed micelle with large water-filled cavities (Fig. 7.1). The remaining residues, 172-325, are suggested to provide the binding site for the periplasmic peptidodoglycans.

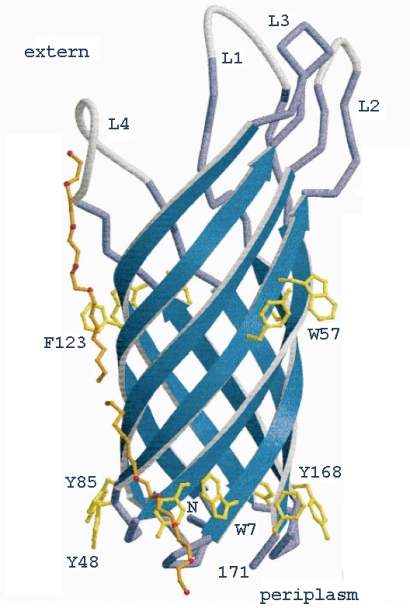

Figure 7.1. Ribbon representation of the OmpA transmembrane domain. The protein resembles a cylinder with a diameter of 26 Å and a length of 57 Å. β-strands are drawn in blue, loops in magenta and the aromatic girdle in yellow. The highly mobile loop moieties are grey. The modeled detergent molecule (orange, oxygen atoms red) and its symmetry-related neighbor are included. (Adapted from Pautsch and Schulz, 1998)

Since GPCR TM1 and TM7 are physically very close to each other (as exemplified by the structures of the bovine rhodopsine[1] and the β_2-adrenoreceptor[2,3]), my idea was to insert a small β-barrel in the vicinity of these two helices. By doing so one would expect to reduce domain swapping, aggregation, and higher-order oligomerization from the earliest stages of GPCR biogenesis in the endoplasmic reticulum and the Golgi, to their final insertion in the plasma membrane.

Moreover, N-terminal ends of most GPCRs are known to interact in a flexible fashion with extracellular helices, rendering efficient accessibility to tag fusions at these N-terminal parts somehow tedious. My second objective was therefore to fuse the FLAG and decahistidine tags onto the N-terminal end of OmpA, which in turn would be fused to the N-terminal domain of DRD2, thereby facilitating the purification of a such multi-fusion protein.

In the case in which this latter would be easy to purify, my final goal was to perform crystallization trials in bicelles or in a lipidic-cubic phase.

For instance, such targeted protein engineering was very successful in providing a high-resolution structure of β_2AR, in which the third intracellular loop was replaced by the T4 lysozyme, a well-folded protein that restricted the movement of TM5 and TM6 (Fig. 7.2) (see Chapter 1, paragraph 1.6).

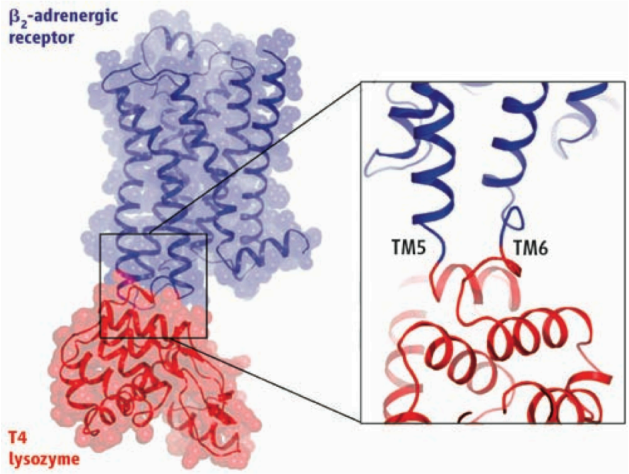

Figure 7.2. Replacement of an intracellular loop of the β_2-adrenergic receptor with a T4 lysozyme stabilized two flexible helices (5 and 6), thus allowing crystallization of the fusion protein and determination of its structure. (Rosenbaum *et al.*, 2007)

7.2 Results & Discussion

Preliminary expression results in *Pichia pastoris* show that, surprisingly, the OmpA–DRD2 fusion protein was successfully expressed (at its correct calculated size, i.e. ~115 kDa) and inserted in the *Pichia* membrane. Indeed, OmpA–DRD2, FLAG epitope (N-ter) and Bio-tag (C-ter) were detected by immunodetection with M2 anti-FLAG antibody and alkaline phosphatase-linked streptavidin, respectively (Fig. 7.3). These results are surprisingly amazing, because β-barrel membrane proteins are always inserted into the outer membrane of bacteria, mitochondria and chloroplasts by pre-existing translocation machineries that do not exist in yeast. This is probably the first successful expression trial of a β-barrel protein using a yeast system!

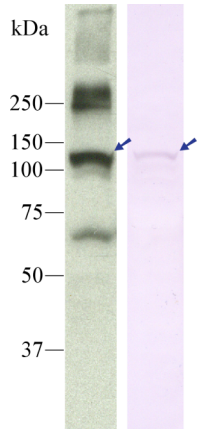

Figure 7.3. Immunoblot analysis of membrane proteins prepared from recombinant *P. pastoris* cells producing the OmpA–D_2 fusion protein. *Pichia* membranes were separated by SDS-PAGE, transferred to a nitrocellulose filter, and probed using either the M2 anti-FLAG antibody (left) or an alkaline phosphatase-linked streptavidin (right) as described in Chapter 3. OmpA–D_2 is indicated by arrows. Molecular mass markers (kDa) are shown on the left side. Each lane was loaded with 10 µg of membrane protein.

I cannot prove, at least not for the moment, that OmpA is correctly folded in the membrane, as there is no functional test for this protein yet. Nevertheless, taking into consideration the overall results of Western-blotting assays, where there is clearly no visible proteolytic degradation, it would be reasonable to assume that OmpA is correctly folded in the membranes. However, only circular dichroism measurements of the purified OmpA–DRD2 fusion in its detergent micelle should be able to assess the presence of β-sheets and prove their correct folding.

A second fusion construct between OmpA and our best expressed and easy to purify receptor, the human cannabinoid receptor type-2 (CNR2), was also successfully expressed (data not shown).

Purification trials using IMAC (batch or FPLC), streptavidine-coated beads and ion exchange chromatography are still ongoing, but the preliminary results are quite encouraging.

Chapter 8

Summary and Outlook

During the course of this study, successful production and isolation strategies for recombinant GPCRs have been established. Indeed, the yeast *Pichia pastoris* was demonstrated to be a reliable expression system for many different GPCRs, yielding large amounts of membrane-bound active protein, regardless of whether cultures were managed in shake flasks or in bioreactors. In some cases, GPCRs were purified in milligram quantities, implying that quantity should no longer be a major impediment to determining a structure.

However, since the receptor aggregation problem was not completely solved, further efforts in this direction are needed. For instance, it would be interesting to address the question of receptor (higher order) oligomerization by means of FRET or BRET experiments, which have proven informative in the case of some other GPCRs (for a review, see[359]) and which could ultimately provide interesting insights concerning the endogenously active form of GPCRs when expressed in *Pichia*.

Another major barrier in crystallography involves stabilizing a particular conformation of the protein that enables the growth of diffractable crystals. For example, a key feature in the crystallization of β_2AR was the presence of the β-blocker carazolol, an inverse agonist, and the replacement of the third intracellular loop with a T4 lysozyme, which both contributed to stabilizing the active conformation of the receptor.

Similar strategies were used in this work in order to stabilize GPCRs; in particular, we engineered different GPCR–Gα and OmpA–GPCR fusion proteins. These constructions were successfully expressed in *Pichia pastoris* and pharmacological studies, as well purification trials, revealed promising results.

In addition, co-crystallization of GPCRs with additional proteins such as G proteins, GRKs, arrestins, venom peptide toxins and antibodies is significantly promising in helping to stabilize receptor conformation and increasing the polar surface area.

But although a crystal structure usually constitutes a breakthrough, other biophysical methods will also provide structural information about GPCRs. For example, recent developments in NMR technology[360] suggest that the determination of small membrane proteins should be feasible using this technique, and possibly provide information complementary to X-ray crystallography. Small-angle neutron scattering can provide important structural information on protein complexes in which GPCRs are involved, such as the mean radius and the molecular mass of the complex. This recently allowed to demonstrate that a dimeric GPCR is associated with a single heterotrimeric G protein[361].

Solid-state NMR studies on purified neurokinin receptors may also provide some new insight into the binding of endogenous tachykinins to their cognate receptors. Hartmut Michel and colleagues successfully used such an approach to get the receptor bound conformation of bradykinin, another peptide ligand, to the bradykinin receptor[362].

But the real revolution in the GPCR research community is yet just about to be revealed. Indeed, astounding recent findings were presented, again, by Gebhard Schertler at a Gordon Conference on “Ligand Recognition and Molecular Gating” last March 2-7 in Ventura Beach (CA, USA), and again at the Collège de France (Paris, France) two weeks later…

References

1. Palczewski, K., Kumasaka, T., Hori, T., Behnke, C.A., Motoshima, H., Fox, B.A., Trong, I.L., Teller, D.C., Okada, T., Stenkamp, R.E., Yamamoto, M. & Miyano, M. Crystal structure of rhodopsin: a G protein-coupled receptor. *Science* **289**, 739-745 (2000).
2. Cherezov, V., Rosenbaum, D.M., Hanson, M.A., Rasmussen, S.G.F., Thian, F.S., Kobilka, T.S., Choi, H.-J., Kuhn, P., Weis, W.I., Kobilka, B.K. & Stevens, R.C. High-resolution crystal structure of an engineered human β_2-adrenergic G protein-coupled receptor. *Science* **318**, 1258-1265 (2007).
3. Rosenbaum, D.M., Cherezov, V., Hanson, M.A., Rasmussen, S.G.F., Thian, F.S., Kobilka, T.S., Choi, H.-J., Yao, X.-J., Weis, W.I., Stevens, R.C. & Kobilka, B.K. GPCR engineering yields high-resolution structural insights into β_2-adrenergic receptor function. *Science* **318**, 1266-1273 (2007).
4. Rasmussen, S.G.F., Choi, H.-J., Rosenbaum, D.M., Kobilka, T.S., Thian, F.S., Edwards, P.C., Burghammer, M., Ratnala, V.R.P., Sanishvili, R., Fischetti, R.F., Schertler, G.F.X., Weis, W.I. & Kobilka, B.K. Crystal structure of the human β_2-adrenergic G protein-coupled receptor. *Nature* **450**, 383-387 (2007).
5. Lundstrom, K. Structural genomics on membrane proteins: the MePNet approach. *Curr. Opin. Drug Discov. Dev.* **7**, 342-346 (2004).
6. Nathans, J. & Hogness, D.S. Isolation and nucleotide sequence of the gene encoding human rhodopsin. *Proc. Natl. Acad. Sci. U. S. A.* **81**, 4851-4855 (1984).
7. Kobilka, B.K., Dixon, R.A.F., Frielle, T., Dohlman, H.G., Bolanowski, M.A., Sigal, I.S., Yang-Feng, T.L., Francke, U., Caron, M.G. & Lefkowitz, R.J. cDNA for the human β_2-adrenergic receptor: a protein with multiple membrane-spanning domains and encoded by a gene whose chromosomal location is shared with that of the receptor for platelet-derived growth factor. *Proc. Natl. Acad. Sci. U. S. A.* **84**, 46-50 (1987).
8. Nathans, J., Thomas, D. & Hogness, D.S. Molecular genetics of human color vision: the genes encoding blue, green, and red pigments. *Science* **232**, 193-202 (1986).
9. Nathans, J., Piantanida, T.P., Eddy, R.L., Shows, T.B. & Hogness, D.S. Molecular genetics of inherited variation in human color vision. *Science* **232**, 203-210 (1986).
10. Buck, L. & Axel, R. A novel multigene family may encode odorant receptors: a molecular basis for odor recognition. *Cell* **65**, 175-187 (1991).
11. Gershengorn, M.C. & Osman, R. Minireview: insights into G protein-coupled receptor function using molecular models. *Endocrinology* **142**, 2-10 (2001).
12. Perez, D.M. The evolutionarily triumphant G protein-coupled receptor. *Mol. Pharmacol.* **63**, 1202-1205 (2003).
13. Bissantz, C., Logean, A. & Rognan, D. High-throughput modeling of human G protein-coupled receptors: amino acid sequence alignment, three-dimensional model building, and receptor library screening. *J. Chem. Inf. Comput. Sci.* **44**, 1162-1176 (2004).

14. Fredriksson, R. & Schiöth, H.B. The repertoire of G protein-coupled receptors in fully sequenced genomes. *Mol. Pharmacol.* **67**, 1414-1425 (2005).
15. Klein, P.S., Sun, T.J., Saxe III, C.L., Kimmel, A.R., Johnson, R.L. & Devreotes, P.N. A chemoattractant receptor controls development in *Dictyostelium discoideum*. *Science* **241**, 1467-1472 (1988).
16. Versele, M., Lemaire, K. & Thevelein, J.M. Sex and sugar in yeast: two distinct GPCR systems. *EMBO Rep.* **2**, 574-579 (2001).
17. Horn, F., Bettler, E., Oliveira, L., Campagne, F., Cohen, F.E. & Vriend, G. GPCRDB information system for G protein-coupled receptors. *Nucleic Acids Res.* **31**, 294-297 (2003).
18. Foord, S.M., Bonner, T.I., Neubig, R.R., Rosser, E.M., Pin, J.-P., Davenport, A.P., Spedding, M. & Harmar, A.J. International Union of Pharmacology. XLVI. G Protein-Coupled Receptor List. *Pharmacol. Rev.* **57**, 279-288 (2005).
19. Lander, E.S. *et al.* Initial sequencing and analysis of the human genome. *Nature* **409**, 860-921 (2001).
20. Venter, J.C. *et al.* The sequence of the human genome. *Science* **291**, 1304-1351 (2001).
21. Reed, R.R. After the holy grail: establishing a molecular basis for mammalian olfaction. *Cell* **116**, 329-336 (2004).
22. Adler, E., Hoon, M.A., Mueller, K.L., Chandrashekar, J., Ryba, N.J.P. & Zuker, C.S. A novel family of mammalian taste receptors. *Cell* **100**, 693-702 (2000).
23. Okada, T., Ernst, O.P., Palczewski, K. & Hofmann, K.P. Activation of rhodopsin: new insights from structural and biochemical studies. *Trends Biochem. Sci.* **26**, 318-324 (2001).
24. Brown, E.M., Pollak, M. & Hebert, S.C. The extracellular calcium-sensing receptor: its role in health and disease. *Annu. Rev. Med.* **49**, 15-29 (1998).
25. Vernier, P., Cardinaud, B., Valdenaire, O., Philippe, H. & Vincent, J.-D. An evolutionary view of drug-receptor interaction: the bioamine receptor family. *Trends Pharmacol. Sci.* **16**, 375-381 (1995).
26. Brown, A.J., Jupe, S. & Briscoe, C.P. A family of fatty acid binding receptors. *DNA Cell Biol.* **24**, 54-61 (2005).
27. Luján, R., Shigemoto, R. & López-Bendito, G. Glutamate and GABA receptor signalling in the developing brain. *Neuroscience* **130**, 567-580 (2005).
28. Janecka, A., Fichna, J. & Janecki, T. Opioid receptors and their ligands. *Curr. Top. Med. Chem.* **4**, 1-17 (2004).
29. Horuk, R. Chemokine receptors. *Cytokine Growth Factor Rev.* **12**, 313-335 (2001).
30. Fredholm, B.B., Ijzerman, A.P., Jacobson, K.A., Klotz, K.-N. & Linden, J. International Union of Pharmacology. XXV. Nomenclature and Classification of Adenosine Receptors. *Pharmacol. Rev.* **53**, 527-552 (2001).
31. Chun, J., Goetzl, E.J., Hla, T., Igarashi, Y., Lynch, K.R., Moolenaar, W., Pyne, S. & Tigyi, G. International Union of Pharmacology. XXXIV. Lysophospholipid Receptor Nomenclature. *Pharmacol. Rev.* **54**, 265-269 (2002).
32. Brink, C., Dahlén, S.-E., Drazen, J., Evans, J.F., Hay, D.W.P., Rovati, G.E., Serhan, C.N., Shimizu, T. & Yokomizo, T. International Union of Pharmacology XLIV. Nomenclature for the Oxoeicosanoid Receptor. *Pharmacol. Rev.* **56**, 149-157 (2004).
33. Kostenis, E. A glance at G protein-coupled receptors for lipid mediators: a growing receptor family with remarkably diverse ligands. *Pharmacol. Ther.* **102**, 243-257 (2004).

34. He, W., Miao, F.J.-P., Lin, D.C.-H., Schwandner, R.T., Wang, Z., Gao, J., Chen, J.-L., Tian, H. & Ling, L. Citric acid cycle intermediates as ligands for orphan G protein-coupled receptors. *Nature* **429**, 188-193 (2004).
35. Revankar, C.M., Cimino, D.F., Sklar, L.A., Arterburn, J.B. & Prossnitz, E.R. A transmembrane intracellular estrogen receptor mediates rapid cell signalling. *Science* **307**, 1625-1630 (2005).
36. Hopkins, A.L. & Groom, C.R. The druggable genome. *Nat. Rev. Drug Discov.* **1**, 727-730 (2002).
37. Klabunde, T. & Hessler, G. Drug design strategies for targeting G protein-coupled receptors. *ChemBioChem* **3**, 928-944 (2002).
38. Vanti, W.B., Swaminathan, S., Blevins, R., Bonini, J.A., Dowd, B.F., George, S.R., Weinshank, R.L., Smith, K.E. & Bailey, W.J. Patent status of the therapeutically important G protein-coupled receptors. *Expert Opinion on Therapeutic Patents* **11**, 1861-1887 (2001).
39. Fredriksson, R., Lagerström, M.C., Lundin, L.-G. & Schiöth, H.B. The G protein-coupled receptors in the human genome form five main families. Phylogenetic analysis, paralogon groups, and fingerprints. *Mol. Pharmacol.* **63**, 1256-1272 (2003).
40. Wise, A., Jupe, S.C. & Rees, S. The identification of ligands at orphan G protein-coupled receptors. *Annu. Rev. Pharmacol. Toxicol.* **44**, 43-66 (2004).
41. Civelli, O. GPCR deorphanizations: the novel, the known and the unexpected transmitters. *Trends Pharmacol. Sci.* **26**, 15-19 (2005).
42. Hein, P., Goepel, M., Cotecchia, S. & Michel, M.C. A quantitative analysis of antagonism and inverse agonism at wild-type and constitutively active hamster α_{1B}-adrenoceptors. *Naunyn-Schmiedeberg's Arch. Pharmacol.* **363**, 34-39 (2001).
43. Burstein, E.S., Spalding, T.A. & Brann, M.R. Pharmacology of muscarinic receptor subtypes constitutively activated by G Proteins. *Mol. Pharmacol.* **51**, 312-319 (1997).
44. Alewijnse, A.E., Timmerman, H., Jacobs, E.H., Smit, M.J., Roovers, E., Cotecchia, S. & Leurs, R. The effect of mutations in the DRY motif on the constitutive activity and structural instability of the histamine H_2 receptor. *Mol. Pharmacol.* **57**, 890-898 (2000).
45. Hall, D.A. & Strange, P.G. Evidence that antipsychotic drugs are inverse agonists at D_2 dopamine receptors. *Br. J. Pharmacol.* **121**, 731-736 (1997).
46. Gether, U. Uncovering molecular mechanisms involved in activation of G protein-coupled receptors. *Endocr. Rev.* **21**, 90-113 (2000).
47. Rader, A.J., Anderson, G., Isin, B., Khorana, H.G., Bahar, I. & Klein-Seetharaman, J. Identification of core amino acids stabilizing rhodopsin. *Proc. Natl. Acad. Sci. U. S. A.* **101**, 7246-7251 (2004).
48. Howard, A.D., McAllister, G., Feighner, S.D., Liu, Q., Nargund, R.P., Van der Ploeg, L.H.T. & Patchett, A.A. Orphan G protein-coupled receptors and natural ligand discovery. *Trends Pharmacol. Sci.* **22**, 132-140 (2001).
49. Saito, Y. & Civelli, O. G protein-coupled receptor deorphanizations. *Int. Rev. Neurobiol.* **65**, 179-209 (2005).
50. Saugstad, J.A., Segerson, T.P. & Westbrook, G.L. Metabotropic glutamate receptors activate G protein-coupled inwardly rectifying potassium channels in *Xenopus* oocytes. *J. Neurosci.* **16**, 5979-5985 (1996).
51. Wang, Y.-X., Dhulipala, P.D.K., Li, L., Benovic, J.L. & Kotlikoff, M.I. Coupling of M_2 muscarinic receptors to membrane ion channels via phosphoinositide 3-kinase γ and atypical protein kinase C. *J. Biol. Chem.* **274**, 13859-13864 (1999).
52. Hildebrandt, J.D. Role of subunit diversity in signalling by heterotrimeric G proteins. *Biochem. Pharmacol.* **54**, 325-339 (1997).

53. Yang, W. & Hildebrandt, J.D. Genomic analysis of G protein γ-subunits in human and mouse: the relationship between conserved gene structure and G protein βγ-dimer formation. *Cell. Signal.* **18**, 194-201 (2006).
54. Baker, E.K., Colley, N.J. & Zuker, C.S. The cyclophilin homolog NinaA functions as a chaperone, forming a stable complex *in vivo* with its protein target rhodopsin. *EMBO J.* **13**, 4886-4895 (1994).
55. Daviet, L., Lehtonen, J.Y.A., Tamura, K., Griese, D.P., Horiuchi, M. & Dzau, V.J. Cloning and characterization of ATRAP, a novel protein that interacts with the angiotensin II type 1 receptor. *J. Biol. Chem.* **274**, 17058-17062 (1999).
56. Cui, T.-X., Nakagami, H., Iwai, M., Takeda, Y., Shiuchi, T., Tamura, K., Daviet, L. & Horiuchi, M. ATRAP, novel AT1 receptor associated protein, enhances internalization of AT1 receptor and inhibits vascular smooth muscle cell growth. *Biochem. Biophys. Res. Commun.* **279**, 938-941 (2000).
57. Strittmatter, S.M., Cannon, S.C., Ross, E.M., Higashijima, T. & Fishman, M.C. GAP-43 augments G protein-coupled receptor transduction in *Xenopus laevis* oocytes. *Proc. Natl. Acad. Sci. U. S. A.* **90**, 5327-5331 (1993).
58. Neubig, R.R. Membrane organization in G protein mechanisms. *FASEB J.* **8**, 939-946 (1994).
59. de Weerd, W.F.C. & Leeb-Lundberg, L.M.F. Bradykinin sequesters B_2 bradykinin receptors and the receptor-coupled Gα subunits $G_q\alpha$ and $G_i\alpha$ in caveolae in DDT_1 MF-2 smooth muscle cells. *J. Biol. Chem.* **272**, 17858-17866 (1997).
60. Feron, O., Smith, T.W., Michel, T. & Kelly, R.A. Dynamic targeting of the agonist-stimulated M_2 muscarinic acetylcholine receptor to caveolae in cardiac myocytes. *J. Biol. Chem.* **272**, 17744-17748 (1997).
61. Haasemann, M., Cartaud, J., Müller-Esterl, W. & Dunia, I. Agonist-induced redistribution of bradykinin B_2 receptor in caveolae. *J. Cell Sci.* **111**, 917-928 (1998).
62. Ostrom, R.S., Post, S.R. & Insel, P.A. Stoichiometry and compartmentation in G protein-coupled receptor signalling: implications for therapeutic interventions involving G_s. *J. Pharmacol. Exp. Ther.* **294**, 407-412 (2000).
63. Seno, K., Kishimoto, M., Abe, M., Higuchi, Y., Mieda, M., Owada, Y., Yoshiyama, W., Liu, H. & Hayashi, F. Light- and guanosine 5'-3-*O*-(thio)triphosphate-sensitive localization of a G protein and its effector on detergent-resistant membrane rafts in rod photoreceptor outer segments. *J. Biol. Chem.* **276**, 20813-20816 (2001).
64. Nair, K.S., Balasubramanian, N. & Slepak, V.Z. Signal-dependent translocation of transducin, RGS9-1-Gβ5L complex, and arrestin to detergent-resistant membrane rafts in photoreceptors. *Curr. Biol.* **12**, 421-425 (2002).
65. Chini, B. & Parenti, M. G protein-coupled receptors in lipid rafts and caveolae: how, when and why do they go there? *J. Mol. Endocrinol.* **32**, 325-338 (2004).
66. Ostrom, R.S. & Insel, P.A. The evolving role of lipid rafts and caveolae in G protein-coupled receptor signalling: implications for molecular pharmacology. *Br. J. Pharmacol.* **143**, 235-245 (2004).
67. Ianoul, A., Grant, D.D., Rouleau, Y., Bani-Yaghoub, M., Johnston, L.J. & Pezacki, J.P. Imaging nanometer domains of β-adrenergic receptor complexes on the surface of cardiac myocytes. *Nat. Chem. Biol.* **1**, 196-202 (2005).
68. Insel, P.A., Head, B.P., Ostrom, R.S., Patel, H.H., Swaney, J.S., Tang, C.-M. & Roth, D.M. Caveolae and lipid rafts: G protein-coupled receptor signalling microdomains in cardiac myocytes. *Ann. N. Y. Acad. Sci.* **1047**, 166-172 (2005).
69. Morris, D.P., Lei, B., Wu, Y.-X., Michelotti, G.A. & Schwinn, D.A. The α_{1a}-adrenergic receptor occupies membrane rafts with its G protein effectors but internalizes via clathrin-coated pits. *J. Biol. Chem.* **283**, 2973-2985 (2008).

70. Lisanti, M.P., Scherer, P.E., Tang, Z. & Sargiacomo, M. Caveolae, caveolin and caveolin-rich membrane domains: a signalling hypothesis. *Trends Cell Biol.* **4**, 231-235 (1994).
71. Limbird, L.E., De Meyts, P. & Lefkowitz, R.J. β-Adrenergic receptors: evidence for negative cooperativity. *Biochem. Biophys. Res. Commun.* **64**, 1160-1168 (1975).
72. Limbird, L.E. & Lefkowitz, R.J. Negative cooperativity among beta-adrenergic receptors in frog erythrocyte membranes. *J. Biol. Chem.* **251**, 5007-5014 (1976).
73. Mattera, R., Pitts, B.J., Entman, M.L. & Birnbaumer, L. Guanine nucleotide regulation of a mammalian myocardial muscarinic receptor system. Evidence for homo- and heterotropic cooperativity in ligand binding analyzed by computer-assisted curve fitting. *J. Biol. Chem.* **260**, 7410-7421 (1985).
74. Whorton, M.R., Bokoch, M.P., Rasmussen, S.G.F., Huang, B., Zare, R.N., Kobilka, B. & Sunahara, R.K. A monomeric G protein-coupled receptor isolated in a high-density lipoprotein particle efficiently activates its G protein. *Proc. Natl. Acad. Sci. U. S. A.* **104**, 7682-7687 (2007).
75. Milligan, G. Constitutive activity and inverse agonists of G protein-coupled receptors: a current perspective. *Mol. Pharmacol.* **64**, 1271-1276 (2003).
76. Kroeger, K.M. & Eidne, K.A. Study of G protein-coupled receptor-protein interactions by bioluminescence resonance energy transfer. *Methods Mol. Biol.* **259**, 323-333 (2004).
77. Terrillon, S. & Bouvier, M. Roles of G protein-coupled receptor dimerization: from ontogeny to signalling regulation. *EMBO Rep.* **5**, 30-34 (2004).
78. Bulenger, S., Marullo, S. & Bouvier, M. Emerging role of homo- and heterodimerization in G protein-coupled receptor biosynthesis and maturation. *Trends Pharmacol. Sci.* **26**, 131-137 (2005).
79. Maggio, R., Vogel, Z. & Wess, J. Coexpression studies with mutant muscarinic/adrenergic receptors provide evidence for intermolecular "cross-talk" between G protein-linked receptors. *Proc. Natl. Acad. Sci. U. S. A.* **90**, 3103-3107 (1993).
80. Margeta-Mitrovic, M., Jan, Y.N. & Jan, L.Y. A trafficking checkpoint controls $GABA_B$ receptor heterodimerization. *Neuron* **27**, 97-106 (2000).
81. Issafras, H., Angers, S., Bulenger, S., Blanpain, C., Parmentier, M., Labbé-Jullié, C., Bouvier, M. & Marullo, S. Constitutive agonist-independent CCR_5 oligomerization and antibody-mediated clustering occurring at physiological levels of receptors. *J. Biol. Chem.* **277**, 34666-34673 (2002).
82. Overton, M.C. & Blumer, K.J. The extracellular N-terminal domain and transmembrane domains 1 and 2 mediate oligomerization of a yeast G protein-coupled receptor. *J. Biol. Chem.* **277**, 41463-41472 (2002).
83. Terrillon, S., Durroux, T., Mouillac, B., Breit, A., Ayoub, M.A., Taulan, M., Jockers, R., Barberis, C. & Bouvier, M. Oxytocin and vasopressin V_{1A} and V_2 receptors form constitutive homo- and heterodimers during biosynthesis. *Mol. Endocrinol.* **17**, 677-691 (2003).
84. Floyd, D.H., Geva, A., Bruinsma, S.P., Overton, M.C., Blumer, K.J. & Baranski, T.J. C_{5a} receptor oligomerization: II. Fluorescence resonance energy transfer studies of a human G protein-coupled receptor expressed in yeast. *J. Biol. Chem.* **278**, 35354-35361 (2003).
85. Zhu, X. & Wess, J. Truncated V_2 vasopressin receptors as negative regulators of wild-type V_2 receptor function. *Biochemistry (Wash.)* **37**, 15773-15784 (1998).

86. Karpa, K.D., Lin, R., Kabbani, N. & Levenson, R. The dopamine D_3 receptor interacts with itself and the truncated D_3 splice variant D_3nf: D_3-D_3nf interaction causes mislocalization of D_3 receptors. *Mol. Pharmacol.* **58**, 677-683 (2000).
87. Grosse, R., Schöneberg, T., Schultz, G. & Gudermann, T. Inhibition of gonadotropin-releasing hormone receptor signalling by expression of a splice variant of the human receptor. *Mol. Endocrinol.* **11**, 1305-1318 (1997).
88. Benkirane, M., Jin, D.-Y., Chun, R.F., Koup, R.A. & Jeang, K.-T. Mechanism of transdominant inhibition of CCR_5-mediated HIV-1 infection by $ccr_5\Delta32$. *J. Biol. Chem.* **272**, 30603-30606 (1997).
89. Shioda, T., Nakayama, E.E., Tanaka, Y., Xin, X., Liu, H., Kawana-Tachikawa, A., Kato, A., Sakai, Y., Nagai, Y. & Iwamoto, A. Naturally occurring deletional mutation in the C-terminal cytoplasmic tail of CCR_5 affects surface trafficking of CCR_5. *J. Virol.* **75**, 3462-3468 (2001).
90. Colley, N.J., Cassill, J.A., Baker, E.K. & Zuker, C.S. Defective intracellular transport is the molecular basis of rhodopsin-dependent dominant retinal degeneration. *Proc. Natl. Acad. Sci. U. S. A.* **92**, 3070-3074 (1995).
91. Jordan, B.A. & Devi, L.A. G protein-coupled receptor heterodimerization modulates receptor function. *Protein Expression Purif.* **399**, 697-700 (1999).
92. Galvez, T., Duthey, B., Kniazeff, J., Blahos, J., Rovelli, G., Bettler, B., Prézeau, L. & Pin, J.-P. Allosteric interactions between GB_1 and GB_2 subunits are required for optimal $GABA_B$ receptor function. *EMBO J.* **20**, 2152–2159 (2001).
93. Gomes, I., Jordan, B.A., Gupta, A., Trapaidze, N., Nagy, V. & Devi, L.A. Heterodimerization of μ- and δ-opioid receptors: a role in opiate synergy. *J. Neurosci.* **20**, 110RC (2000).
94. Maggio, R., Barbier, P., Colelli, A., Salvadori, F., Demontis, G. & Corsini, G.U. G protein-linked receptors: pharmacological evidence for the formation of heterodimers. *J. Pharmacol. Exp. Ther.* **291**, 251-257 (1999).
95. Rocheville, M., Lange, D.C., Kumar, U., Patel, S.C., Patel, R.C. & Patel, Y.C. Receptors for dopamine and somatostatin: formation of hetero-oligomers with enhanced functional activity. *Science* **288**, 154-157 (2000).
96. Franco, R., Ferré, S., Agnati, L., Torvinen, M., Ginés, S., Hillion, J., Casadó, V., Lledó, P.-M., Zoli, M., Lluis, C. & Fuxe, K. Evidence for adenosine/dopamine receptor interactions: indications for heteromerization. *Neuropsychopharmacology* **23**, S50-S59 (2000).
97. Strange, P.G. Oligomers of D_2 dopamine receptors: evidence from ligand binding. *J. Mol. Neurosci.* **26**, 155-160 (2005).
98. Vivo, M., Lin, H. & Strange, P.G. Investigation of cooperativity in the binding of ligands to the D_2 dopamine receptor. *Mol. Pharmacol.* **69**, 226-235 (2006).
99. Springael, J.-Y., Urizar, E. & Parmentier, M. Dimerization of chemokine receptors and its functional consequences. *Cytokine Growth Factor Rev.* **16**, 611-623 (2005).
100. Springael, J.-Y., Le Minh, P.N., Urizar, E., Costagliola, S., Vassart, G. & Parmentier, M. Allosteric modulation of binding properties between units of chemokine receptor homo- and hetero-oligomers. *Mol. Pharmacol.* **69**, 1652-1661 (2006).
101. Sohy, D., Parmentier, M. & Springael, J.-Y. Allosteric trans-inhibition by specific antagonists in CCR_2/$CXCR_4$ heterodimers. *J. Biol. Chem.*, *in press* (2007).
102. Fotiadis, D., Liang, Y., Filipek, S., Saperstein, D.A., Engel, A. & Palczewski, K. Atomic-force microscopy: rhodopsin dimers in native disc membranes. *Nature* **421**, 127-128 (2003).

103. Liang, Y., Fotiadis, D., Filipek, S., Saperstein, D.A., Palczewski, K. & Engel, A. Organization of the G protein-coupled receptors rhodopsin and opsin in native membranes. *J. Biol. Chem.* **278**, 21655-21662 (2003).
104. Chidiac, P., Hebert, T.E., Valiquette, M., Dennis, M. & Bouvier, M. Inverse agonist activity of β-adrenergic antagonists. *Mol. Pharmacol.* **45**, 490-499 (1994).
105. Barker, E.L., Westphal, R.S., Schmidt, D. & Sanders-Bush, E. Constitutively active 5-hydroxytryptamine$_{2C}$ receptors reveal novel inverse agonist activity of receptor ligands. *J. Biol. Chem.* **269**, 11687-11690 (1994).
106. Costa, T. & Herz, A. Antagonists with negative intrinsic activity at δ-opioid receptors coupled to GTP-binding proteins. *Proc. Natl. Acad. Sci. U. S. A.* **86**, 7321-7325 (1989).
107. Leeb-Lundberg, L.M., Mathis, S.A. & Herzig, M.C. Antagonists of bradykinin that stabilize a G protein-uncoupled state of the B_2 receptor act as inverse agonists in rat myometrial cells. *J. Biol. Chem.* **269**, 25970-25973 (1994).
108. Hanf, R., Li, Y., Szabo, G. & Fischmeister, R. Agonist-independent effects of muscarinic antagonists on Ca^{2+} and K^+ currents in frog and rat cardiac cells. *J. Physiol. (Lond)*. **461**, 743-765 (1993).
109. Soudijn, W., van Wijngaarden, I. & Ijzerman, A.P. Structure-activity relationships of inverse agonists for G protein-coupled receptors. *Med. Res. Rev.* **25**, 398-426 (2005).
110. Bond, R.A., Leff, P., Johnson, T.D., Milano, C.A., Rockman, H.A., McMinn, T.R., Apparsundaram, S., Hyek, M.F., Kenakin, T.P., Allen, L.F. & Lefkowitz, R.J. Physiological effects of inverse agonists in transgenic mice with myocardial overexpression of the β_2-adrenoceptor. *Nature* **374**, 272-276 (1995).
111. Nagaraja, S., Iyer, S., Liu, X., Eichberg, J. & Bond, R.A. Treatment with inverse agonists enhances baseline atrial contractility in transgenic mice with chronic β_2-adrenoceptor activation. *Br. J. Pharmacol.* **127**, 1099-1104 (1999).
112. Seifert, R. & Wenzel-Seifert, K. Unmasking different constitutive activity of four chemoattractant receptors using Na^+ as universal stabilizer of the inactive (R) state. *Receptors Channels* **7**, 357-369 (2001).
113. Dryja, T.P., Berson, E.L., Rao, V.R. & Oprian, D.D. Heterozygous missense mutation in the rhodopsin gene as a cause of congenital stationary night blindness. *Nat. Genet.* **4**, 280-283 (1993).
114. Han, M., Smith, S.O. & Sakmar, T.P. Constitutive activation of opsin by mutation of methionine 257 on transmembrane helix 6. *Biochemistry (Mosc)*. **37**, 8253-8261 (1998).
115. Yang, T.-Y., Chen, S.-C., Leach, M.W., Manfra, D., Homey, B., Wiekowski, M., Sullivan, L., Jenh, C.-H., Narula, S.K., Chensue, S.W. & Lira, S.A. Transgenic expression of the chemokine receptor encoded by human herpesvirus 8 induces an angioproliferative disease resembling Kaposi's sarcoma. *J. Exp. Med.* **191**, 445-454 (2000).
116. Burger, M., Burger, J.A., Hoch, R.C., Oades, Z., Takamori, H. & Schraufstatter, I.U. Point mutation causing constitutive signalling of $CXCR_2$ leads to transforming activity similar to Kaposi's sarcoma herpesvirus-G protein-coupled receptor. *J. Immunol.* **163**, 2017-2022 (1999).
117. Lunn, C.A., Fine, J.S., Rojas-Triana, A., Jackson, J.V., Fan, X., Kung, T.T., Gonsiorek, W., Schwarz, M.A., Lavey, B., Kozlowski, J.A., Narula, S.K., Lundell, D.J., Hipkin, R.W. & Bober, L.A. A novel cannabinoid peripheral cannabinoid receptor-selective inverse agonist blocks leukocyte recruitment *in vivo*. *J. Pharmacol. Exp. Ther.* **316**, 780-788 (2006).

118. Rosenkilde, M.M. & Schwartz, T.W. Potency of ligands correlates with affinity measured against agonist and inverse agonists but not against neutral ligand in constitutively active chemokine receptor. *Mol. Pharmacol.* **57**, 602-609 (2000).
119. Oesterhelt, D. & Stoeckenius, W. Functions of a new photoreceptor membrane. *Proc. Natl. Acad. Sci. U. S. A.* **70**, 2853-2857 (1973).
120. Henderson, R. & Unwin, P.N.T. Three-dimensional model of purple membrane obtained by electron microscopy. *Nature* **257**, 28-32 (1975).
121. Henderson, R., Baldwin, J.M., Ceska, T.A., Zemlin, F., Beckmann, E. & Downing, K.H. Model for the structure of bacteriorhodopsin based on high-resolution electron cryo-microscopy. *J. Mol. Biol.* **213**, 899-929 (1990).
122. Tsygannik, I.N. & Baldwin, J.M. Three-dimensional structure of deoxycholate-treated purple membrane at 6 Å resolution and molecular averaging of three crystal forms of bacteriorhodopsin. *Eur. Biophys. J.* **14**, 263-272 (1987).
123. Pebay-Peyroula, E., Rummel, G., Rosenbusch, J.P. & Landau, E.M. X-ray structure of bacteriorhodopsin at 2.5 Å from microcrystals grown in lipidic cubic phases. *Science* **277**, 1676-1681 (1997).
124. Luecke, H., Schobert, B., Richter, H.-T., Cartailler, J.-P. & Lanyi, J.K. Structure of bacteriorhodopsin at 1.55 Å resolution. *J. Mol. Biol.* **291**, 899-911 (1999).
125. Lanyi, J.K. Molecular mechanism of ion transport in bacteriorhodopsin: insights from crystallographic, spectroscopic, kinetic, and mutational studies. *Journal of Physical Chemistry B* **104**, 11441-11448 (2000).
126. Kolbe, M., Besir, H., Essen, L.-O. & Oesterhelt, D. Structure of the light-driven chloride pump halorhodopsin at 1.8 Å resolution. *Science* **288**, 1390-1396 (2000).
127. Edman, K., Royant, A., Nollert, P., Maxwell, C.A., Pebay-Peyroula, E., Navarro, J., Neutze, R. & Landau, E.M. Early structural rearrangements in the photocycle of an integral membrane sensory receptor. *Structure* **10**, 473-482 (2002).
128. Gordeliy, V.I., Labahn, J., Moukhametzianov, R., Efremov, R., Granzin, J., Schlesinger, R., Büldt, G., Savopol, T., Scheidig, A.J., Klare, J.P. & Engelhard, M. Molecular basis of transmembrane signalling by sensory rhodopsin II-transducer complex. *Nature* **419**, 484-487 (2002).
129. Moukhametzianov, R., Klare, J.P., Efremov, R., Baeken, C., Göppner, A., Labahn, J., Engelhard, M., Büldt, G. & Gordeliy, V.I. Development of the signal in sensory rhodopsin and its transfer to the cognate transducer. *Nature* **440**, 115-119 (2006).
130. Li, J., Edwards, P.C., Burghammer, M., Villa, C. & Schertler, G.F.X. Structure of bovine rhodopsin in a trigonal crystal form. *J. Mol. Biol.* **343**, 1409-1438 (2004).
131. Ovchinnikov, Y.A. Rhodopsin and bacteriorhodopsin: structure-function relationships. *FEBS Lett.* **148**, 179-191 (1982).
132. Fung, B.K.-K. & Stryer, L. Photolyzed rhodopsin catalyzes the exchange of GTP for bound GDP in retinal rod outer segments. *Proc. Natl. Acad. Sci. U. S. A.* **77**, 2500-2504 (1980).
133. McBee, J.K., Palczewski, K., Baehr, W. & Pepperberg, D.R. Confronting complexity: the interlink of phototransduction and retinoid metabolism in the vertebrate retina. *Prog. Retin. Eye Res.* **20**, 469-529 (2001).
134. Kuksa, V., Imanishi, Y., Batten, M., Palczewski, K. & Moise, A.R. Retinoid cycle in the vertebrate retina: experimental approaches and mechanisms of isomerization. *Vision Res.* **43**, 2959-2981 (2003).
135. Zhao, X., Nagai, Y., Reeves, P.J., Kiley, P., Khorana, H.G. & Zhang, S. Designer short peptide surfactants stabilize G protein-coupled receptor bovine rhodopsin. *Proc. Natl. Acad. Sci. U. S. A.* **103**, 17707-17712 (2006).

136. Gether, U., Ballesteros, J.A., Seifert, R., Sanders-Bush, E., Weinstein, H. & Kobilka, B.K. Structural instability of a constitutively active G protein-coupled receptor. Agonist-independent activation due to conformational flexibility. *J. Biol. Chem.* **272**, 2587-2590 (1997).
137. Samama, P., Bond, R.A., Rockman, H.A., Milano, C.A. & Lefkowitz, R.J. Ligand-induced overexpression of a constitutively active β_2-adrenergic receptor: pharmacological creation of a phenotype in transgenic mice. *Proc. Natl. Acad. Sci. U. S. A.* **94**, 137-141 (1997).
138. Kobilka, B.K. Amino and carboxyl terminal modifications to facilitate the production and purification of a G protein-coupled receptor. *Anal. Biochem.* **231**, 269-271 (1995).
139. Day, P.W., Rasmussen, S.G.F., Parnot, C., Fung, J.J., Masood, A., Kobilka, T.S., Yao, X.-J., Choi, H.-J., Weis, W.I., Rohrer, D.K. & Kobilka, B.K. A monoclonal antibody for G protein-coupled receptor crystallography. *Nat. Methods* **4**, 927-929 (2007).
140. Schwartz, T.W., Frimurer, T.M., Holst, B., Rosenkilde, M.M. & Elling, C.E. Molecular mechanism of 7TM receptor activation: a global toggle switch model. *Annu. Rev. Pharmacol. Toxicol.* **46**, 481-519 (2006).
141. Kobilka, B.K. & Deupi, X. Conformational complexity of G protein-coupled receptors. *Trends Pharmacol. Sci.* **28**, 397-406 (2007).
142. Parnot, C., Miserey-Lenkei, S., Bardin, S., Corvol, P. & Clauser, E. Lessons from constitutively active mutants of G protein-coupled receptors. *Trends Endocrinol. Metab.* **13**, 336-343 (2002).
143. Huang, P., Visiers, I., Weinstein, H. & Liu-Chen, L.Y. The local environment at the cytoplasmic end of TM6 of the μ-opioid receptor differs from those of rhodopsin and monoamine receptors: introduction of an ionic lock between the cytoplasmic ends of helices 3 and 6 by a L6.30(275)E mutation inactivates the μ-opioid receptor and reduces the constitutive activity of its T6.34(279)K mutant. *Biochemistry (Wash.)* **41**, 11972-11980 (2002).
144. Springael, J.-Y., de Poorter, C., Deupi, X., Van Durme, J., Pardo, L. & Parmentier, M. The activation mechanism of chemokine receptor CCR_5 involves common structural changes but a different network of interhelical interactions relative to rhodopsin. *Cell. Signal.* **19**, 1446-1456 (2007).
145. Baker, J.G. & Hill, S.J. Multiple GPCR conformations and signalling pathways: implications for antagonist affinity estimates. *Trends Pharmacol. Sci.* **28**, 374-381 (2007).
146. Overington, J.P., Al-Lazikani, B. & Hopkins, A.L. How many drug targets are there? *Nat. Rev. Drug Discov.* **5**, 993-996 (2006).
147. Klabunde, T. & Jäger, R. Chemogenomics approaches to G protein-coupled receptor lead finding. *Ernst Schering Res Found Workshop*, 31-46 (2006).
148. Evers, A. & Klabunde, T. Structure-based drug discovery using GPCR homology modeling: successful virtual screening for antagonists of the α_{1A}-adrenergic receptor. *J. Med. Chem.* **48**, 1088-1097 (2005).
149. Strader, C.D., Sigal, I.S. & Dixon, R.A. Structural basis of beta-adrenergic receptor function. *FASEB J.* **3**, 1825-1832 (1989).
150. Govaerts, C., Blanpain, C., Deupi, X., Ballet, S., Ballesteros, J.A., Wodak, S.J., Vassart, G., Pardo, L. & Parmentier, M. The T*X*P motif in the second transmembrane helix of CCR_5. A structural determinant of chemokine-induced activation. *J. Biol. Chem.* **276**, 13217-13225 (2001).
151. Govaerts, C., Bondue, A., Springael, J.-Y., Olivella, M., Deupi, X., Le Poul, E., Wodak, S.J., Parmentier, M., Pardo, L. & Blanpain, C. Activation of CCR_5 by

chemokines involves an aromatic cluster between transmembrane helices 2 and 3. *J. Biol. Chem.* **278**, 1892-1903 (2003).
152. Jongejan, A., Bruysters, M., Ballesteros, J.A., Haaksma, E., Bakker, R.A., Pardo, L. & Leurs, R. Linking agonist binding to histamine H_1 receptor activation. *Nat. Chem. Biol.* **1**, 98-103 (2005).
153. Oliveira, L., Hulsen, T., Lutje Hulsik, D., Paiva, A.C.M. & Vriend, G. Heavier-than-air flying machines are impossible. *FEBS Lett.* **564**, 269-273 (2004).
154. Evers, A. & Klebe, G. Successful virtual screening for a submicromolar antagonist of the neurokinin-1 receptor based on a ligand-supported homology model. *J. Med. Chem.* **47**, 5381-5392 (2004).
155. Vaidehi, N., Floriano, W.B., Trabanino, R., Hall, S.E., Freddolino, P., Choi, E.J., Zamanakos, G. & Goddard III, W.A. Prediction of structure and function of G protein-coupled receptors. *Proc. Natl. Acad. Sci. U. S. A.* **99**, 12622-12627 (2002).
156. Freddolino, P.L., Kalani, M.Y.S., Vaidehi, N., Floriano, W.B., Hall, S.E., Trabanino, R.J., Kam, V.W.T. & Goddard III, W.A. Predicted 3D structure for the human β_2-adrenergic receptor and its binding site for agonists and antagonists. *Proc. Natl. Acad. Sci. U. S. A.* **101**, 2736-2741 (2004).
157. Kalani, M.Y.S., Vaidehi, N., Hall, S.E., Trabanino, R.J., Freddolino, P.L., Kalani, M.A., Floriano, W.B., Kam, V.W.T. & Goddard III, W.A. The predicted 3D structure of the human D_2 dopamine receptor and the binding site and binding affinities for agonists and antagonists. *Proc. Natl. Acad. Sci. U. S. A.* **101**, 3815-3820 (2004).
158. Peng, J.Y.-c., Vaidehi, N., Hall, S.E. & Goddard III, W.A. The predicted 3D structures of the human M_1 muscarinic acetylcholine receptor with agonist or antagonist bound. *ChemMedChem* **1**, 878-890 (2006).
159. Vaidehi, N., Schlyer, S., Trabanino, R.J., Floriano, W.B., Abrol, R., Sharma, S., Kochanny, M., Koovakat, S., Dunning, L., Liang, M., Fox, J.M., de Mendonça, F.L., Pease, J.E., Goddard III, W.A. & Horuk, R. Predictions of CCR_1 chemokine receptor structure and BX 471 antagonist binding followed by experimental validation. *J. Biol. Chem.* **281**, 27613-27620 (2006).
160. Shacham, S., Marantz, Y., Bar-Haim, S., Kalid, O., Warshaviak, D., Avisar, N., Inbal, B., Heifetz, A., Fichman, M., Topf, M., Naor, Z., Noiman, S. & Becker, O.M. PREDICT modeling and *in silico* screening for G protein-coupled receptors. *Proteins: Structure, Function, and Bioinformatics* **57**, 51-86 (2004).
161. Becker, O.M., Marantz, Y., Shacham, S., Inbal, B., Heifetz, A., Kalid, O., Bar-Haim, S., Warshaviak, D., Fichman, M. & Noiman, S. G protein-coupled receptors: *in silico* drug discovery in 3D. *Proc. Natl. Acad. Sci. U. S. A.* **101**, 11304-11309 (2004).
162. Raman, P., Cherezov, V. & Caffrey, M. The Membrane Protein Data Bank. *Cellular and Molecular Life Sciences (CMLS)* **63**, 36-51 (2006).
163. White, S.H. http://blanco.biomol.uci.edu/Membrane_Proteins_xtal.html Membrane Proteins of Known 3D Structure. (Last Modified: 8 March, 2008).
164. RCSB PDB http://www.pdb.org/.
165. Wimalawansa, S.J. Purification and biochemical characterization of neuropeptide Y_2 receptor. *J. Biol. Chem.* **270**, 18523-18530 (1995).
166. Sarramegna, V., Talmont, F., Demange, P. & Milon, A. Heterologous expression of G protein-coupled receptors: comparison of expression systems from the standpoint of large-scale production and purification. *Cellular and Molecular Life Sciences (CMLS)* **60**, 1529-1546 (2003).
167. Schertler, G.F.X. Overproduction of membrane proteins. *Curr. Opin. Struct. Biol.* **2**, 534-544 (1992).

168. Grisshammer, R. & Tate, C.G. Overexpression of integral membrane proteins for structural studies. *Q. Rev. Biophys.* **28**, 315-422 (1995).
169. Sautel, M. & Milligan, G. Molecular manipulation of G protein-coupled receptors: a new avenue into drug discovery. *Curr. Med. Chem.* **7**, 889-896 (2000).
170. Tate, C.G. & Grisshammer, R. Heterologous expression of G protein-coupled receptors. *Trends Biotechnol.* **14**, 426-430 (1996).
171. Ogata, K., Nishikawa, H. & Ohsugi, M. Yeast capable of utilizing methanol. *Agric. Biol. Chem.* **33**, 1519-1520 (1969).
172. Weiss, H.M., Haase, W., Michel, H. & Reiländer, H. Comparative biochemical and pharmacological characterization of the mouse $5HT_{5A}$ 5-hydroxytryptamine receptor and the human β_2-adrenergic receptor produced in the methylotrophic yeast *Pichia pastoris*. *Biochem. J.* **330**, 1137-1147 (1998).
173. Schiller, H., Haase, W., Molsberger, E., Janssen, P., Michel, H. & Reiländer, H. The human ET_B endothelin receptor heterologously produced in the methylotrophic yeast *Pichia pastoris* shows high-affinity binding and induction of stacked membranes. *Receptors Channels* **7**, 93-107 (2000).
174. Sarramegna, V., Demange, P., Milon, A. & Talmont, F. Optimizing functional versus total expression of the human μ-opioid receptor in *Pichia pastoris*. *Protein Expression Purif.* **24**, 212-220 (2002).
175. Weiss, H.M., Haase, W., Michel, H. & Reiländer, H. Expression of functional mouse $5HT_{5A}$ serotonin receptor in the methylotrophic yeast *Pichia pastoris*: pharmacological characterization and localization. *FEBS Lett.* **377**, 451-456 (1995).
176. Abdulaev, N.G., Popp, M.P., Smith, W.C. & Ridge, K.D. Functional expression of bovine opsin in the methylotrophic yeast *Pichia pastoris*. *Protein Expression Purif.* **10**, 61-69 (1997).
177. Cereghino, J.L. & Cregg, J.M. Heterologous protein expression in the methylotrophic yeast *Pichia pastoris*. *FEMS Microbiol. Rev.* **24**, 45-66 (2000).
178. Reiländer, H. & Weiss, H.M. Production of G protein-coupled receptors in yeast. *Curr. Opin. Biotechnol.* **9**, 510-517 (1998).
179. Kaushal, S., Ridge, K.D. & Khorana, H.G. Structure and function in rhodopsin: the role of asparagine-linked glycosylation. *Proc. Natl. Acad. Sci. U. S. A.* **91**, 4024-4028 (1994).
180. Ohvo-Rekilä, H., Ramstedt, B., Leppimäki, P. & Peter Slotte, J. Cholesterol interactions with phospholipids in membranes. *Prog. Lipid Res.* **41**, 66-97 (2002).
181. Gimpl, G., Burger, K. & Fahrenholz, F. A closer look at the cholesterol sensor. *Trends Biochem. Sci.* **27**, 596-599 (2002).
182. Lee, A.G. How lipids affect the activities of integral membrane proteins. *Biochimica et Biophysica Acta (BBA) - Biomembranes* **1666**, 62-87 (2004).
183. Lagane, B., Gaibelet, G., Meilhoc, E., Masson, J.-M., Cézanne, L. & Lopez, A. Role of sterols in modulating the human μ-opioid receptor function in *Saccharomyces cerevisiae*. *J. Biol. Chem.* **275**, 33197-33200 (2000).
184. Déméné, H., Granier, S., Müller, D., Guillon, G., Dufour, M.-N., Delsuc, M.-A., Hibert, M., Pascal, R. & Mendre, C. Active peptidic mimics of the second intracellular loop of the V_{1A} vasopressin receptor are structurally related to the second intracellular rhodopsin loop: a combined ^1H NMR and biochemical study. *Biochemistry (Wash.)* **42**, 8204-8213 (2003).
185. Grace, C.R.R., Perrin, M.H., DiGruccio, M.R., Miller, C.L., Rivier, J.E., Vale, W.W. & Riek, R. NMR structure and peptide hormone binding site of the first extracellular domain of a type B_1 G protein-coupled receptor. *Proc. Natl. Acad. Sci. U. S. A.* **101**, 12836-12841 (2004).

186. Estephan, R., Englander, J., Arshava, B., Samples, K.L., Becker, J.M. & Naider, F. Biosynthesis and NMR analysis of a 73-residue domain of a *Saccharomyces cerevisiae* G protein-coupled receptor. *Biochemistry (Wash.)* **44**, 11795-11810 (2005).
187. Ichiyama, S., Oka, Y., Haga, K., Kojima, S., Tateishi, Y., Shirakawa, M. & Haga, T. The structure of the third intracellular loop of the muscarinic acetylcholine receptor M_2 subtype. *FEBS Lett.* **580**, 23-26 (2006).
188. Zhao, J., Zheng, H. & Xie, X.-Q. NMR characterization of recombinant transmembrane protein CB_2 fragment CB_2(180-233). *Protein Peptide Lett.* **13**, 335-342 (2006).
189. Zheng, H., Zhao, J., Sheng, W. & Xie, X.-Q. A transmembrane helix-bundle from G protein-coupled receptor CB_2: biosynthesis, purification, and NMR characterization. *Biopolymers* **83**, 46-61 (2006).
190. Weiss, H.M. & Grisshammer, R. Purification and characterization of the human adenosine A_{2A} receptor functionally expressed in *Escherichia coli*. *Eur. J. Biochem.* **269**, 82-92 (2002).
191. Yao, Z. & Kobilka, B. Using synthetic lipids to stabilize purified β_2-adrenoceptor in detergent micelles. *Anal. Biochem.* **343**, 344-346 (2005).
192. Michel, H. General and practical aspects of membrane protein crystallization. in *Crystallization of membrane proteins* (ed. Michel, H.) 73-88 (CRC Press, Boca Raton, FL, USA, 1991).
193. Abramson, J. & Iwata, S. Crystallization of membrane proteins. in *Protein crystallization: Techniques, strategies, and tips: A laboratory manual* (ed. Bergfors, T.M.) 199-210 (International University Line, La Jolla, CA, USA, 1999).
194. Ostermeier, C., Harrenga, A., Ermler, U. & Michel, H. Structure at 2.7 Å resolution of the *Paracoccus denitrificans* two-subunit cytochrome *c* oxidase complexed with an antibody Fv fragment. *Proc. Natl. Acad. Sci. U. S. A.* **94**, 10547-10553 (1997).
195. Harrenga, A. & Michel, H. The cytochrome *c* oxidase from *Paracoccus denitrificans* does not change the metal center ligation upon reduction. *J. Biol. Chem.* **274**, 33296-33299 (1999).
196. Hunte, C., Koepke, J., Lange, C., Roßmanith, T. & Michel, H. Structure at 2.3 Å resolution of the cytochrome bc_1 complex from the yeast *Saccharomyces cerevisiae* co-crystallized with an antibody Fv fragment. *Structure* **8**, 669-684 (2000).
197. Zhou, Y., Morais-Cabral, J.H., Kaufman, A. & MacKinnon, R. Chemistry of ion coordination and hydration revealed by a K^+ channel-Fab complex at 2.0 Å resolution. *Nature* **414**, 43-48 (2001).
198. Jiang, Y., Lee, A., Chen, J., Ruta, V., Cadene, M., Chait, B.T. & MacKinnon, R. X-ray structure of a voltage-dependent K^+ channel. *Nature* **423**, 33-41 (2003).
199. Dutzler, R., Campbell, E.B. & MacKinnon, R. Gating the selectivity filter in ClC chloride channels. *Science* **300**, 108-112 (2003).
200. Kaufmann, M., Lindner, P., Honegger, A., Blank, K., Tschopp, M., Capitani, G., Plückthun, A. & Grütter, M.G. Crystal structure of the anti-His tag antibody 3D5 single-chain fragment complexed to its antigen. *J. Mol. Biol.* **318**, 135-147 (2002).
201. Roosild, T.P., Castronovo, S. & Choe, S. Structure of anti-FLAG M2 Fab domain and its use in the stabilization of engineered membrane proteins. *Acta Crystallographica Section F* **62**, 835-839 (2006).
202. Abramson, J., Larsson, G., Byrne, B., Puustinen, A., Garcia-Horsmanb, A. & Iwata, S. Purification, crystallization and preliminary crystallographic studies of an integral membrane protein, cytochrome bo_3 ubiquinol oxidase from *Escherichia coli*. *Acta Crystallogr. D. Biol. Crystallogr.* **56**, 1076-1078 (2000).

203. Pebay-Peyroula, E., Neutze, R. & Landau, E.M. Lipidic cubic phase crystallization of bacteriorhodopsin and cryotrapping of intermediates: towards resolving a revolving photocycle. *Biochimica et Biophysica Acta (BBA) - Bioenergetics* **1460**, 119-132 (2000).
204. Royant, A., Edman, K., Ursby, T., Pebay-Peyroula, E., Landau, E.M. & Neutze, R. Helix deformation is coupled to vectorial proton transport in the photocycle of bacteriorhodopsin. *Nature* **406**, 645-648 (2000).
205. Sass, H.J., Büldt, G., Gessenich, R., Hehn, D., Neff, D., Schlesinger, R., Berendzen, J. & Ormos, P. Structural alterations for proton translocation in the M state of wild-type bacteriorhodopsin. *Nature* **406**, 649-653 (2000).
206. Chiu, M.L., Nollert, P., Loewen, M.C., Belrhali, H., Pebay-Peyroula, E., Rosenbusch, J.P. & Landau, E.M. Crystallization in cubo: general applicability to membrane proteins. *Acta Crystallogr. D. Biol. Crystallogr.* **56**, 781-784 (2000).
207. Katona, G., Andréasson, U., Landau, E.M., Andréasson, L.-E. & Neutze, R. Lipidic cubic phase crystal structure of the photosynthetic reaction centre from *Rhodobacter sphaeroides* at 2.35 Å resolution. *J. Mol. Biol.* **331**, 681-692 (2003).
208. Riekel, C., Burghammer, M. & Schertler, G. Protein crystallography microdiffraction. *Curr. Opin. Struct. Biol.* **15**, 556-562 (2005).
209. Standfuss, J., Xie, G., Edwards, P.C., Burghammer, M., Oprian, D.D. & Schertler, G.F.X. Crystal structure of a thermally stable rhodopsin mutant. *J. Mol. Biol.* **372**, 1179-1188 (2007).
210. Gonen, T., Cheng, Y., Sliz, P., Hiroaki, Y., Fujiyoshi, Y., Harrison, S.C. & Walz, T. Lipid-protein interactions in double-layered two-dimensional AQP0 crystals. *Nature* **438**, 633-638 (2005).
211. Lundstrom, K. Structural genomics of GPCRs. *Trends Biotechnol.* **23**, 103-108 (2005).
212. Giros, B., Sokoloff, P., Martres, M.-P., Riou, J.-F., Emorine, L.J. & Schwartz, J.-C. Alternative splicing directs the expression of two D_2 dopamine receptor isoforms. *Nature* **342**, 923-926 (1989).
213. Fishburn, C.S., Belleli, D., David, C., Carmon, S. & Fuchs, S. A novel short isoform of the D_3 dopamine receptor generated by alternative splicing in the third cytoplasmic loop. *J. Biol. Chem.* **268**, 5872-5878 (1993).
214. Cravchik, A., Sibley, D.R. & V. Gejman, P. Functional analysis of the human D_2 dopamine receptor missense variants. *J. Biol. Chem.* **271**, 26013-26017 (1996).
215. Van Tol, H.H.M., Wu, C.M., Guan, H.-C., Ohara, K., Bunzow, J.R., Civelli, O., Kennedy, J., Seeman, P., Niznik, H.B. & Jovanovic, V. Multiple dopamine D_4 receptor variants in the human population. *Nature* **358**, 149-152 (1992).
216. Castro, S.W. & Strange, P.G. Coupling of D_2 and D_3 dopamine receptors to G proteins. *FEBS Lett.* **315**, 223-226 (1993).
217. Guiramand, J., Montmayeur, J.-P., Ceraline, J., Bhatia, M. & Borrelli, E. Alternative splicing of the dopamine D_2 receptor directs specificity of coupling to G proteins. *J. Biol. Chem.* **270**, 7354-7358 (1995).
218. Castro, S.W. & Strange, P.G. Differences in the ligand binding properties of the short and long versions of the D_2 dopamine receptor. *J. Neurochem.* **60**, 372-375 (1993).
219. Malmberg, A., Jackson, D.M., Eriksson, A. & Mohell, N. Unique binding characteristics of antipsychotic agents interacting with human dopamine D_{2A}, D_{2B}, and D_3 receptors. *Mol. Pharmacol.* **43**, 749-754 (1993).
220. Kazmi, M.A., Snyder, L.A., Cypess, A.M., Graber, S.G. & Sakmar, T.P. Selective reconstitution of human D_4 dopamine receptor variants with $G_i\alpha$ subtypes. *Biochemistry (Mosc).* **39**, 3734-3744 (2000).

221. Neve, K.A. & Neve, R.L. *The Dopamine Receptors*, (Humana Press, Totowa, NJ, USA, 1997).
222. Vallar, L., Muca, C., Magni, M., Albert, P., Bunzow, J., Meldolesi, J. & Civelli, O. Differential coupling of dopaminergic D_2 receptors expressed in different cell types. Stimulation of phosphatidylinositol 4,5-bisphosphate hydrolysis in LtK^- fibroblasts, hyperpolarization, and cytosolic-free Ca^{2+} concentration decrease in GH_4C_1 cells. *J. Biol. Chem.* **265**, 10320-10326 (1990).
223. Kanterman, R.Y., Mahan, L.C., Briley, E.M., Monsma, F.J., Jr., Sibley, D.R., Axelrod, J. & Felder, C.C. Transfected D_2 dopamine receptors mediate the potentiation of arachidonic acid release in Chinese hamster ovary cells. *Mol. Pharmacol.* **39**, 364-369 (1991).
224. Lledo, P.M., Homburger, V., Bockaert, J. & Vincent, J.-D. Differential G protein-mediated coupling of D_2 dopamine receptors to K^+ and Ca^{2+} currents in rat anterior pituitary cells. *Neuron* **8**, 455-463 (1992).
225. Seabrook, G.R., Knowles, M., Brown, N., Myers, J., Sinclair, H., Patel, S., Freedman, S.B. & McAllister, G. Pharmacology of high-threshold calcium currents in GH_4C_1 pituitary cells and their regulation by activation of human D_2 and D_4 dopamine receptors. *Br. J. Pharmacol.* **112**, 728-734 (1994).
226. Coldwell, M.C., Boyfield, I., Brown, A.M., Stemp, G. & Middlemiss, D.N. Pharmacological characterization of extracellular acidification rate responses in human $D_{2(long)}$, D_3 and $D_{4.4}$ receptors expressed in Chinese hamster ovary cells. *Br. J. Pharmacol.* **127**, 1135-1144 (1999).
227. Livingstone, C.D., Strange, P.G. & Naylor, L.H. Molecular modelling of D_2-like dopamine receptors. *Biochem. J.* **287**, 277–282 (1992).
228. Trumpp-Kallmeyer, S., Hoflack, J., Bruinvels, A. & Hibert, M. Modeling of G protein-coupled receptors: application to dopamine, adrenaline, serotonin, acetylcholine, and mammalian opsin receptors. *J. Med. Chem.* **35**, 3448-3462 (1992).
229. Hibert, M.F., Trumpp-Kallmeyer, S., Bruinvels, A. & Hoflack, J. Three-dimensional models of neurotransmitter G-binding protein-coupled receptors. *Mol. Pharmacol.* **40**, 8-15 (1991).
230. Baldwin, J.M. Structure and function of receptors coupled to G proteins. *Curr. Opin. Cell Biol.* **6**, 180-190 (1994).
231. Ahlquist, R.P. A study of the adrenotropic receptors. *Am. J. Physiol.* **153**, 586-600 (1948).
232. Langer, S.Z. Presynaptic regulation of catecholamine release. *Biochem. Pharmacol.* **23**, 1793-1800 (1974).
233. Kobilka, B.K., Matsui, H., Kobilka, T.S., Yang-Feng, T.L., Francke, U., Caron, M.G., Lefkowitz, R.J. & Regan, J.W. Cloning, sequencing, and expression of the gene coding for the human platelet α_2-adrenergic receptor. *Science* **238**, 650-656 (1987).
234. Regan, J.W., Kobilka, T.S., Yang-Feng, T.L., Caron, M.G., Lefkowitz, R.J. & Kobilka, B.K. Cloning and expression of a human kidney cDNA for an α_2-adrenergic receptor subtype. *Proc. Natl. Acad. Sci. U. S. A.* **85**, 6301-6305 (1988).
235. Lomasney, J.W., Lorenz, W., Allen, L.F., King, K., Regan, J.W., Yang-Feng, T.L., Caron, M.G. & Lefkowitz, R.J. Expansion of the α_2-adrenergic receptor family: cloning and characterization of a human α_2-adrenergic receptor subtype, the gene for which is located on chromosome 2. *Proc. Natl. Acad. Sci. U. S. A.* **87**, 5094-5098 (1990).
236. Bylund, D.B., Blaxall, H.S., Iversen, L.J., Caron, M.G., Lefkowitz, R.J. & Lomasney, J.W. Pharmacological characteristics of α_2-adrenergic receptors: comparison of

pharmacologically defined subtypes with subtypes identified by molecular cloning. *Mol. Pharmacol.* **42**, 1-5 (1992).
237. Eason, M.G., Kurose, H., Holt, B.D., Raymond, J.R. & Liggett, S.B. Simultaneous coupling of α_2-adrenergic receptors to two G proteins with opposing effects. Subtype-selective coupling of α_2C10, α_2C4, and α_2C2 adrenergic receptors to G_i and G_s. *J. Biol. Chem.* **267**, 15795-15801 (1992).
238. Limbird, L.E. Receptors linked to inhibition of adenylate cyclase: additional signalling mechanisms. *FASEB J.* **2**, 2686-2695 (1988).
239. Alblas, J., van Corven, E.J., Hordijk, P.L., Milligan, G. & Moolenaar, W.H. G_i-mediated activation of the $p21^{ras}$-mitogen-activated protein kinase pathway by α_2-adrenergic receptors expressed in fibroblasts. *J. Biol. Chem.* **268**, 22235-22238 (1993).
240. Flordellis, C.S., Berguerand, M., Gouache, P., Barbu, V., Gavras, H., Handy, D.E., Béréziat, G. & Masliah, J. α_2-Adrenergic receptor subtypes expressed in Chinese hamster ovary cells activate differentially mitogen-activated protein kinase by a $p21^{ras}$ independent pathway. *J. Biol. Chem.* **270**, 3491-3494 (1995).
241. Stamer, W.D., Huang, Y., Seftor, R.E., Svensson, S.S., Snyder, R.W. & Regan, J.W. Cultured human trabecular meshwork cells express functional α_{2A}-adrenergic receptors. *Invest. Ophthalmol. Vis. Sci.* **37**, 2426-2433 (1996).
242. Richman, J.G. & Regan, J.W. α_2-Adrenergic receptors increase cell migration and decrease F-actin labeling in rat aortic smooth muscle cells. *Am. J. Physiol. Cell Physiol.* **274**, C654-662 (1998).
243. Jones, S.B., Halenda, S.P. & Bylund, D.B. α_2-Adrenergic receptor stimulation of phospholipase A_2 and of adenylate cyclase in transfected Chinese hamster ovary cells is mediated by different mechanisms. *Mol. Pharmacol.* **39**, 239-245 (1991).
244. Seuwen, K., Magnaldo, I., Kobilka, B.K., Caron, M.G., Regan, J.W., Lefkowitz, R.J. & Pouysségur, J. α_2-Adrenergic agonists stimulate DNA synthesis in Chinese hamster lung fibroblasts transfected with a human α_2-adrenergic receptor gene. *Cell Regul.* **1**, 445-451 (1990).
245. Koch, W.J., Hawes, B.E., Inglese, J., Luttrell, L.M. & Lefkowitz, R.J. Cellular expression of the carboxyl terminus of a G protein-coupled receptor kinase attenuates Gβγ-mediated signalling. *J. Biol. Chem.* **269**, 6193-6197 (1994).
246. Dorn II, G.W., Oswald, K.J., McCluskey, T.S., Kuhel, D.G. & Liggett, S.B. α_{2A}-Adrenergic receptor stimulated calcium release is transduced by G_i-associated Gβγ-mediated activation of phospholipase C. *Biochemistry (Mosc).* **36**, 6415-6423 (1997).
247. MacNulty, E.E., McClue, S.J., Carr, I.C., Jess, T., Wakelam, M.J. & Milligan, G. α_2-C10 adrenergic receptors expressed in rat 1 fibroblasts can regulate both adenylylcyclase and phospholipase D-mediated hydrolysis of phosphatidylcholine by interacting with pertussis toxin-sensitive guanine nucleotide-binding proteins. *J. Biol. Chem.* **267**, 2149-2156 (1992).
248. Ruffolo, R.R. & Hieble, J.P. α-Adrenoceptors. *Pharmacol. Ther.* **61**, 1-64 (1994).
249. Ruffolo, R.R., Bondinell, W. & Hieble, J.P. α- and β-Adrenoceptors: from the gene to the clinic. 2. Structure-activity relationships and therapeutic applications. *J. Med. Chem.* **38**, 3681-3716 (1995).
250. Lakhlani, P.P., McMillan, L.B., Guo, T.Z., McCool, B.A., Lovinger, D.M., Maze, M. & Limbird, L.E. Substitution of a mutant α_{2a}-adrenergic receptor via "hit and run" gene targeting reveals the role of this subtype in sedative, analgesic, and anesthetic-sparing responses *in vivo*. *Proc. Natl. Acad. Sci. U. S. A.* **94**, 9950-9955 (1997).
251. Arnsten, A.F.T. The biology of being frazzled. *Science* **280**, 1711-1712 (1998).

252. Robinson, E. & Hudson, A. Adrenoceptor Pharmacology. *Tocris Reviews No. 8* (1998).
253. Bes, A., Eyssette, M., Pierrot-Deseilligny, E., Rohmer, F. & Warter, J.M. A multi-centre, double-blind trial of tizanidine, a new antispastic agent, in spasticity associated with hemiplegia. *Curr. Med. Res. Opin.* **10**, 709-718 (1988).
254. Eyssette, M., Rohmer, F., Serratrice, G., Warter, J.M. & Boisson, D. Multi-centre, double-blind trial of a novel antispastic agent, tizanidine, in spasticity associated with multiple sclerosis. *Curr. Med. Res. Opin.* **10**, 699-708 (1988).
255. Hutchinson, D.R. Modified release tizanidine: a review. *J. Int. Med. Res.* **17**, 565-573 (1989).
256. Serle, J.B., Lustgarten, J.S. & Podos, S.M. A clinical trial of metipranolol, a noncardioselective beta-adrenergic antagonist, in ocular hypertension. *Am. J. Ophthalmol.* **112**, 302-307 (1991).
257. Linden, J. Adenosine in tissue protection and tissue regeneration. *Mol. Pharmacol.* **67**, 1385-1387 (2005).
258. Kull, B., Svenningsson, P. & Fredholm, B.B. Adenosine A_{2A} receptors are colocalized with and activate G_{olf} in rat striatum. *Mol. Pharmacol.* **58**, 771-777 (2000).
259. Fresco, P., Diniz, C. & Gonçalves, J. Facilitation of noradrenaline release by activation of adenosine A_{2A} receptors triggers both phospholipase C and adenylate cyclase pathways in rat-tail artery. *Cardiovasc. Res.* **63**, 739-746 (2004).
260. Offermanns, S. & Simon, M.I. $G\alpha_{15}$ and $G\alpha_{16}$ couple a wide variety of receptors to phospholipase C. *J. Biol. Chem.* **270**, 15175-15180 (1995).
261. Schindler, C.W., Karcz-Kubicha, M., Thorndike, E.B., Müller, C.E., Tella, S.R., Ferré, S. & Goldberg, S.R. Role of central and peripheral adenosine receptors in the cardiovascular responses to intraperitoneal injections of adenosine A_1 and A_{2A} subtype receptor agonists. *Br. J. Pharmacol.* **144**, 642-650 (2005).
262. Varani, K., Portaluppi, F., Gessi, S., Merighi, S., Ongini, E., Belardinelli, L. & Borea, P.A. Dose and time effects of caffeine intake on human platelet adenosine A_{2A} receptors: functional and biochemical aspects. *Circulation* **102**, 285-289 (2000).
263. Hendel, R.C., Bateman, T.M., Cerqueira, M.D., Iskandrian, A.E., Leppo, J.A., Blackburn, B. & Mahmarian, J.J. Initial clinical experience with regadenoson, a novel selective A_{2A} agonist for pharmacologic stress single-photon emission computed tomography myocardial perfusion imaging. *J. Am. Coll. Cardiol.* **46**, 2069-2075 (2005).
264. Barrett, R.J., Lamson, M.J., Johnson, J. & Smith, W.B. Pharmacokinetics and safety of binodenoson after intravenous dose escalation in healthy volunteers. *J. Nucl. Cardiol.* **12**, 166-171 (2005).
265. Devane, W.A., Hanus, L., Breuer, A., Pertwee, R.G., Stevenson, L.A., Griffin, G., Gibson, D., Mandelbaum, A., Etinger, A. & Mechoulam, R. Isolation and structure of a brain constituent that binds to the cannabinoid receptor. *Science* **258**, 1946-1949 (1992).
266. Mechoulam, R., Ben-Shabat, S., Hanus, L., Ligumsky, M., Kaminski, N.E., Schatz, A.R., Gopher, A., Almog, S., Martin, B.R., Compton, D.R., Pertwee, R.G., Griffin, G., Bayewitch, M., Barg, J. & Vogel, Z. Identification of an endogenous 2-monoglyceride, present in canine gut, that binds to cannabinoid receptors. *Biochem. Pharmacol.* **50**, 83-90 (1995).
267. Matsuda, L.A., Lolait, S.J., Brownstein, M.J., Young, A.C. & Bonner, T.I. Structure of a cannabinoid receptor and functional expression of the cloned cDNA. *Nature* **346**, 561-564 (1990).

268. Munro, S., Thomas, K.L. & Abu-Shaar, M. Molecular characterization of a peripheral receptor for cannabinoids. *Nature* **365**, 61-65 (1993).
269. Howlett, A.C., Barth, F., Bonner, T.I., Cabral, G., Casellas, P., Devane, W.A., Felder, C.C., Herkenham, M., Mackie, K., Martin, B.R., Mechoulam, R. & Pertwee, R.G. International Union of Pharmacology. XXVII. Classification of Cannabinoid Receptors. *Pharmacol. Rev.* **54**, 161-202 (2002).
270. Roth, M.D., Baldwin, G.C. & Tashkin, D.P. Effects of delta-9-tetrahydrocannabinol on human immune function and host defense. *Chem. Phys. Lipids* **121**, 229-239 (2002).
271. Felder, C.C., Joyce, K.E., Briley, E.M., Mansouri, J., Mackie, K., Blond, O., Lai, Y., Ma, A.L. & Mitchell, R.L. Comparison of the pharmacology and signal transduction of the human cannabinoid CB_1 and CB_2 receptors. *Mol. Pharmacol.* **48**, 443-450 (1995).
272. Slipetz, D.M., O'Neill, G.P., Favreau, L., Dufresne, C., Gallant, M., Gareau, Y., Guay, D., Labelle, M. & Metters, K.M. Activation of the human peripheral cannabinoid receptor results in inhibition of adenylyl cyclase. *Mol. Pharmacol.* **48**, 352-361 (1995).
273. Howlett, A.C., Qualy, J.M. & Khachatrian, L.L. Involvement of G_i in the inhibition of adenylate cyclase by cannabimimetic drugs. *Mol. Pharmacol.* **29**, 307-313 (1986).
274. Mackie, K. & Hille, B. Cannabinoids inhibit N-type calcium channels in neuroblastoma-glioma cells. *Proc. Natl. Acad. Sci. U. S. A.* **89**, 3825-3829 (1992).
275. Mackie, K., Lai, Y., Westenbroek, R. & Mitchell, R. Cannabinoids activate an inwardly rectifying potassium conductance and inhibit Q-type calcium currents in AtT20 cells transfected with rat brain cannabinoid receptor. *J. Neurosci.* **15**, 6552-6561 (1995).
276. Vaughan, C.W. & Christie, M.J. Retrograde signalling by endocannabinoids. in *Cannabinoids* (ed. Heidelberg, S.B.) 367-383 (2005).
277. Walter, L. & Stella, N. Cannabinoids and neuroinflammation. *Br. J. Pharmacol.* **141**, 775-785 (2004).
278. Cabral, G.A. & Staab, A. Effects on the immune system. in *Cannabinoids* (ed. Heidelberg, S.B.) 385-423 (2005).
279. Pertwee, R. The therapeutic potential of drugs that target cannabinoid receptors or modulate the tissue levels or actions of endocannabinoids. *The AAPS Journal* **7**, E625-E654 (2005).
280. Kieffer, B.L., Befort, K., Gaveriaux-Ruff, C. & Hirth, C.G. The δ-opioid receptor: isolation of a cDNA by expression cloning and pharmacological characterization. *Proc. Natl. Acad. Sci. U. S. A.* **89**, 12048-12052 (1992).
281. Chen, Y., Mestek, A., Liu, J., Hurley, J.A. & Yu, L. Molecular cloning and functional expression of a μ-opioid receptor from rat brain. *Mol. Pharmacol.* **44**, 8-12 (1993).
282. Minami, M., Toya, T., Katao, Y., Maekawa, K., Nakamura, S., Onogi, T., Kaneko, S. & Satoh, M. Cloning and expression of a cDNA for the rat κ-opioid receptor. *FEBS Lett.* **329**, 291-295 (1993).
283. Chaturvedi, K., Christoffers, K.H., Singh, K. & Howells, R.D. Structure and regulation of opioid receptors. *Peptide Science* **55**, 334-346 (2000).
284. Matthes, H.W.D., Maldonado, R., Simonin, F., Valverde, O., Slowe, S., Kitchen, I., Befort, K., Dierich, A., Le Meur, M., Dollé, P., Tzavara, E., Hanoune, J., Roques, B.P. & Kieffer, B.L. Loss of morphine-induced analgesia, reward effect and withdrawal symptoms in mice lacking the μ-opioid receptor gene. *Nature* **383**, 819-823 (1996).
285. Grudt, T.J. & Williams, J.T. κ-Opioid receptors also increase potassium conductance. *Proc. Natl. Acad. Sci. U. S. A.* **90**, 11429-11432 (1993).

286. Von Euler, U.S. & Gaddum, J.H. An unidentified depressor substance in certain tissue extracts. *J. Physiol. (Lond).* **72**, 74-87 (1931).
287. Almeida, T.A., Rojo, J., Nieto, P.M., Pinto, F.M., Hernandez, M., Martín, J.D. & Candenas, M.L. Tachykinins and tachykinin receptors: structure and activity relationships. *Curr. Med. Chem.* **11**, 2045-2081 (2004).
288. Mussap, C.J., Geraghty, D.P. & Burcher, E. Tachykinin receptors: a radioligand binding perspective. *J. Neurochem.* **60**, 1987-2009 (1993).
289. Buck, S.H. *The Tachykinin Receptors*, (Humana Press, Totowa, NJ, USA, 1994).
290. Prado, C.M., Leick-Maldonado, E.A., Miyamoto, L., Yano, L.M., Kasahara, D.I., Martins, M.A. & Tibério, I.F.L.C. Capsaicin-sensitive nerves and neurokinins modulate non-neuronal nNOS expression in lung. *Respiratory Physiology & Neurobiology* **160**, 37-44 (2008).
291. Nakajima, Y., Tsuchida, K., Negishi, M., Ito, S. & Nakanishi, S. Direct linkage of three tachykinin receptors to stimulation of both phosphatidylinositol hydrolysis and cyclic AMP cascades in transfected Chinese hamster ovary cells. *J. Biol. Chem.* **267**, 2437-2442 (1992).
292. Kramer, M.S. *et al.* Distinct mechanism for antidepressant activity by blockade of central substance P receptors. *Science* **281**, 1640-1645 (1998).
293. Emonds-Alt, X., Bichon, D., Ducoux, J.-P., Heaulme, M., Miloux, B., Poncelet, M., Proietto, V., Van Broeck, D., Vilain, P., Neliat, G., Soubrié, P., Le Fur, G. & Brelière, J.-C. SR 142801, the first potent non-peptide antagonist of the tachykinin NK_3 receptor. *Life Sci.* **56**, PL27-PL32 (1994).
294. Sarau, H.M., Griswold, D.E., Potts, W., Foley, J.J., Schmidt, D.B., Webb, E.F., Martin, L.D., Brawner, M.E., Elshourbagy, N.A., Medhurst, A.D., Giardina, G.A.M. & Hay, D.W.P. Nonpeptide tachykinin receptor antagonists: I. Pharmacological and pharmacokinetic characterization of SB 223412, a novel, potent and selective neurokinin-3 receptor antagonist. *J. Pharmacol. Exp. Ther.* **281**, 1303-1311 (1997).
295. André, N., Cherouati, N., Prual, C., Steffan, T., Zeder-Lutz, G., Magnin, T., Pattus, F., Michel, H., Wagner, R. & Reinhart, C. Enhancing functional production of G protein-coupled receptors in *Pichia pastoris* to levels required for structural studies via a single expression screen. *Protein Sci.* **15**, 1115-1126 (2006).
296. Lundstrom, K., Wagner, R., Reinhart, C., Desmyter, A., Cherouati, N., Magnin, T., Zeder-Lutz, G., Courtot, M., Prual, C., André, N., Hassaine, G., Michel, H., Cambillau, C. & Pattus, F. Structural genomics on membrane proteins: comparison of more than 100 GPCRs in 3 expression systems. *J. Struct. Funct. Genomics* **7**, 77-91 (2006).
297. Cronan, J.E., Jr. Biotination of proteins *in vivo*. A post-translational modification to label, purify, and study proteins. *J. Biol. Chem.* **265**, 10327-10333 (1990).
298. Cregg, J.M., Vedvick, T.S. & Raschke, W.C. Recent advances in the expression of foreign genes in *Pichia pastoris*. *Biotechnology* **11**, 905-910 (1993).
299. Towbin, H., Staehelin, T. & Gordon, J. Electrophoretic transfer of proteins from polyacrylamide gels to nitrocellulose sheets: procedure and some applications. *Biotechnology* **24**, 145-149 (1992).
300. Zeder-Lutz, G., Cherouati, N., Reinhart, C., Pattus, F. & Wagner, R. Dot-blot immunodetection as a versatile and high-throughput assay to evaluate recombinant GPCRs produced in the yeast *Pichia pastoris*. *Protein Expression Purif.* **50**, 118-127 (2006).
301. Cherouati, N. Université Louis Pasteur − Strasbourg I (2005).

302. Vasudevan, S., Hulme, E.C., Bach, M., Haase, W., Pavia, J. & Reiländer, H. Characterization of the rat M_3 muscarinic acetylcholine receptor produced in insect cells infected with recombinant baculovirus. *Eur. J. Biochem.* **227**, 466-475 (1995).
303. Liitti, S., Matikainen, M.-T., Scheinin, M., Glumoff, T. & Goldman, A. Immunoaffinity purification and reconstitution of human α_2-adrenergic receptor subtype C2 into phospholipid vesicles. *Protein Expression Purif.* **22**, 1-10 (2001).
304. Vilardaga, J.-P., Steinmeyer, R., Harms, G.S. & Lohse, M.J. Molecular basis of inverse agonism in a G protein-coupled receptor. *Nat. Chem. Biol.* **1**, 25-28 (2005).
305. Williamson, R.A., Worrall, S., Chazot, P.L. & Strange, P.G. Purification of brain D_2 dopamine receptor. *EMBO J.* **7**, 4129-4133 (1988).
306. Kwatra, M.M., Schreurs, J., Schwinn, D.A., Innis, M.A., Caron, M.G. & Lefkowitz, R.J. Immunoaffinity purification of epitope-tagged human β_2-adrenergic receptor to homogeneity. *Protein Expression Purif.* **6**, 717-721 (1995).
307. Ghanouni, P., Schambye, H., Seifert, R., Lee, T.W., Rasmussen, S.G.F., Gether, U. & Kobilka, B.K. The effect of pH on β_2-adrenoceptor function. Evidence for protonation-dependent activation. *J. Biol. Chem.* **275**, 3121-3127 (2000).
308. Hayashi, M.K. & Haga, T. Purification and functional reconstitution with GTP-binding regulatory proteins of hexahistidine-tagged muscarinic acetylcholine receptors (M_2 subtype). *J. Biochem. (Tokyo).* **120**, 1232-1238 (1996).
309. Park, P.S.-H. & Wells, J.W. Monomers and oligomers of the M_2 muscarinic cholinergic receptor purified from Sf9 cells. *Biochemistry (Wash.)* **42**, 12960-12971 (2003).
310. Doi, T., Hiroaki, Y., Arimoto, I., Fujiyoshi, Y., Okamoto, T., Satoh, M. & Furuichi, Y. Characterization of human endothelin B receptor and mutant receptors expressed in insect cells. *Eur. J. Biochem.* **248**, 139-148 (1997).
311. Kovoor, A., Celver, J., Abdryashitov, R.I., Chavkin, C. & Gurevich, V.V. Targeted construction of phosphorylation-independent β-arrestin mutants with constitutive activity in cells. *J. Biol. Chem.* **274**, 6831-6834 (1999).
312. Gurevich, V.V. & Gurevich, E.V. The structural basis of arrestin-mediated regulation of G protein-coupled receptors. *Pharmacol. Ther.* **110**, 465-502 (2006).
313. Bertin, B., Freissmuth, M., Jockers, R., Strosberg, A.D. & Marullo, S. Cellular signalling by an agonist-activated receptor/$G_s\alpha$ fusion protein. *Proc. Natl. Acad. Sci. U. S. A.* **91**, 8827-8831 (1994).
314. Ransnäs, L.A. & Insel, P.A. Quantitation of the guanine nucleotide binding regulatory protein G_s in S49 cell membranes using antipeptide antibodies to α_s. *J. Biol. Chem.* **263**, 9482-9485 (1988).
315. Bertin, B., Jockers, R., Strosberg, A.D. & Marullo, S. Activation of a β_2-adrenergic receptor/$G_s\alpha$ fusion protein elicits a desensitization-resistant cAMP signal capable of inhibiting proliferation of two cancer cell lines. *Receptors Channels* **5**, 41-51 (1997).
316. Bertin, B., Strosberg, A.D. & Marullo, S. Human β_2-adrenergic receptor/$G_s\alpha$ fusion protein, expressed in 2 *ras*-dependent murine carcinoma cell lines, prevents tumor growth in syngeneic mice. *Int. J. Cancer* **71**, 1029-1034 (1997).
317. Medici, R., Bianchi, E., Di Segni, G. & Tocchini-Valentini, G.P. Efficient signal transduction by a chimeric yeast-mammalian G protein α-subunit Gpa1−$G_s\alpha$ covalently fused to the yeast receptor Ste2. *EMBO J.* **16**, 7241-7249 (1997).
318. Wise, A., Carr, I.C., Groarke, D.A. & Milligan, G. Measurement of agonist efficacy using an α_{2A}-adrenoceptor−$G_{i1}\alpha$ fusion protein. *FEBS Lett.* **419**, 141-146 (1997).
319. Wise, A., Carr, I.C. & Milligan, G. Measurement of agonist-induced guanine nucleotide turnover by the G protein $G_{i1}\alpha$ when constrained within an α_{2A}-adrenoceptor−$G_{i1}\alpha$ fusion protein. *Biochem. J.* **325**, 17-21 (1997).

320. Wise, A. & Milligan, G. Rescue of functional interactions between the α_{2A}-adrenoreceptor and acylation-resistant forms of $G_{i1}\alpha$ by expressing the proteins from chimeric open reading frames. *J. Biol. Chem.* **272**, 24673-24678 (1997).
321. Burt, A.R., Sautel, M., Wilson, M.A., Rees, S., Wise, A. & Milligan, G. Agonist occupation of an α_{2A}-adrenoreceptor−$G_{i1}\alpha$ fusion protein results in activation of both receptor-linked and endogenous G_i proteins. Comparisons of their contributions to GTPase activity and signal transduction and analysis of receptor−G protein activation stoichiometry. *J. Biol. Chem.* **273**, 10367-10375 (1998).
322. Carr, I.C., Burt, A.R., Jackson, V.N., Wright, J., Wise, A., Rees, S. & Milligan, G. Quantitative analysis of a cysteine^{351}glycine mutation in the G protein $G_{i1}\alpha$: effect on α_{2A}-adrenoceptor−$G_{i1}\alpha$ fusion protein activation. *FEBS Lett.* **428**, 17-22 (1998).
323. Seifert, R., Lee, T.W., Lam, V.T. & Kobilka, B.K. Reconstitution of β_2-adrenoceptor−GTP-binding protein interaction in Sf9 cells. High coupling efficiency in a β_2-adrenoceptor−$G_s\alpha$ fusion protein. *Eur. J. Biochem.* **255**, 369-382 (1998).
324. Seifert, R., Wenzel-Seifert, K., Lee, T.W., Gether, U., Sanders-Bush, E. & Kobilka, B.K. Different effects of $G_s\alpha$ splice variants on β_2-adrenoreceptor-mediated signalling. The β_2-adrenoreceptor coupled to the long splice variant of $G_s\alpha$ has properties of a constitutively active receptor. *J. Biol. Chem.* **273**, 5109-5116 (1998).
325. Wenzel-Seifert, K., Lee, T.W., Seifert, R. & Kobilka, B.K. Restricting mobility of $G_s\alpha$ relative to the β_2-adrenoceptor enhances adenylate cyclase activity by reducing $G_s\alpha$ GTPase activity. *Biochem. J.* **334**, 519-524 (1998).
326. Kobilka, B. Adrenergic receptors as models for G protein-coupled receptors. *Annu. Rev. Neurosci.* **15**, 87-114 (1992).
327. Ostrowski, J., Kjelsberg, M.A., Caron, M.G. & Lefkowitz, R.J. Mutagenesis of the β_2-adrenergic receptor: how structure elucidates function. *Annu. Rev. Pharmacol. Toxicol.* **32**, 167-183 (1992).
328. Wess, J. G protein-coupled receptors: molecular mechanisms involved in receptor activation and selectivity of G protein recognition. *FASEB J.* **11**, 346-354 (1997).
329. Iiri, T., Farfel, Z. & Bourne, H.R. G protein diseases furnish a model for the turn-on switch. *Nature* **394**, 35-38 (1998).
330. Irie, A., Sugimoto, Y., Namba, T., Asano, T., Ichikawa, A. & Negishi, M. The C-terminus of the prostaglandin-E-receptor EP_3 subtype is essential for activation of GTP-binding protein. *Eur. J. Biochem.* **224**, 161-166 (1994).
331. Bommakanti, R.K., Dratz, E.A., Siemsen, D.W. & Jesaitis, A.J. Extensive contact between G_{i2} and *N*-formyl peptide receptor of human neutrophils: mapping of binding sites using receptor-mimetic peptides. *Biochemistry (Wash.)* **34**, 6720-6728 (1995).
332. Kai, H., Alexander, R.W., Ushio-Fukai, M., Lyons, P.R., Akers, M. & Griendling, K.K. G protein binding domains of the angiotensin II AT_{1A} receptors mapped with synthetic peptides selected from the receptor sequence. *Biochem. J.* **332**, 781-787 (1998).
333. Milligan, G. & Rees, S. Chimaeric Gα proteins: their potential use in drug discovery. *Trends Pharmacol. Sci.* **20**, 118-124 (1999).
334. Seifert, R., Gether, U., Wenzel-Seifert, K. & Kobilka, B.K. Effects of guanine, inosine, and xanthine nucleotides on β_2-adrenergic receptor/G_s interactions: evidence for multiple receptor conformations. *Mol. Pharmacol.* **56**, 348-358 (1999).
335. Seifert, R., Wenzel-Seifert, K., Gether, U., Lam, V.T. & Kobilka, B.K. Examining the efficiency of receptor/G protein coupling with a cleavable β_2-adrenoceptor−$G_s\alpha$ fusion protein. *Eur. J. Biochem.* **260**, 661-666 (1999).
336. Molinari, P., Ambrosio, C., Riitano, D., Sbraccia, M., Grò, M.C. & Costa, T. Promiscuous coupling at receptor−Gα fusion proteins. The receptor of one covalent

complex interacts with the α-subunit of another. *J. Biol. Chem.* **278**, 15778-15788 (2003).
337. Sautel, M. & Milligan, G. Loss of activation of G_s but not G_i following expression of an α_{2A}-adrenoceptor−$G_{i1}\alpha$ fusion protein. *FEBS Lett.* **436**, 46-50 (1998).
338. Jackson, V.N., Bahia, D.S. & Milligan, G. Modulation of relative intrinsic activity of agonists at the α_{2A}-adrenoceptor by mutation of residue 351 of G protein $G_{i1}\alpha$. *Mol. Pharmacol.* **55**, 195-201 (1999).
339. Waldhoer, M., Wise, A., Milligan, G., Freissmuth, M. & Nanoff, C. Kinetics of ternary complex formation with fusion proteins composed of the A_1 adenosine receptor and G protein α-subunits. *J. Biol. Chem.* **274**, 30571-30579 (1999).
340. Wise, A., Sheehan, M., Rees, S., Lee, M. & Milligan, G. Comparative analysis of the efficacy of A_1 adenosine receptor activation of $G_{i/o}\alpha$ G proteins following coexpression of receptor and G protein and expression of A_1 adenosine receptor−$G_{i/o}\alpha$ fusion proteins. *Biochemistry (Wash.)* **38**, 2272-2278 (1999).
341. Dupuis, D.S., Tardif, S., Wurch, T., Colpaert, F.C. & Pauwels, P.J. Modulation of $5HT_{1A}$ receptor signalling by point-mutation of cysteine^{351} in the rat $G\alpha_o$ protein. *Neuropharmacology* **38**, 1035-1041 (1999).
342. Welsby, P.J., Carr, I.C., Wilkinson, G. & Milligan, G. Regulation of the avidity of ternary complexes containing the human $5HT_{1A}$ receptor by mutation of a receptor contact site on the interacting G protein α-subunit. *Br. J. Pharmacol.* **137**, 345-352 (2002).
343. Wenzel-Seifert, K., Arthur, J.M., Liu, H.-Y. & Seifert, R. Quantitative analysis of formyl peptide receptor coupling to $G_i\alpha_1$, $G_i\alpha_2$, and $G_i\alpha_3$. *J. Biol. Chem.* **274**, 33259-33266 (1999).
344. Shi, M., Bennett, T.A., Cimino, D.F., Maestas, D.C., Foutz, T.D., Gurevich, V.V., Sklar, L.A. & Prossnitz, E.R. Functional capabilities of an *N*-formyl peptide receptor−$G_{i2}\alpha$ fusion protein: assemblies with G proteins and arrestins. *Biochemistry (Mosc).* **42**, 7283-7293 (2003).
345. Takeda, S., Okada, T., Okamura, M., Haga, T., Isoyama-Tanaka, J., Kuwahara, H. & Minamino, N. The receptor−Gα fusion protein as a tool for ligand screening: a model study using a nociceptin receptor−$G\alpha_{i2}$ fusion protein. *J. Biochem., Tokyo* **135**, 597-604 (2004).
346. Zhang, Q., Okamura, M., Guo, Z.-D., Niwa, S. & Haga, T. Effects of partial agonists and Mg^{2+} ions on the interaction of M_2 muscarinic acetylcholine receptor and G protein $G\alpha_{i1}$ subunit in the M_2−$G\alpha_{i1}$ fusion protein. *J. Biochem., Tokyo* **135**, 589-596 (2004).
347. Armstrong, D. & Strange, P.G. Dopamine D_2 receptor dimer formation. Evidence from ligand binding. *J. Biol. Chem.* **276**, 22621-22629 (2001).
348. Sonntag, I., Schwarz, H., Hirota, Y. & Henning, U. Cell envelope and shape of *Escherichia coli*: multiple mutants missing the outer membrane lipoprotein and other major outer membrane proteins. *J. Bacteriol.* **136**, 280-285 (1978).
349. Schweizer, M. & Henning, U. Action of a major outer cell envelope membrane protein in conjugation of *Escherichia coli* K-12. *J. Bacteriol.* **129**, 1651-1652 (1977).
350. Ried, G. & Henning, U. A unique amino acid substitution in the outer membrane protein OmpA causes conjugation deficiency in *Escherichia coli* K-12. *FEBS Lett.* **223**, 387-390 (1987).
351. Morona, R., Krämer, C. & Henning, U. Bacteriophage receptor area of outer membrane protein OmpA of *Escherichia coli* K-12. *J. Bacteriol.* **164**, 539-543 (1985).

352. Foulds, J. & Barrett, C. Characterization of *Escherichia coli* mutants tolerant to bacteriocin JF246: two new classes of tolerant mutants. *J. Bacteriol.* **116**, 885-892 (1973).
353. Weiser, J.N. & Gotschlich, E.C. Outer membrane protein A (OmpA) contributes to serum resistance and pathogenicity of *Escherichia coli* K-1. *Infect. Immun.* **59**, 2252-2258 (1991).
354. Prasadarao, N.V., Wass, C.A., Weiser, J.N., Stins, M.F., Huang, S.H. & Kim, K.S. Outer membrane protein A of *Escherichia coli* contributes to invasion of brain microvascular endothelial cells. *Infect. Immun.* **64**, 146-153 (1996).
355. Freudl, R., Klose, M. & Henning, U. Export and sorting of the *Escherichia coli* outer membrane protein OmpA. *J. Bioenerg. Biomembr.* **22**, 441-449 (1990).
356. Kleinschmidt, J.H. & Tamm, L.K. Folding intermediates of a β-barrel membrane protein. Kinetic evidence for a multi-step membrane insertion mechanism. *Biochemistry (Mosc)*. **35**, 12993-13000 (1996).
357. Pautsch, A. & Schulz, G.E. Structure of the outer membrane protein A transmembrane domain. *Nat. Struct. Mol. Biol.* **5**, 1013-1017 (1998).
358. Pautsch, A., Vogt, J., Model, K., Siebold, C. & Schulz, G.E. Strategy for membrane protein crystallization exemplified with OmpA and OmpX. *Proteins: Structure, Function, and Genetics* **34**, 167-172 (1999).
359. Bouvier, M. Oligomerization of G protein-coupled transmitter receptors. *Nat. Rev. Neurosci.* **2**, 274-286 (2001).
360. Fernández, C. & Wüthrich, K. NMR solution structure determination of membrane proteins reconstituted in detergent micelles. *FEBS Lett.* **555**, 144-150 (2003).
361. Banères, J.-L., Mesnier, D., Martin, A., Joubert, L., Dumuis, A. & Bockaert, J. Molecular characterization of a purified $5HT_4$ receptor: a structural basis for drug efficacy. *J. Biol. Chem.* **280**, 20253-20260 (2005).
362. Lopez, J.J., Shukla, A.K., Reinhart, C., Schwalbe, H., Michel, H. & Glaubitz, C. The structure of the neuropeptide bradykinin bound to the human G protein-coupled receptor bradykinin B_2 as determined by solid-state NMR spectroscopy. *Angewandte Chemie International Edition* **47**, 1668-1671 (2008).

Abbreviations

AA2AR_HUMAN, A_{2A}AR	Human adenosine A_{2A} receptor
ADA1B_MESAU	Mesau α_{1B}-adrenergic receptor
ADA2B_HUMAN, α_{2B}AR	Human α_{2B}-adrenergic receptor
ADA2C_RAT	Rat α_{2C}-adrenergic receptor
α_2AR(s)	α_2-Adrenergic receptor(s)
β_2AR	Human β_2-adrenoreceptor
AFM	Atomic force microscopy
ANRT	Association Nationale de la Recherche Technique
AR(s)	Adenosine receptor(s)
BCA	Bicinchoninic acid assay
B_{max}	Receptor specific binding activity
cAMP	Cyclic adenosine monophosphate
CB(s)	Cannabinoid receptor(s)
cDNA	Complementary DNA
CHS	Cholesteryl hemisuccinate
CIFRE	Conventions Industrielles de Formation par la Recherche
CMC	Critical micelle concentration
CNR2_HUMAN, CB_2R	Human cannabinoid receptor type-2
CNS	Central nervous system
cryo-EM	Cryo-electron microscopy
CV	Column/bed volume
Da	Dalton
DAG	Diacylglycerol
DDM	n-dodecyl-β-D-maltopyranoside
DRD2_HUMAN, D_2DR	Human dopamine D_2 receptor (long isoform)
DM	n-decyl-β-D-maltopyranoside
DMSO	Dimethyl sulfoxide
DO_2	Dissolved oxygen
DR(s)	Dopaminergic receptor(s)
EDTA	Ethylenediaminetetraacetic acid
ER	Endoplasmic reticulum
E-MeP	European Membrane Protein Consortium
FPLC	Fast protein liquid chromatography
$GABA_B$	Metabotropic γ-aminobutyric acid B
GDP	Guanosine diphosphate
GPCR	G protein-coupled receptor
G protein	Heterotrimeric GTP-binding protein
[^{35}S]GTPγS	[^{35}S]Guanosine-5′-*O*-(3-thio)triphosphate
5HT1B_HUMAN, $5HT_{1B}$R	Human serotonin $5HT_{1B}$ receptor
HRH1_HUMAN	Human histamine H_1 receptor
IEX	Ion-exchange chromatography
IgG	Immunoglobulin-G

IMAC	Immobilised metal-affinity chromatography
IP3	Inositol triphosphate
Kd	Dissociation constant
LDAO	Lauryldimethylamine-*N*-oxide
MAPKs	Mitogen-activated protein kinases
MePNet	Membrane Protein Network
MRC	Medical Research Council
MWCO	Molecular weight cut-off
NK1R_HUMAN	Human neurokinin-1 receptor
NK2R_RAT, NK_2R	Rat neurokinin-2 receptor
NK3R_HUMAN, NK_3R	Human neurokinin-3 receptor
NKRs	Neurokinin receptors
NMDG	N-methyl-D-glucamine
NMR	Nuclear magnetic resonance
OD	Optical density
OG	n-octyl-β-D-glucopyranoside
OPRD_HUMAN, δOR	Human delta-opioid receptor
OPRK_HUMAN, κOR	Human kappa-opioid receptor
ORF	Open reading frame
PAR1_HUMAN	Human proteinase-activated receptor 1 precursor
PI	Protease inhibitor
PLC	Phospholipase C
P2RY1_HUMAN, $P2Y_1R$	Human neuropeptide Y receptor type-1
SDS-PAGE	Sodium dodecyl sulphate-polyacrylamide gel electrophoresis
TEV	Tobacco etch virus protease
TM	Transmembrane helix

Acknowledgments

First of all, I would like to thank Mr. Etienne L'Hermite, founder and CEO of Bio-Xtal, Dr. Franc Pattus and Prof. So Iwata for giving me the opportunity to fulfill this thesis in their laboratories. I highly enjoyed the independence and confidence they entrusted in me, which allowed me to successfully pursue my project in the ever-challenging field of membrane proteins.

I would like to thank all the members of Franc and So's groups, former and present, for the friendly and warm atmosphere, which made working in their respective departments a great pleasure. My special thanks go to Rim Benmaamar for carefully reading some parts of this manuscript.

A load of greatful thanks to Drs. Renaud Wagner and Thierry Magnin for their many ideas, precious advice and their endless support throughout my work. Thank you for always being around when mostly needed.

One of my projects, as described in chapter 6, concerned GPCR–Gα fusion proteins. This work would not have been possible without the expert collaboration with Prof. Philip G. Strange. I would like to take this opportunity to personally thank him.

I would also like to thank Prof. Eva Pebay-Peyroula, Prof. Andreas Engel and Prof. Marcel Hibert for critically reading the manuscript to this thesis. To them and to Dr. Niek Dekker I am indebted for agreeing to participate in the defense of this thesis.

This research was funded by the Membrane Protein Network (Abbott, AstraZeneca, Daiichi-Sankyo, Evotec, GlaxoSmithKline, Kyowa, Novartis, Pfizer, Sanofi Aventis), the European Membrane Protein Consortium (E-MeP), and the French government (ANRT/CIFRE 174/2005).

Curriculum vitæ

Cédric Fiez-Vandal
Born on April 15, 1974 in Paris

Since April 2008	Postdoctoral position at the Karolinska Institute in Prof. Pär Nordlund's group
2005-2008	Ph.D. thesis under the supervision of Dr. Franc Pattus and Prof. So Iwata at the Louis Pasteur University and Imperial College London
2002-2005	Research engineer at the Pasteur Institute in Prof. Pedro Alzari's group
2000-2001	French Institute for Agronomical Research, Microbiology Department, Diploma work: Cloning, characterization, and inactivation of the major esterase gene of *Lactococcus lactis*

2003	Pasteur advanced course in bioinformatics, Paris
2001	French Civil Engineering degree, Paris
1992	Baccalauréat C, Paris

Notes

Notes